SET-UP OF OIL ON WATER

BY WIND

by

Edmund B. Spencer and Robert M. Sorensen
Coastal and Ocean Engineering Division
Texas A&M University

Partially supported by the National Science Foundation
Sea Grant Program
Institutional Grant GH-59 to
Texas A&M University

Sea Grant Publication No. TAMU-SG-70-220
Coastal and Ocean Engineering Division
Report No. 128 - C.O.E.

August 1970

ABSTRACT

Set-up of various density and viscosity oils on water's surface when subjected to wind was studied analytically and experimentally using a two-dimensional wind-wave channel. The primary objective of the study was to verify the controlling equations and establish dimensionless parameters by experimental analysis. Analysis of the results shows that set-up of oil is a function of wind stress and wind generated wave action. The empirical parameters developed allow prediction of oil set-up when subjected to various steady state wind conditions.

PREFACE

Research described in this report was conducted as part of the research program in Coastal and Ocean Engineering at Texas A&M University.

The report was primarily written by the senior author in partial fulfillment of the Master of Science requirement under the supervision of the junior author who was his major advisor.

The review of this report and comments by Dr. Ron Darby and Dr. John B. Herbich are also appreciated.

The research set forth in this report was partially supported by the United States Coast Guard through a contract with Wilson Industries, Houston and through a sub-contract with Texas A&M University, and by the National Science Foundation Sea Grant Program, Institutional Grant GH-59 to Texas A&M University.

TABLE OF CONTENTS

LIST OF TABLES

LIST OF FIGURES

LIST OF FIGURES (Continued)

CHAPTER I

INTRODUCTION

The economical and ecological impact of recent at-sea oil spill incidents has created an engineering requirement to design and deploy containment systems capable of retaining large volumes of oil. As a result of this requirement, a study was begun to develop theoretical and empirical expressions describing the interactions of wind, water and oil.

The primary objective of this research is to study set-up of oil by wind and to experimentally verify equations which describe the interaction of a wind, oil and water system. The utilization of these equations allows predictions of the two-dimensional set-up of oil on the water surface when subjected to a steady and uniform wind. From this, it is possible to make engineering estimates for the design of containment devices required to limit the spread of oil on water.

Much work has been done regarding the prediction of water set-up by wind, both in confined bodies of water and in the open ocean. As a result of these efforts, and by utilizing some of the theoretical and experimental considerations developed in these studies, it is possible to extend the theory to include the case of

---

The citations on the following pages follow the style of the Journal of the Hydraulic Division, Proceedings of the American Society of Civil Engineers.

oil floating on water.

The experiments utilized three different oils ranging in specific gravity from 0.85 to 0.91, and kinematic viscosity from 4.3 to 388 centipoise. The viscosity was varied to determine the oil set-up dependence on the Reynolds number. By using a a densimetric Froude Number, based on the density ratio of the and water, the relationship between oil set-up, fetch, wind speed and oil density was established.

CHAPTER II

LITERATURE REVIEW

No previously published work has been found regarding the study of oil set-up on water by wind. Set-up of oil will be defined as the observed increase in oil thickness, floating on the water's surface at the windward side of a barrier, at the leeward end of an oil fetch.

Keulegan (1) studied wind set-up of water in a closed uniform rectangular cross section laboratory flume, 11.21 in. deep, 4.45 in. wide and approximately 65 ft long. Water depths varied from 0.79 in. to 5.72 in. and the cross sectional average wind velocity ranged up to 40 ft per sec. Set-up of the water surface was measured at various wind velocities with the water surface smooth and with wind generated waves. He determined that when sugar was added (thus increasing water viscosity and density) the set-up varied directly as the square of the wind speed, U and was inversely proportional to the water depth h,

$$S \alpha \frac{U^2}{h} \quad \ldots\ldots\ldots\ldots\ldots\ldots \quad (1)$$

Keulegan's studies give insight into the relationship between wind velocity, fluid surface condition and resulting surface shear stress. This is particularly significant for fluids of different viscosity as will be the case when considering the set-up of oil.

By treating Eq. 1 as a dimensionless quantity,

$$\frac{S}{L} = \frac{AU^2}{gh} \quad \ldots\ldots\ldots\ldots \quad (2)$$

where A is an experimentally determined constant having the value, $A = 3.3 \times 10^{-6}$, L is the water fetch length, and g is gravity, Keulegan showed that this relationship described the set-up of water by wind when no waves were generated on the water's surface.

In this work, Keulegan made many correlations to see if a relationship existed between the air and water surface velocities, as affected by water depth and viscosity. He established the dimensionless relationship,

$$\frac{u_s}{U} = f\left(\frac{u_s h}{\nu}\right) \quad \ldots\ldots\ldots\ldots \quad (3)$$

where u_s is the water surface velocity and ν is the water kinematic viscosity. Through a series of tests with varied water depth and viscosity, and without producing waves, he showed that at Reynolds number greater than 1000, the ratio of the two velocities approached a constant value. This indicated that the effects of kinematic viscosity and depth were negligible. It was further shown that the ratio of velocities was constant regardless of the water surface condition, i.e., regardless of the presence of waves. Further, Keulegan showed that the constant relating the dimensionless quantities in Eq. 3 was a coefficient equal to 7.6×10^{-4} for small Reynolds numbers. Above Reynolds number of 1000, the ratio

of the two velocities reached a limiting value of $u_s/U = 0.333$. In addition, Keulegan inferred from his data that this relationship held when the wind velocities or water viscosity were of such value as to produce waves.

A relationship was developed wherein the coefficient, A, of Eq. 2 was expressed in terms of wind velocity instead of the liquid surface velocity. This surface coefficient is also independent of Reynolds number and has the value of 3.35×10^{-6}. Using this surface coefficient, Keulegan developed an equation for surface shear stress, T_s,

$$T_s = \frac{0.0037 \rho_a U^2}{2} \quad \ldots\ldots\ldots \quad (4)$$

where ρ_a is the density of air. The coefficient 0.0037 is very close to the accepted values of C_d (drag coefficient) for air flow across a smooth flat plate. From Eq. 4, Keulegan developed,

$$\frac{dS}{dx} = \frac{nT_s}{\rho_w g h} \quad \ldots\ldots\ldots \quad (5)$$

where $\frac{dS}{dx}$ is the surface gradient, ρ_w is the density of water, n is the flow form constant, and T_s is the shear stress. This says the shear stress, acting on the water's surface, produces the resulting gradient. By substituting Eq. 4 into 5,

$$\frac{dS}{dx} = 0.0037n \frac{\rho_a}{\rho_w} \frac{U^2}{2gh} \quad (6)$$

it can be seen

$$\frac{S}{x} = f\left(\frac{\rho_a}{\rho_w}, \frac{U}{\sqrt{gh}}\right) \quad \ldots\ldots\ldots\ldots \quad (7)$$

which is basically the same dimensionless form shown in Eq. 2.

Keulegan's experiments, conducted for set-up of water in the presence of waves, indicated that there are two relationships which governed the total set-up, S,

$$S = S_1 + S_2 \quad \ldots\ldots\ldots \quad (8)$$

S_1 is expressed by Eq. 2 and is that part of the set-up caused by the surface friction between the wind and the fluid, and S_2 is that set-up caused by waves. He found that as the wind velocity was increased, waves were generated (for a given fluid viscosity) when the velocity exceeded a certain value. At that point, there was a marked increase in the set-up. He reasoned that

$$\frac{S_2}{L} = f\left(\frac{U}{\sqrt{gh}}, \frac{U_o}{\sqrt{gh}}, \frac{\rho_a}{\rho_w}, \frac{h}{L}\right) \quad \ldots\ldots \quad (9)$$

and when added to the set-up due to skin friction,

$$\frac{S}{L} = \frac{AU^2}{gh} + \frac{B(U - U_o)^2}{gh} \times (h/L)^{1/2} \quad (10)$$

where the constants $A = 3.3 \times 10^{-6}$, $B = 2.08 \times 10^{-4}$ and U_o is defined as the formula characteristic (to a particular fluid) velocity at which wave generation occurs. By analyzing S_2 for liquids of various viscosities and plotting S_2 versus wind velocity, a family of curves was generated, each of which re-

presents the viscosity of a liquid. However, what was shown to be significant, was that the slope of the family of lines was nearly the same, thus indicating that the constant B, in Eq. 10, is unaffected by viscosity. In summary, Keulegan said that the only effect of the increase in viscosity of a liquid was to increase the formula characteristic velocity, U_o of Eq. 11. The result of this therefore, is to increase the total set-up observed for a given wind when the kinematic viscosity of the liquid is decreased.

By observing the beginning of wave formation, Keulegan attempted to determine a critical velocity, U_c at which waves were generated. He found the relationship to be,

$$U_c = 16.2\left(\frac{g\rho_w\nu}{\rho_a}\right)^{1/3} \quad \ldots\ldots\ldots \quad (11)$$

In relating this critical velocity to the formula characteristic velocity, U_o, he showed,

$$U_o = 21.0\left(\frac{g\rho_w\nu}{\rho_a}\right)^{1/3} \quad \ldots\ldots\ldots \quad (12)$$

which verifies the previous statement that total set-up is a function of two forms of set-up, one independent of, and the other dependent on the liquid's viscosity.

Van Dorn (2) conducted tests to determine the set-up of water by wind in an 800-ft model-yacht pond. His tests were modeled closely after the studies conducted by Keulegan in the 60-ft laboratory channel as discussed above. In his paper, Van Dorn

proposed equations similar to Eq. 10 for set-up caused by surface friction and by waves. Essentially Van Dorn proposed that the set-up due to waves was,

$$S_1 = \frac{L\alpha^2}{gh} \quad \text{and} \quad S_2 = \frac{L\beta^2}{gh} \quad . \quad . \quad . \quad . \quad . \quad (13)$$

where α and β are empirical wind stress parameters for water surface without and with waves respectively. In evaluating α, β, and $V_{critical}$, Van Dorn was able to reach agreement between his work, under field conditions, and those obtained by Keulegan in the laboratory. This was achieved by selecting the elevations above the pond at which to measure the wind velocity.

Van Dorn could see no physical change in the water's surface when the critical velocity was reached. However, by comparing his results with those of Keulegan, he concluded that the water surface velocity both in the laboratory and in the open pond were equal when the critical wind velocity was reached in either case. From this he concluded that the surface stress is dependent on a "specific" value of the surface current and is therefore independent of scale.

In looking only at wind stress over smooth water, Van Dorn showed that,

$$\tau_s = \gamma^2 \rho_a U^2 \quad . \quad . \quad . \quad . \quad . \quad . \quad . \quad . \quad . \quad . \quad (14)$$

where $\gamma^2 = (\rho_w/\rho_a)\ \alpha^2$. Using a value of α^2, taken at an elevation of 25 cm, the elevation at which closest agreement was reached

with Keulegan's data, it was shown that $\gamma^2 = 0.0037$ and therefore

$$T_s = 3.7 \times 10^{-3} \rho_a U^2 \quad \ldots\ldots\ldots \quad (15)$$

This coefficient, determined from field data, is the same as the one in Eq. 5 as developed by Keulegan.

Qualitative observations were made by Van Dorn to support his relationship for total stress when the water surface was rough. He proposed

$$T_s = \rho_w \alpha^2 U^2 + \rho_w \beta^2 (U - U_c)^2 \quad \ldots\ldots \quad (16)$$

which is a combination of the stresses developed for water that is smooth and rough and is similar to the Eq. 10 and 13, the former developed by Keulegan. Van Dorn's observations were that the water surface current was not decreased when soap was added to reduce wave action. In addition, when there was soap on the surface, a very sharp velocity gradient existed from the surface, below which there was a low speed area of motion which was steady and horizontal. With waves however, the water moved in typical orbital motion with a mean horizontal velocity that was roughly independent of depth. His conclusion was that the waves themselves, caused by the wind, increased the transport, thus the set-up of the water with waves was greater than the set-up without waves.

Van Dorn also attempted to measure bottom stress by use of a pressure disc roughened to approximate the bottom roughness of the pond. Bottom stress measurements were recorded for a wide

range of wind speeds, up to 10 m/sec, and no stress was recorded. The lower value for measurement of stress. as limited by the instrument used, was 0.1 dynes/cm^2 and it was concluded that the bottom stress was negligible when compared to the magnitude of surface stress.

Wilson (3) made a correlation of drag coefficients for set-up by wind for work that had been done prior to 1960. Through the use of the Karman-Prandtl equation for vertical velocity distribution, he achieved values for a drag coefficient which were related to a common height above the water's surface.

Using the results of Keulegan (1), which indicated the need for considering set-up as a combination of events resulting from surface friction and waves, Wilson indicated that the surface stress T_s was,

$$T_s = k \rho_w U^2 \quad \ldots\ldots\ldots\ldots \quad (17)$$

in which k is a constant. Neglecting bottom friction, the set-up should then be,

$$\frac{S}{L} \simeq \frac{kU^2}{gh} \quad \ldots\ldots\ldots\ldots \quad (18)$$

at low wind speeds.

Using Eq. 10, Wilson wrote,

$$\frac{S}{L} = \left[A + B\left(1 - \frac{U_c}{U}\right)^2 \left(\frac{h}{L}\right)^{1/2}\right] \frac{U^2}{gh} \quad \ldots\ldots \quad (19)$$

in which

$$k = \left[A + B\left(1 - \frac{U_c}{U}\right)^2 \left(\frac{h}{L}\right)^{1/2}\right] \quad \ldots\ldots\ldots \quad (20)$$

As the drag coefficient C_d equals $k(\rho_w/\rho_a)$, and using h/L between 0.0021 and 0.0076, $\rho_w/\rho_a = 8.51 \times 10^2$ (at 20°C and 1013 mb pressure), and Keulegan's values for A and B, Wilson found

$$C_d = 2.81 \times 10^{-3} + (8.15 \text{ to } 15.2) \times 10^{-3} \left(1 - \frac{U_o}{U}\right)^2. \quad (21)$$

Using the Karman-Prandtl relationship,

$$\frac{U}{U_*} = \left(\frac{1}{k_o}\right) \ln \frac{z}{z_o} \quad (22)$$

where U is the wind speed at z, U_* is the shear velocity defined as $\sqrt{\tau_s/\rho_a}$, k_o is the Karman constant taken as 0.40, and z_o is the equivalent roughness height at which the logarithmic velocity profile is zero for a stationary surface, Wilson states,

$$U_* = U\sqrt{C_d} \quad (23)$$

and, therefore,

$$C_d^{-1/2} = \frac{U}{U_*} = 2.5 \ln \frac{z}{z_o} \quad (24)$$

The purpose of Wilson's work was to relate values of C_d for various elevations. Assuming there was a relationship for C_d at z_o, z_1, z_2, etc., he concluded that

$$[C_d]_{z_2}^{-1/2} - [C_d]_{z_1}^{-1/2} = 2.5 \ln \frac{z_2}{z_1} \quad (25)$$

or

$$[C_d]_{z_2}^{-1/2} = 2.5 \ln \frac{z_2}{z_1} + [C_d]_{z_1}^{-1/2} \quad (26)$$

Assuming that Keulegan took his measurements at 10 cm, Wilson

developed,

$$(C_d)_{10m}^{-1/2} = (C_d)_{0.1m}^{-1/2} + 11.5 \quad . \quad . \quad . \quad . \quad (27)$$

Then, using Keulegan's results and calculating for prototype conditions, i.e. surface wind speeds taken at 10 meters, Wilson found, for low wind speeds,

$$(C_d)_{10m} = 1.1 \times 10^{-3} \quad . \quad . \quad . \quad . \quad . \quad . \quad . \quad (28)$$

and for high wind speeds,

$$(C_d)_{10m} = 2.2 \text{ to } 2.8 \times 10^{-3} \quad . \quad . \quad . \quad . \quad (29)$$

Wilson then used Eq. 26 to calculate values for C_d for all experimental work done prior to 1960 and relate them to a specific elevation, i.e. 10 meters. The results of his work were that for light winds, $C_d = 1.49 \times 10^{-3}$, with a standard deviation of 0.86×10^{-3}. For strong winds, $C_d = 2.37 \times 10^{-3}$ with a standard deviation of 0.56×10^{-3}. In addition, he concluded that between light and strong winds, C_d increases from about 1.5×10^{-3} to 2.4×10^{-3} in a non-linear fashion, becoming asymptotic for very high velocities.

Reid and Bodine (4), in their prediction of storm surge in Galveston Bay, utilized the drag coefficients presented by Van Dorn (3), in calculating wind stress components. Utilizing an air density to water density ratio of 1.2×10^{-3} and a resistance (C_d) coefficient of 3.0×10^{-3}, they calculated $k = 3.6 \times 10^{-6}$, which they used as an upper limit for high wind speeds.

Using data from Hurricane Carla to calibrate their method of predicting surge, the computed surge was found to be in close agreement with the actual record of water levels in the Galveston Bay area during the storm.

Bretschneider (5), recommended using a value of $k = 3.3 \times 10^{-6}$ for a wind stress coefficient in predicting wind set-up by a synthetic hurricane in Corpus Christi Bay. This value was derived from

$$k = (1 + \frac{T_b}{T_s}) \times 3.0 \times 10^{-6} = 3.3 \times 10^{-6} \quad . \quad . \quad . \quad (30)$$

where $T_b/T_s = 0.1$, taken from Saville's (6) studies at Lake Okeechobee, and T_b is the bottom stress and T_s is surface stress. The dimensionless coefficient, 3.0×10^{-6} was also determined experimentally by Saville (6) in his work at Lake Okeechobee.

When Bretschneider used the value of $k = 3.0 \times 10^{-6}$ to determine a predicted wind set-up at Port Aransas, the predicted value was close to the observed values obtained by calibration of his method using Hurricane Carla. Bretschneider indicated that the variation in the values of k depended on the type of bottom conditions and water depth encountered at the area of interest.

Another approach to determine the shear stress of wind over a moving surface is that taken by experimenters in studying movement of sand by wind. Belly (7) in his work on "Sand Movement by Wind" utilized the Karman-Prandtl relationship to determine the shear stress required for sand motion by wind action. Taking

a value of 0.40 for k the Karman constant, the Karman equation was expressed as

$$\frac{U}{U_*} = 5.75 \log \frac{z}{z_o} \quad \ldots\ldots\ldots \quad (31)$$

where z_o is a roughness factor associated with the sand grain diameter.

When Belly plotted wind velocity profiles versus z on semi-log paper, the velocity distributions remained as straight lines and met at a common point or "focus". The height of the focus, z_o was described as a function of the surface roughness and sand grain diameter.

In an earlier work, Horikawa and Shen (8) used the same relationship and achieved similar results. They made the point that the Prandtl equation holds good when wind conditions do not create sand motion. When the wind becomes strong enough to cause motion, the profile of the wind is changed, which causes the distribution to concentrate at the "focus" or focal point. They said that to express this, the Karman equation should be stated, as originally attributed to Bagnold (9), as follows,

$$U = U_* \; 5.75 \log \frac{z}{z'} + U' \quad \ldots\ldots\ldots \quad (32)$$

in which z' and U' describe the conditions at the focal point.

Using their techniques, by plotting the wind velocity profile on semi-log paper it is possible to determine the value for U_*, for a given wind speed and surface condition. As $U_* = \sqrt{\tau_s/\rho_a}$, it is

possible to determine values for the surface shear stress. Recalling that Keulegan used the surface shear stress τ_s = constant x $\rho_a U^2$, (Eq. 4), and that the constant he found was very nearly that for C_d, the drag coefficient associated with air across a smooth flat plate, it follows that it is possible to determine C_d for any surface condition by measuring and plotting the wind velocity profile.

From the foregoing, it can be seen that the use of a similar wind stress coefficient has predominated. Additionally, there are means for relating meaningful stress coefficients to any height, at which wind measurements could be taken. From this work accurate prediction of wind set-up of water has been achieved. Further, by relating all the data for stress coefficients to a similar point of measurement of wind velocity, a form of universal constant becomes evident. The developed constants therefore give confidence for their use in predicting the set-up of oil on water.

CHAPTER III

THEORETICAL CONSIDERATIONS

The theoretical relationships required to describe the effects of wind stress and the subsequent set-up of oil against a barrier can be developed in several ways. One method involves use of the Navier-Stokes equations of motion. A similar but less sophisticated approach involves the use of a control volume of oil and water on which a two-dimensional summation of horizontal forces can be conducted. A third, and more general method, requires dimensional analysis of the significant parameters in an air-oil-water system. Each of these developments will be summarized here, along with the assumptions required to make solution of the problem more tenable.

Equations of Motion

The Navier-Stokes equations for an incompressible Newtonian fluid (an oil in this case), with non-varying density and viscosity, in a uniform gravitational field, assuming two-dimensional flow, can be written

$$\rho_o g_x - \frac{\partial P}{\partial x} + \mu_o\left[\frac{\partial^2 u}{\partial x^2} + \frac{\partial^2 u}{\partial z^2}\right] = \rho_o a_x \quad . \quad . \quad . \quad . \quad . \quad (33)$$

$$\rho_o g_z - \frac{\partial P}{\partial z} + \mu_o\left[\frac{\partial^2 w}{\partial x^2} + \frac{\partial^2 w}{\partial z^2}\right] = \rho_o a_z \quad . \quad . \quad . \quad . \quad . \quad (34)$$

where:

μ_o = the oil viscosity,

P = fluid pressure,

u, w = fluid velocities in the x - and z - directions,

a_x, a_z = the total fluid accelerations in the x - and z - directions, and

g_x, g_z = gravity constant in the x - and z - directions.

For the case of oil floating on water, it us assumed that steady state conditions will exist.

Because of the low liquid velocities which exist when steady state is established, the convective acceleration terms can also be neglected. Hence,

$$a_x = \frac{\partial u}{\partial t} + u \frac{\partial u}{\partial x} + w \frac{\partial u}{\partial z} = 0 \quad \ldots\ldots \quad (35)$$

and

$$a_z = \frac{\partial w}{\partial t} + u \frac{\partial w}{\partial x} + w \frac{\partial u}{\partial z} = 0 \quad \ldots\ldots \quad (36)$$

Eq. 33 and 34 can now be written,

$$\rho_o g_x - \frac{\partial P}{\partial x} + \mu_o \left[\frac{\partial^2 u}{\partial x^2} + \frac{\partial^2 u}{\partial z^2}\right] = 0 \quad \ldots\ldots \quad (37)$$

$$\rho_o g_z - \frac{\partial P}{\partial z} + \mu_o \left[\frac{\partial^2 w}{\partial x^2} + \frac{\partial^2 w}{\partial z^2}\right] = 0 \quad \ldots\ldots \quad (38)$$

The surface curvature and displacement will be small when the oil is set-up against the barrier. It is assumed that w=0, therefore,

$$\frac{\partial w}{\partial x} = 0 \quad \ldots\ldots\ldots\ldots \quad (39)$$

and

$$\frac{\partial w}{\partial z} = 0 \quad \ldots\ldots\ldots\ldots \quad (40)$$

and Eq. 38 becomes

$$g_z = \frac{\partial P}{\partial z}\frac{1}{\rho_o} \quad \ldots\ldots\ldots\ldots \quad (41)$$

As uniform conditions exist, and thus

$$\frac{\partial u}{\partial x} = 0 \quad \ldots\ldots\ldots\ldots \quad (42)$$

and the last term in Eq. 37 becomes

$$\mu_o\left[\frac{\partial^2 u}{\partial z^2}\right] = \frac{\partial}{\partial z}\left[\mu_o\left(\frac{\partial u}{\partial z}\right)\right] \quad \ldots\ldots\ldots \quad (43)$$

As,

$$T = \mu_o\left(\frac{\partial u}{\partial z}\right)$$

where T is the shear stress in the fluid, Eq. 37 can be written

$$\rho_o\, g_x - \frac{\partial P}{\partial x} - \frac{\partial T}{\partial z} = 0 \quad \ldots\ldots\ldots \quad (44)$$

Assuming the system is a horizontal plane, g_x is zero. Therefore,

$$-\frac{\partial P}{\partial x} + \frac{\partial T}{\partial z} = 0 \quad \ldots\ldots\ldots\ldots \quad (45)$$

Integrating Eq. 41 between $z = 0$ and $z = d_{ox}$ (the oil depth) at x,

$$P = \rho_o\, g_z\, d_{ox} \quad \ldots\ldots\ldots\ldots \quad (46)$$

Substituting into Eq. 45, yields

$$-\rho_o \, g_z \frac{\partial d_{ox}}{\partial x} + \frac{\partial T}{\partial z} = 0$$

or,

$$\frac{\partial d_{ox}}{\partial x} = \frac{1}{\rho_o g} \frac{\partial T}{\partial z} \quad \ldots\ldots\ldots\ldots\ldots (47)$$

Multiplying both sides by ∂z, and again integrating with respect to z, between 0 and d_o, the result is,

$$(\frac{\partial d_o}{\partial x}) d_o = \frac{1}{\rho_o g} (T_{d_o} - T_o) \quad \ldots\ldots\ldots (48)$$

As $\partial d_o / \partial x$ is the ratio of the change in the oil depth to the length along the oil fetch, and T can be expressed in terms of, $T = (T_s + T_b)$, where it is assumed (as before) $T_b << T_s$, T_o can be neglected from Eq. 48. Eq. 48 can now be integrated to yield

$$(\frac{d_o}{2L}) d_o = \frac{T_s}{\rho_o g} \quad \ldots\ldots\ldots\ldots (49)$$

where T_s is independent of x.

The surface shear stress can be written

$$T_s = C \, \rho_a \, U^2 \quad \ldots\ldots\ldots\ldots (50)$$

where C is the wind stress coefficient. Substituting

$$\frac{d_o^2}{2L} = \frac{C \, \rho_a \, U^2}{\rho_o g} \quad \ldots\ldots\ldots\ldots (51)$$

and dividing by the oil fetch length L,

$$\frac{d_o^2}{L^2} = \frac{2C \, \rho_a \, U^2}{\rho_o \, gL}$$

or

$$\frac{d_o}{L} = \left[\frac{2C\ \rho_a\ U^2}{\rho_o\ gL}\right]^{1/2} \quad \ldots\ldots\ldots\ldots (52)$$

Considering the air-oil-water system, it is correct to replace the gravity term with a densimetric gravity based on the ratio of the buoyant force to the unit mass of the oil, expressed as

$$g' = g\left(1 - \frac{\rho_o}{\rho_w}\right) \quad \ldots\ldots\ldots\ldots (53)$$

and substituting, where,

$$C' = \frac{\rho_a}{\rho_w} C$$

or

$$C = C' \frac{\rho_w}{\rho_a} \quad \ldots\ldots\ldots\ldots (54)$$

$$\frac{d_o}{L} = \left[\frac{2C'\rho_w}{\rho_o}\right]^{1/2} x \frac{U}{\sqrt{g'L}} \quad \ldots\ldots\ldots (55)$$

This expression says that,

$$\frac{d_o}{L} = f\left(\frac{U}{\sqrt{g'L}}\right) \quad \ldots\ldots\ldots\ldots (56)$$

To determine the functional relationship, it is necessary to determine the set-up of oil d_o, for a given oil length L, and wind speed U, and express them as described above.

Control Volume

Dr. R. M. Sorensen of Texas A&M University developed the following simplified approach for predicting the wind set-up of oil against a barrier. His development was part of the research conducted by Texas A&M University while under contract to the U.S. Coast Guard for the development of an oil containment system during the period December 1969 to June 1970.

Referring to Fig. 1, assume an oil-water system as shown, which represent a two-dimensional control volume. A summation of the forces acting on the volume may be accomplished in the x - direction.

The previous assumptions can be applied, and the acceleration terms either neglected or assumed to be zero. The resulting equation is

$$\Sigma F_x = F_w + (T_s + T_b)L - F_o = 0 \quad \ldots\ldots (57)$$

where:

F_w = force on the left of the control volume

F_o = the force on the right and,

L = oil fetch length.

At the barrier, it can be seen from hydrostatics that,

$$g\, d_o\, \rho_o = g\, d_w\, \rho_w$$

or

$$d_w = d_o \frac{\rho_o}{\rho_w} \quad \ldots\ldots\ldots\ldots (58)$$

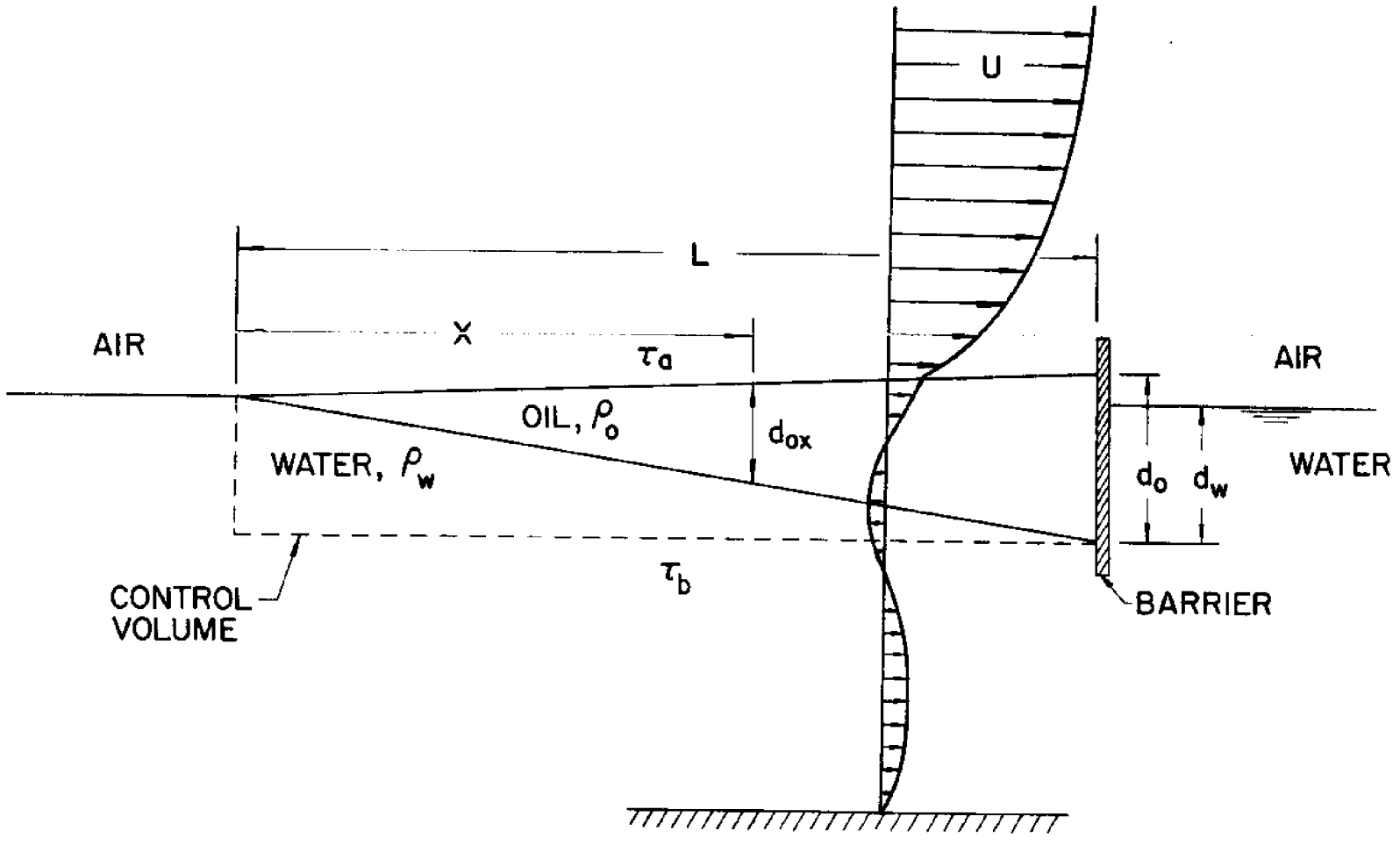

FIG. 1 - SCHEMATIC, TWO-DIMENSIONAL WEDGE OF FLOATING OIL

where:

d_o = oil depth

d_w = water depth to the bottom of the oil wedge

ρ_o = oil mass density

Note, that the increase in the surface level at the barrier is $d_o - d_w$ and from Eq. 58, the increase is $d_o - d_o(\rho_o/\rho_w) = d_o(1 - \rho_o/\rho_w)$.

Assuming that

$$T_s + T_b = K\, T_s,$$

where K is a numerical constant, and as before, $T_b << T_s$, it follows directly that,

$$K \simeq 1.0 \quad . \quad . \quad . \quad . \quad . \quad . \quad . \quad . \quad . \quad . \quad . \quad . \quad (59)$$

Keulegan (1), Van Dorn (2), and Bretschneider (5) have shown that the bottom stress is considerably less than the surface stress and, as before, is negligible.

Assuming a unit width for the control volume, the forces acting are,

$$F_w = 1/2(\rho_w g\, d_w^2) \quad . \quad . \quad . \quad . \quad . \quad . \quad . \quad . \quad . \quad . \quad . \quad (60)$$

and

$$F_o = 1/2(\rho_o g\, d_o^2) \quad . \quad . \quad . \quad . \quad . \quad . \quad . \quad . \quad . \quad . \quad . \quad . \quad (61)$$

Substituting into Eq. 57 yields,

$$1/2(\rho_w g\, d_w^2) + K\, T_s\, L - 1/2(\rho_o g\, d_o^2) = 0 \quad . \quad . \quad . (62)$$

and using $T_s = C\, \rho_w\, U^2$, $d_w = d_o\, \rho_o/\rho_w$ and rearranging,

$$d_o = \left[\frac{2KC\, \rho_w\, U^2 L}{\rho_o g(1 - \frac{\rho_o}{\rho_w})}\right]^{1/2} \quad . \quad . \quad . \quad . \quad . \quad . \quad . \quad (63)$$

Since $g' = g(1 - \rho_o/\rho_w)$, this becomes,

$$\frac{d_o}{L} = [2KC \frac{\rho_w}{\rho_o}]^{1/2} \frac{U}{\sqrt{g'L}} \quad . \quad . \quad . \quad . \quad . \quad . \quad . \quad (64)$$

which is the same as Eq. 55. As before, plotting the dimensionless terms d_o/L versus $U/\sqrt{g'L}$ will result in a curve which allows evaluation of the wind stress coefficient, C.

The relationship developed is independent of fluid viscosity and is therefore independent of Reynolds number. It is believed, however, that Reynolds number and hence, fluid viscosity play an important role in the development of waves in the liquid. If waves are developed, the set-up can be expressed as a two-part phenomenon. The set-up will occur due to wind stress on the liquid surface and because of the transport phenomenon in the wind generated waves. The total oil set-up can then be expressed,

$$d_{o_t} = d_o + d_{o_w} \quad . \quad . \quad . \quad . \quad . \quad . \quad . \quad . \quad . \quad (65)$$

where:

d_{o_t} = the total oil set-up

d_{o_w} = the set-up due to waves.

It is believed that d_{o_w} can be expressed similarly to d_c or,

$$d_{o_w} = [\frac{2BL}{g'} \frac{\rho_w}{\rho_o}]^{1/2} (U - U_c) \quad \ldots\ldots \quad (66)$$

where B is a numerical constant which relates the viscosity of the fluid to U_c, the critical wind speed at which waves are generated in the fluid. B will be called the wind-wave stress coefficient.

Rearranging,

$$\frac{d_{o_w}}{(L)^{1/2}} = [\frac{2B}{g'} \frac{\rho_w}{\rho_o}]^{1/2} U - [\frac{2B}{g'} \frac{\rho_w}{\rho_o}]^{1/2} U_c \quad \ldots \quad (67)$$

and taking the derivative of $d_{o_w}/(L)^{1/2}$ with respect to U, or,

$$\frac{d(\frac{d_{o_w}}{(L)^{1/2}})}{dU} = [\frac{2B}{g'} (\frac{\rho_w}{\rho_o})]^{1/2} \quad \ldots\ldots\ldots (68)$$

Plotting the left-hand term should result in a curve (or a straight line if the exponent is correct), the slope of which is the right-hand term. This will allow determination of the constant B.

To determine the value of d_{o_w}, plot the total set-up, d_c, using the relationship expressed by Eq. 64. When the values begin to depart from the curve, expressed by that relationship, it will

be because an additional set-up has occurred, i.e. the waves generated in the liquid have created an additional oil depth. The oil set-up due to waves, d_{o_w} is that depth greater than d_o, or $d_{o_w} = d_{o_t} - d_o$. Using the wind speed, which generated d_{o_t}, and calculating $d_{o_w}/(L)^{1/2}$, L being the fetch length associated with d_{o_t}, Eq. 68 can be plotted.

The equation for the total set-up of oil can now be written,

$$d_{o_t} = \left[\frac{2KC\ \rho_w\ U^2\ L}{\rho_o\ g'}\right]^{1/2} + \left[\frac{2BL\ \rho_w}{g'\rho_o}\right]^{1/2} (U - U_c). \quad (69)$$

where U_c is that wind speed associated with a given oil, at which set-up due to wave motion begins and U_c is determined from the plot of Eq. 68 where $d_{o_w} = 0$.

The set-up of oil can be related to the wind shear velocity, U_*. Substituting the shear stress, $T_s = C\ \rho_w\ U^2$, and the oil density written as

$$\rho_o = G\ \rho_a \quad \ldots\ldots\ldots\ldots \quad (70)$$

where G is a constant, into Eq. 64, for a given oil the result is

$$\frac{d_o}{L} = \sqrt{\frac{2K\ T_s}{G\ \rho_a g'\ L}} \quad \ldots\ldots\ldots\ldots \quad (71)$$

and

$$\frac{d_o}{L} = \frac{\sqrt{\frac{T_s}{\rho_a}}}{\sqrt{g'L}} \sqrt{\frac{2K}{G}} \quad \ldots\ldots\ldots\ldots \quad (72)$$

The shear velocity is expressed

$$U_* = \sqrt{\frac{T_s}{\rho_a}} \quad \ldots\ldots\ldots\ldots \quad (73)$$

therefore,

$$\frac{d_o}{L} = \frac{U_*}{\sqrt{g'L}} \sqrt{\frac{2K}{G}} \quad \ldots\ldots\ldots \quad (74)$$

This is another method of expressing the original development and provides a means for checking the validity of the wind velocity profiles.

Dimensional Analysis

The dimensional analysis of the air-oil-water system encountered in the set-up of oil by wind can be conducted using the following significant variables,

$$d_o = f(L, U, g', \mu_o, \rho_o, \rho_w) \quad \ldots\ldots \quad (75)$$

or

$$f'(d_o, L, U, g', \mu_o, \rho_o, \rho_w) \quad \ldots\ldots \quad (76)$$

if a mass-length-time system is considered, it can be seen there will be $(n' - m) = (7 - 3) = 4\pi$ terms.

Selecting L, U, and ρ_o as repeating variables, Buckingham π dimensional analysis leads to

$$\frac{d_o}{L} = f\left[\frac{UL\rho_o}{\mu_o}, \frac{U}{g'L}, \left(\frac{\rho_w}{\rho_o}\right)^{1/2}\right] \quad \ldots\ldots\ldots \quad (77)$$

This development shows that the oil depth to oil fetch length

ratio is a function of Froude and Reynolds numbers and a ratio of the densities. This is as expected because as was previously stated, the set-up occurs in two phases, i.e. due to wind stress, where the Froude effects are important because of the gravity acting on the less dense (than water) oil, and due to waves creating the additional set-up. The latter phenomenon is a function of Reynolds number (and therefore viscosity). In this case it has been observed that the wind speed at which waves are initiated in the fluid is a function of viscosity and therefore, Reynolds number,

From Eq. 65,

$$d_{o_t} = d_o + d_{o_w}.$$

Eq. 77 can be arranged,

$$d_o + d_{o_w} = f'\left[\frac{UL^2\rho_o}{\mu_o},\ \left(\frac{L}{g'}\right)^{1/2} U, L\left(\frac{\rho_w}{\rho_o}\right)^{1/2}\right] \quad \ldots\ldots (78)$$

When $d_{o_w} = 0$, the result is that

$$d_o = A\left(\frac{\rho_w}{\rho_o}\right)^{1/2} \left(\frac{L}{g'}\right)^{1/2} U \quad \ldots\ldots\ldots (79)$$

if the viscous effects can be neglected when $U < U_c$, and where A is a constant of proportionality. This is similar to Eq. 63, when,

$$A = [2KC]^{1/2} \quad \ldots\ldots\ldots\ldots (80)$$

When $d_o = 0$ and $U > U_c$,

$$d_{o_w} = B'\left(\frac{L}{g'}\right)^{1/2} (U - U_c) \quad \ldots\ldots\ldots (81)$$

where B' is a functional constant of proportionality relating the viscosity μ_o and the critical velocity U_c. Rearranging Eq. 81 and taking the derivative with respect to U,

$$\frac{d\left(\frac{d_{o_w}}{(U)^{1/2}}\right)}{dU} = \frac{B'}{\sqrt{g'}} \left(\frac{\rho_w}{\rho_o}\right)^{1/2} \quad \ldots\ldots\ldots \quad (82)$$

and, if as before,

$$B' = [2B]^{1/2} \quad \ldots\ldots\ldots\ldots \quad (83)$$

the expression is,

$$\frac{d\left(\frac{d_{o_w}}{(L)^{1/2}}\right)}{dU} = \left[\frac{2B\ \rho_w}{\rho_o\ g'}\right]^{1/2} \quad \ldots\ldots\ldots \quad (84)$$

the same as Eq. 68.

The significance of the foregoing discussion is that three approaches can be used resulting in the same expression for oil set-up. This research will then be conducted so as to measure the two-dimensional set-up of oil and to determine the empirical constants, developed above, which relate the dimensionless terms.

The term d_o/L is a dimensionless ratio in which d_{o_x} is used for d_o and x for L. The dimensionless ratio would then be,

$$\frac{d_{ox}}{x} \quad \ldots\ldots\ldots\ldots \quad (85)$$

where the depth of oil at any point d_{ox}, and at any fetch length x, from the beginning of the oil wedge, is defined. This is

possible by treating the cross-section along x as a two-dimensional system and applying the relationships developed herein. Eq. 69 for the total oil set-up could therefore be written,

$$d_{o_x} = \left[\frac{2KC\,\rho_w\,U^2\,X}{\rho_o\,g'}\right]^{1/2} + \left[\frac{2B\,x\,\rho_w}{g'\,\rho_o}\right]^{1/2}(U - U_c) \quad . \quad . \quad . \quad (86)$$

which describes the oil set-up at any point along a two-dimensional cross-section of an oil wedge contained by a barrier.

Eq. 86 indicates that the top and bottom surfaces of the oil wedge are parabolic in shape. For a unit width of oil, the total oil volume V, is,

$$V = \int_0^L d_{o_x}\,dx \quad . \quad . \quad . \quad . \quad . \quad . \quad . \quad (87)$$

or

$$V = 2/3\left[\frac{2KC\,\rho_w\,U^2L^3}{\rho_o\,g'}\right]^{1/2} + \left[\frac{2BL^3\,\rho_w}{\rho_o\,g'}\right]^{1/2}(U - U_c) \quad . \quad (88)$$

Comparing this to Eq. 69, the volume is seen to be,

$$V = 2/3\;d_o\;L \quad . \quad . \quad . \quad . \quad . \quad . \quad . \quad . \quad . \quad . \quad (89)$$

To determine the oil thickness set-up against a barrier requires knowledge of the volume of oil on the water's surface and the geometric shape of the barrier. From this, calculation of the oil depth at any point along the barrier can be accomplished.

CHAPTER IV

EXPERIMENTAL PROCEDURE

Equipment Arrangement

The work for this investigation was conducted in the two-dimensional wind-wave channel located in the Hydromechanics Laboratory at Texas A&M University. The channel is 120 ft long, 3 ft deep and 2 ft wide. The bottom is a flat steel plate welded on a large wide flange section for support above the laboratory concrete floor. The walls of the channel are constructed of 3/8 in. thick glass panels held in place by steel T-sections. The glass panels allow maximum visibility within the tank. The tank is equipped with a pendulum-type wave generator, and a wave absorber constructed of impermeable steel plates faced with perforated aluminum sheets. These latter features were not required for this investigation.

The wave tank was covered by 25 in. x 48 in. plywood sheets. The seams of the plywood sheets were sealed with masking tape to prevent air from entering. One end of the wave tank has a vertically adjustable filtered air intake, which can be lowered to bring air into the tank parallel to any water surface level not more than 18 in. from the top. The other end of the tank terminates at one of the outside walls of the laboratory through which air is removed from the tank by a centrifugal blower located outside

the laboratory building. A general arrangement of the tank is shown in Fig. 2.

It was necessary to construct barriers to contain the oil within a specific section of the wind-wave channel. These barriers were located approximately 75 ft apart. The downwind barrier was about 70 feet from the air intake. The barriers were necessary to insure the volume of oil tested was constant from one run to the next, to minimize the amount of oil getting into the wave absorbers and to insure a sufficient fetch length was available to contain a representative volume of oil. In addition, it was discovered the oil would dissolve the sealant used around the glass panels and, therefore, by containing the oil in a smaller portion of the tank, this risk was minimized. The barriers were constructed of 1/2 in. plywood,backed by an aluminum frame. Soft rubber strips were attached in layers at the ends of the barrier to act as oil seals along the glass walls. The barriers were held in position by 3/4 in. threaded steel rods screwed into nuts welded to the tank bottom. A brace across the tank top secured the rods at the top to allow lateral adjustment. This arrangement allowed the barriers to be fully adjustable vertically and laterally, and it was possible, therefore, to minimize the profile at the downwind barrier and allow it to be of sufficient height to contain the oil set-up.

The downwind barrier had wave absorbers attached to its face

SCHEMATIC - 2' x 3' x 120' WIND AND WAVE CHANNEL

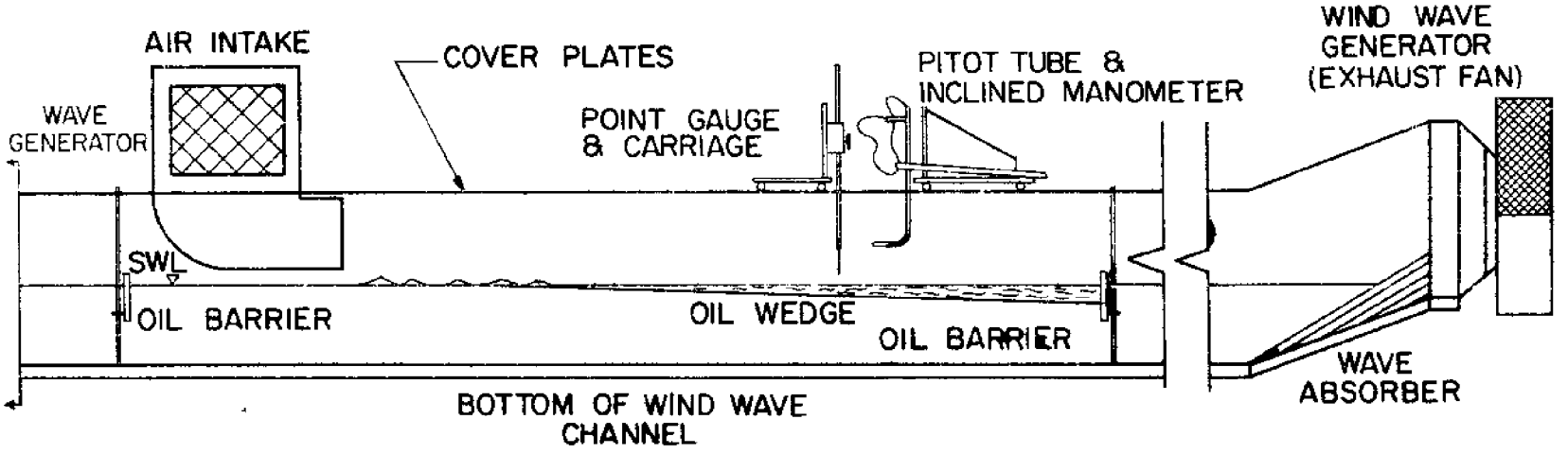

FIG. 2 - EXPERIMENTAL ARRANGEMENT

to minimize wave reflections and thus to prevent standing waves from being established in the oil. The wave absorbers were constructed of wire screen and contained gravel larger than the wire mesh, which provided the wave attenuation desired. The absorbers were made in 1 ft long, triangular-shaped sections, and two were hung on the barrier face after all height adjustment had been made and the barrier secured. The absorbers proved very convenient to work with and were effective to the point that no standing wave was observed throughout the testing, regardless of the wave height generated by the wind.

One inch diameter holes were drilled in the center of the tank covers to allow access of point gauges for measuring the oil thickness. The holes were drilled in the tank covers approximately ten feet apart, along the length of the tank. They extended up wind from the barrier approximately 55 ft. beginning at a point 5 ft upwind of the barrier. The exact location of the holes with respect to the barrier for each set of runs is shown in Table 1.

The wind-wave channel has a steel track mounted along the top of each wall on which there is a rolling carriage. A movable point gauge staff was mounted on the carriage and, for each run, was rolled to a position over each of the holes in the tank top. This permitted measurement of the oil thickness with relative ease and eliminated the need for a fixed reference point at each measurement position.

Table 1 Wind-Wave Tank Arrangement of Stilling Wells (S.W.), Pitot Tube and Oil Barriers (all Distances in Ft.)

	Upwind Barrier	Air Filter and Inlet	Position No. 7	Position No. 6	S.W. No. 5	S.W. No. 4	S.W. No. 3	S.W. No. 2	Pitot Tube	S.W. No. 1	Downwind Barrier
Oil No. 1	76.93	71.96	46.9	47.5	38.1	29.7	20.3	11.9	2.0	2.5	0
Oil No. 2	76.93	71.96	N.A.	N.A.	49.63	36.54	26.5	16.67	3.67	2.33	0
Oil No. 3	76.93	71.96	N.A.	N.A.	46.67	33.63	23.50	13.38	3.67	2.33	0

A fixed point gauge was placed at the position nearest the barrier. This was necessary because the pitot tube (used for wind velocity measurement) was placed just up wind of this position and interfered with the carriage motion.

It was observed that the action of the wind in front of the barrier created a depression in the oil surface and, therefore, the number one position for measuring the oil depth was placed 5 ft up-wind of the barrier.

In order to measure the thickness of the oil wedge, it was found that, for test runs in which waves were generated, it was necessary to construct stilling wells which would dampen the wave motion and produce a still oil level. The stilling basins were construction of 1.5 in. I.D., plexiglas tubing. A series of holes were drilled along a vertical line along the tube at a level which coincided with the oil level in the tank. The stilling tubes were inserted in a short section of pipe welded to steel plates. The plates were used as weights and positioned on the tank bottom under the holes in the tank covers. This arrangement was most satisfactory and, when the tubes filled with water and oil, they gave a means of accurately measuring the oil (and water) levels in the tank. The size of the holes drilled in the tubes was increased in proportion to the oil viscosity to provide the necessary damping of the wave motion. Stilling wells were not required for the tests with the most viscous oil (kinematic viscosity - 388 centistokes).

The thickness of the oil in the stilling wells was measured by the point gauge along the center line of the tank. This measurement was verified by measuring the oil thickness at the side of the tank. This was done with a scale placed on the glass tank wall which permitted a direct reading of the oil thickness. This verification was not possible when waves were generated in the oil as the motion prevented an accurate determination with the ruler.

Because of the surface action of the waves, it was difficult to see when the point gauge was in contact with the oil and oil-water surface in the stilling wells. To facilitate seeing, a strong light was mounted on the point gauge carriage and positioned so that it provided a light shining through the oil. With this arrangement, when the point gauge touched the oil surfaces, the distortion of the surface diffracted the light and thus gave good (and repeatable) indication of the point gauge position. A fixed light was put behind the stilling basin under the fixed point gauge at position number one for the same reasons.

A metal measuring tape secured to the tank cover was used to measure distances along the tank.

Water Conditions

The tank was filled with 18 inches of fresh water during the tests on the first oil. After the water was established at this level, the oil was added in 55 gallon (one drum) increments.

By adjusting the quantity of water in the tank, there was approximately 18 in. total depth at all times.

To lessen the effect of the tank covers on the wind profile during the conduct of the tests on the last two oils, the water and oil level was maintained at 14 in. above the tank bottom.

Oil Conditions

The suggested range of oil fluid properties was predicted by the possibilities of the types of oils that might be encountered by a prototype oil containment system. The suggested (10) range of properties for this investigation were,

Specific gravity: 0.75 ~ 0.95

Absolute viscosity: 1 - 500 centipoise

A search was made to determine which commercially available oils could be obtained easily and in the quantities desired. The three oils used are listed in Table 2.

Each test series consisted of placing one, two or three barrels (55 gallons each) of one of the oils into the wind-wave tank. The still oil depth for each volume was approximately 0.040 ft, 0.090 ft, and 0.140 ft. After each volume of oil was tested, or at the end of a day of testing, an oil sample was taken from the tank and tested for its fluid properties, i.e., density using a calibrated hydrometer, and viscosity using a Saybolt or Furol viscometer. The results of these tests are shown in Table 2, along with the commercial name of the oil.

Table 2 Oil Properties

Test No.	Name	Viscosity, 60°F (Centipoise)	Specific Gravity 60°F
1	Chevron RPM Delo Special	388	0.888
2	Gulf Diesel Oil	3.8	0.858
3	Shell Legion 43	96	0.911

The properties shown are averages of the tests conducted for each volume. Little, if any, variation in the properties of the oil was noted from test to test.

The selection of the test oils was an attempt to cover the range of density and viscosity specified. Although the full range of fluid properties was not covered, the range is considered sufficient to show that the basic equations developed for predicting the oils' behavior have been verified.

Pitot Tube and Manometer

Wind velocities were measured with a pitot tube attached to a movable point gauge staff. The pitot tube was connected with flexible tubing to an inclined air-water manometer. The slope of the manometer was adjusted to 1:48 with a carpenter's level. The manometer was mounted on an adjustable base which allowed securing the base after bringing the manometer to the correct slope prior to commencement of each run.

Calculation of the wind speed for a given deflection of the manometer liquid level utilized Bernoulli's equation.

For each test run, the pitot tube was set a known distance above the surface of the undisturbed oil level and wind velocities were taken at 0.1 ft intervals along a vertical line at the tank centerline. The position of the pitot tube was 5 ft up wind of the down wind oil barrier and directly in front of the oil depth gauge,

position No. 1.

To gain better understanding of the wind patterns that existed in the wind-wave tank, a series of cross-section velocity profiles was taken at the down wind position described above and at positions 25 and 45 ft up wind from the barrier. Similar blower settings were used at each position and isovel patterns were taken for low, medium and high wind velocities. Additional discussion of this procedure will be made later in the chapter and in Chapter V, as the isovel patterns were incorporated in the reduction of wind velocity data to account for the wind patterns and horizontal velocity gradients which existed.

Wind Velocity Determination

The use of an air-water inclined manometer, to measure the pressure differential in the pitot tube, required a means of converting the vertical deflection of the manometer to wind speed. Bernoulli's equations, with elimination of elevation terms (neglected due to relative weight of air to water), is

$$\frac{P_s}{\gamma_a} = \frac{P_o}{\gamma_a} + \frac{U^2}{2g} \quad \ldots\ldots\ldots \quad (90)$$

where:

P_s = the stagnation pressure, in ft of air,

P_o = the free stream pressure, in ft of air,

γ_a = the specific weight of air, and

U = the wind speed in the tank.

The slope, S of the manometer water column is,

$$S = \frac{H}{R \cos \theta} \quad \ldots\ldots\ldots \quad (91)$$

where:

R = horizontal manometer deflection

H = the vertical rise in the water level

θ = the angle whose tangent is 1/48 or = 0.0.

Therefore, $\cos \theta = 1.0$

and we can assume,

$$S = \frac{H}{R}.$$

For our use where the slope was 1:48 we have

$$\frac{H}{R} = \frac{1}{48}$$

or

$$H = \frac{R}{48}.$$

As the differential pressure in the pitot tube is the same as the water column rising the distance H,

$$P_s - P_o = \frac{R}{48} \gamma_w \quad \ldots\ldots\ldots \quad (92)$$

Substituting in to Eq. 90,

$$\frac{R}{48} \gamma_w = \frac{U^2 \gamma_a}{2g} \quad \ldots\ldots\ldots \quad (93)$$

or

$$U = \left(\frac{\gamma_w}{\gamma_a} \frac{2gR}{48}\right)^{1/2} \quad \ldots\ldots\ldots \quad (94)$$

Using $\gamma_w = 1.936$ slugs/ft^3, $\gamma_a = 2.37 \times 10^{-3}$ slugs/ft^3, and

$g = 32.17$ ft/sec^2 and expressing R in inches, the wind velocity, fps, is

$$U = 9.51 \sqrt{R} \quad \ldots\ldots\ldots\ldots \quad (95)$$

This relationship was used through the research to compute the wind velocity, U, in the tank. Care was taken to insure the slope of the manometer remained at 1:48 and to correct R for any initial manometer deflection which existed due to the manometer tubes being tilted out of the same longitudinal plane or due to residual air motion in the tank.

The pitot tube was moved in 0.1 ft increments from the underside of the tank covers to a position as close to the disturbed oil surface level as was possible, depending on the surface condition of the oil. At each incremental position, a manometer deflection was taken and the wind speed calculated. Representative profiles of these readings are shown in Figs. 3, 4 and 5. In addition, complete wind velocity profile data are included in Appendix 1.

To insure that the centerline wind velocity profiles were an accurate representation of the wind creating the surface stress and causing the set-up of oil, it was felt that a correction factor should be applied for it was known that the wind profiles across the tank would not be uniform. This is because the walls of the tank represent a boundary where the wind velocity is zero. Consequently, a gradient must exist. In addition, it was generally

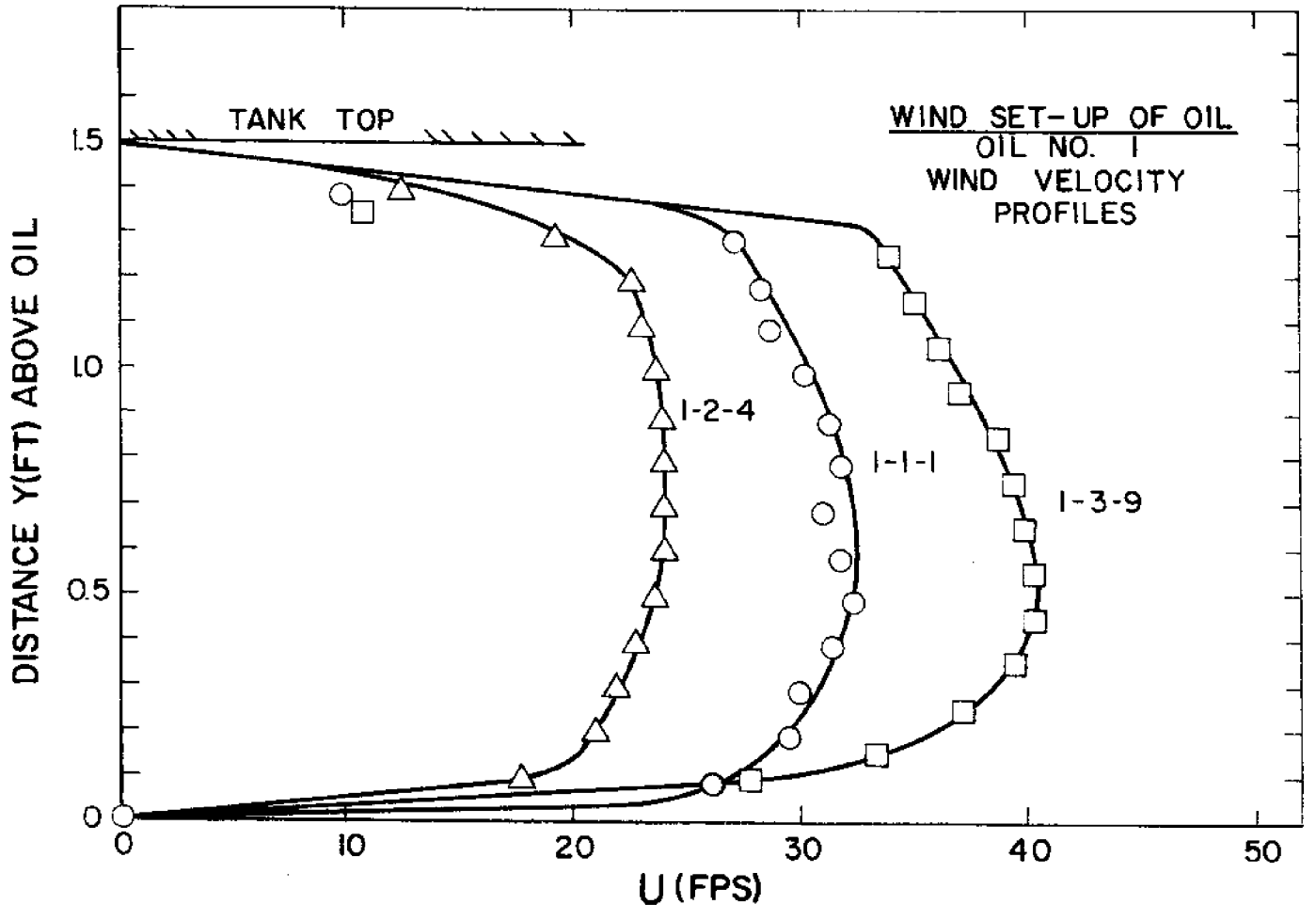

FIG. 3 - WIND VELOCITY PROFILES, OIL NO. 1.

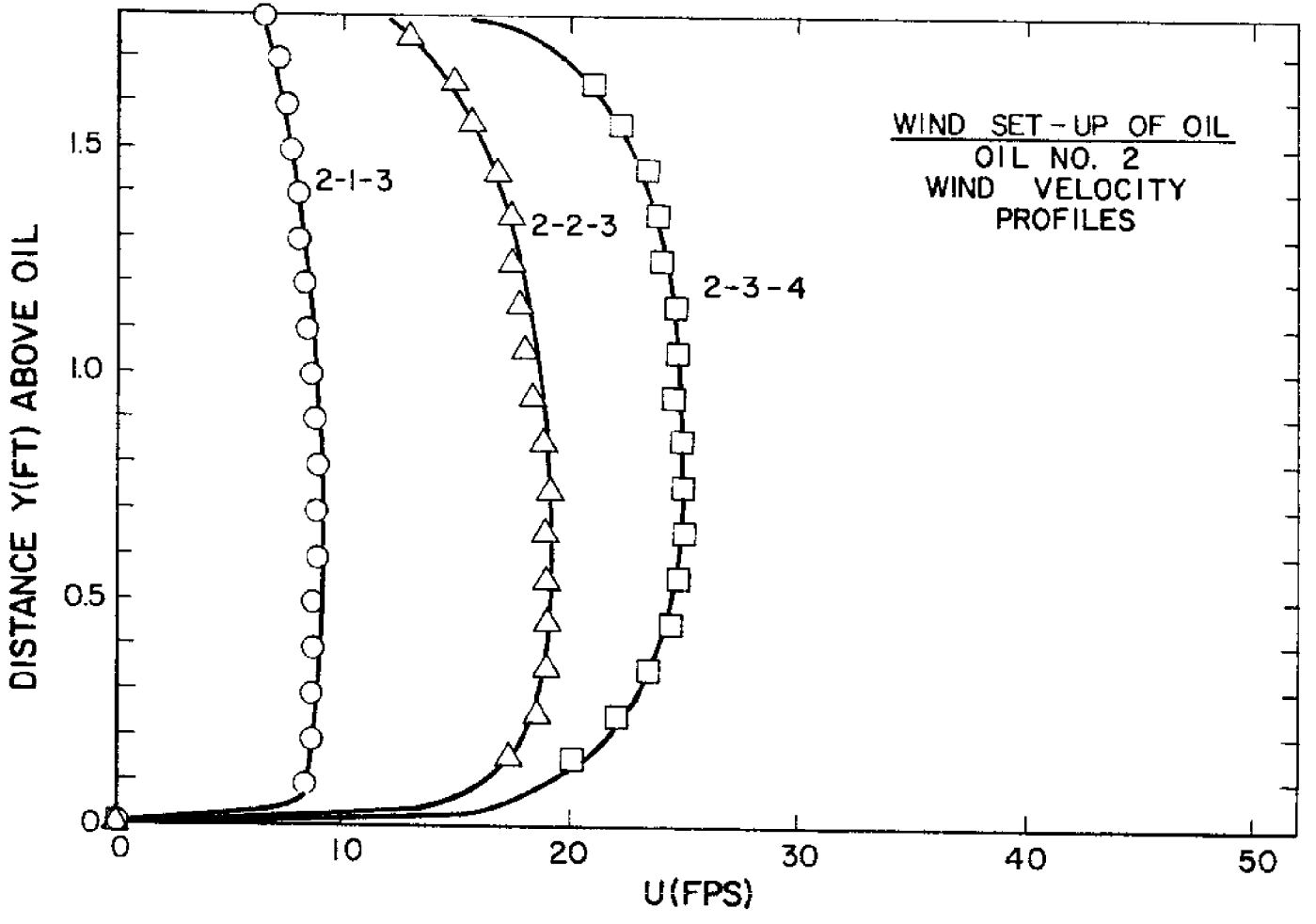

FIG. 4 - WIND VELOCITY PROFILES, OIL NO. 2

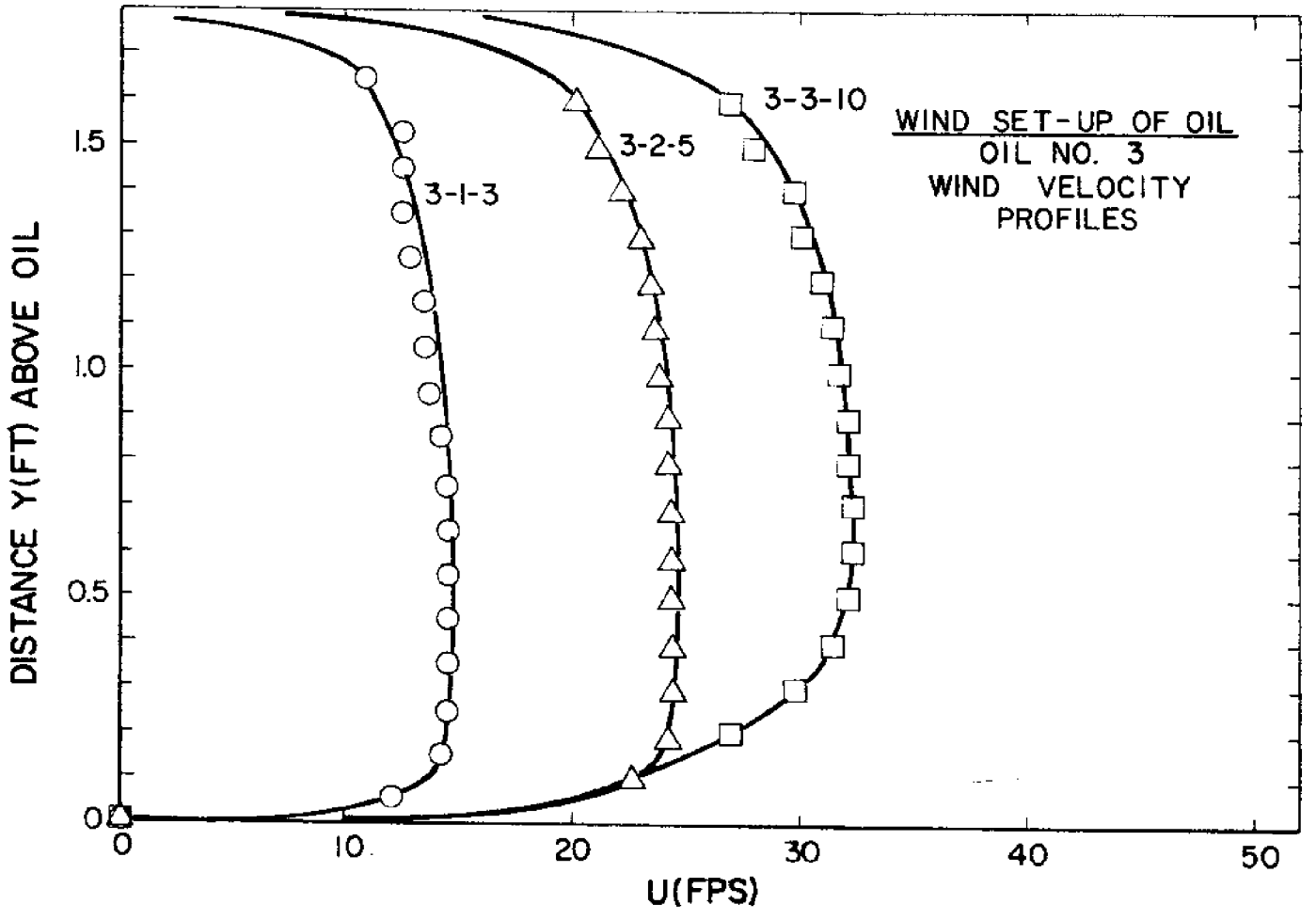

FIG. 5 – WIND VELOCITY PROFILES, OIL NO. 3.

recognized that the ultimate success of this research would depend greatly on the ability to determine the wind speed which created the stress producing the observed oil set-up. A wind profile was provided by the U.S. Coast Guard to be used as a criteria for designing an oil spill containment system. The profile provided the normally accepted relationship for surface boundary layer conditions over water and provided a design wind speed at 10 meters above the water's surface. It was, therefore, necessary to insure the observed wind profiles were representative of the stress causing the oil to set-up against a barrier. Once this stress parameter was determined, use of the Karman-Prandtl relationships would provide the wind speed required to determine anticipated oil set-up.

In a large, open, three-dimensional system, it would be possible to relate directly points on the design profiles and those achieved in the laboratory. However, in a closed system, such as used in this research, it was believed that a correction factor was required.

It was known that boundary layers would occur at the walls and the top of the tank and that the size and shape of these boundary layers would effect the wind stress causing the set-up of the oil. To correct for these boundary layers, isovel patterns were taken at three wind speeds which covered the range of wind velocities used. Examples of the isovels can be seen in Figs. 6 and

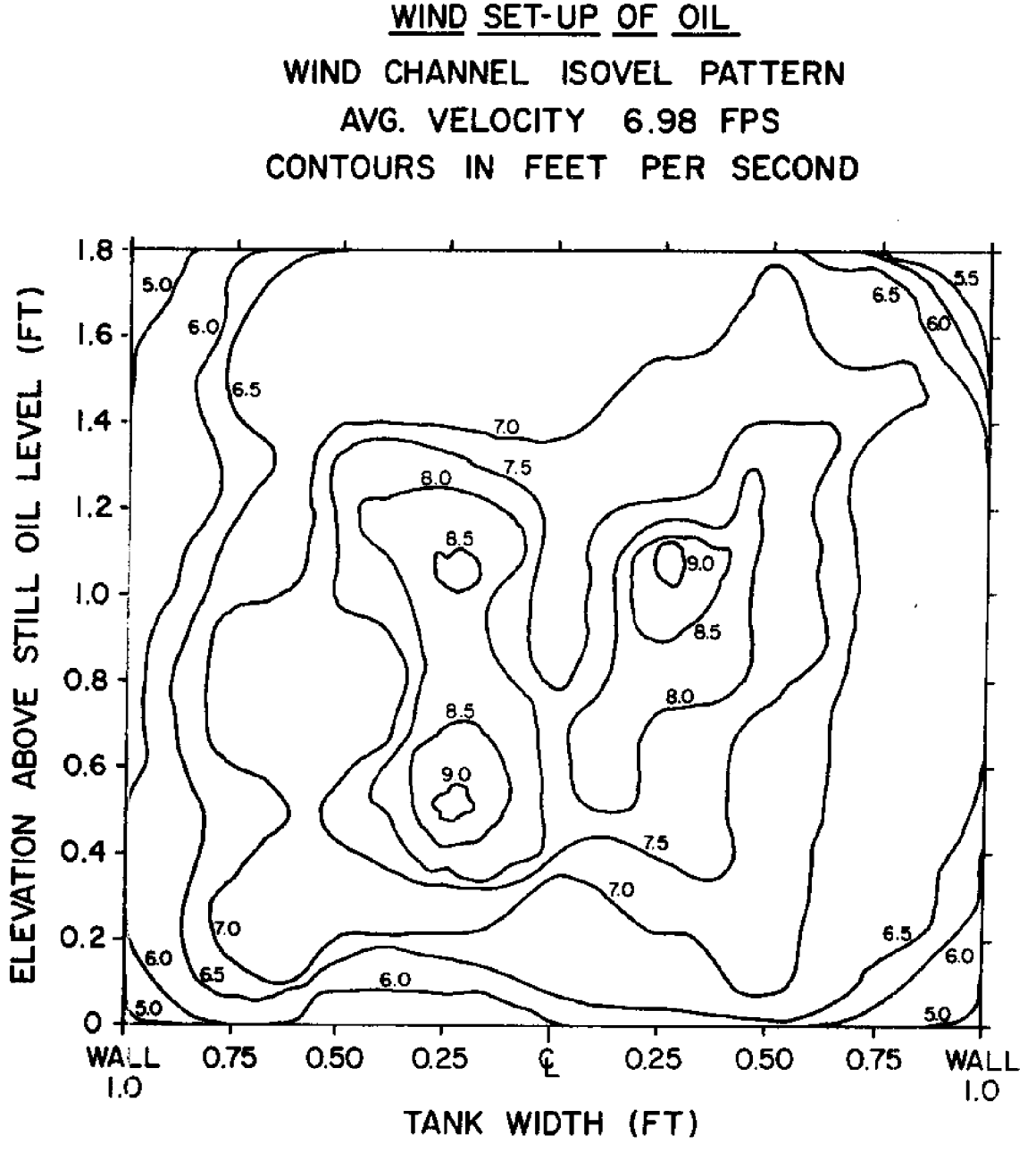

FIG. 6 – LOW WIND VELOCITY, WIND CHANNEL ISOVELS

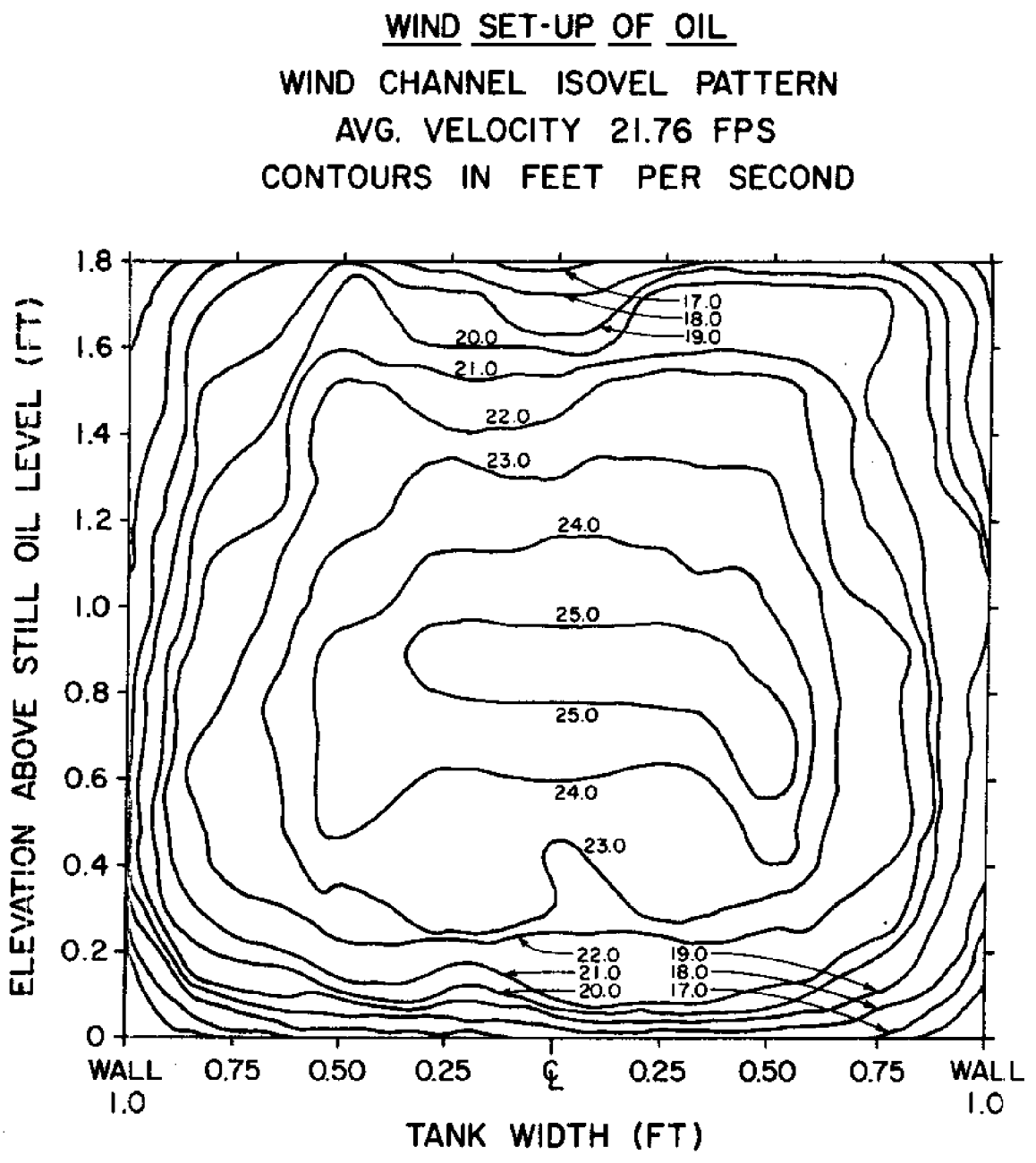

FIG. 7 – HIGH WIND VELOCITY, WIND CHANNEL ISOVELS

7. Oil surface conditions were duplicated during these tests and the water depths used were the same as during the actual testing for the oil set-up.

After determining the wind speed at the three positions mentioned earlier, the RMS (root mean square) value for each elevation in the tank (from the oil surface to the tank top) was calculated (See Fig. 8). Then, for a given wind speed, the vertical profile of RMS wind speed was compared to the actual centerline velocity for the same wind speed (See Fig. 9). The mean variation between the profiles (RMS versus centerline) was determined for the three different tank positions and the average variation was plotted as a function of wind speed. From these plots it was possible to extract a correction factor to apply to the centerline velocity profiles taken during testing of the oil.

Generally, below wind speeds of 30-35 fps the correction factor was less than unity, but ranged up to 1.05 for the lower wind speeds. Above 35 fps the correction factor went down as low as 0.80.

Having determined a means for correcting the observed centerline wind speed, it was then possible to proceed with calculating and plotting the dimensionless terms which represented the oil set-up.

Oil Measurement

The use of five positions for measurement of the oil thickness

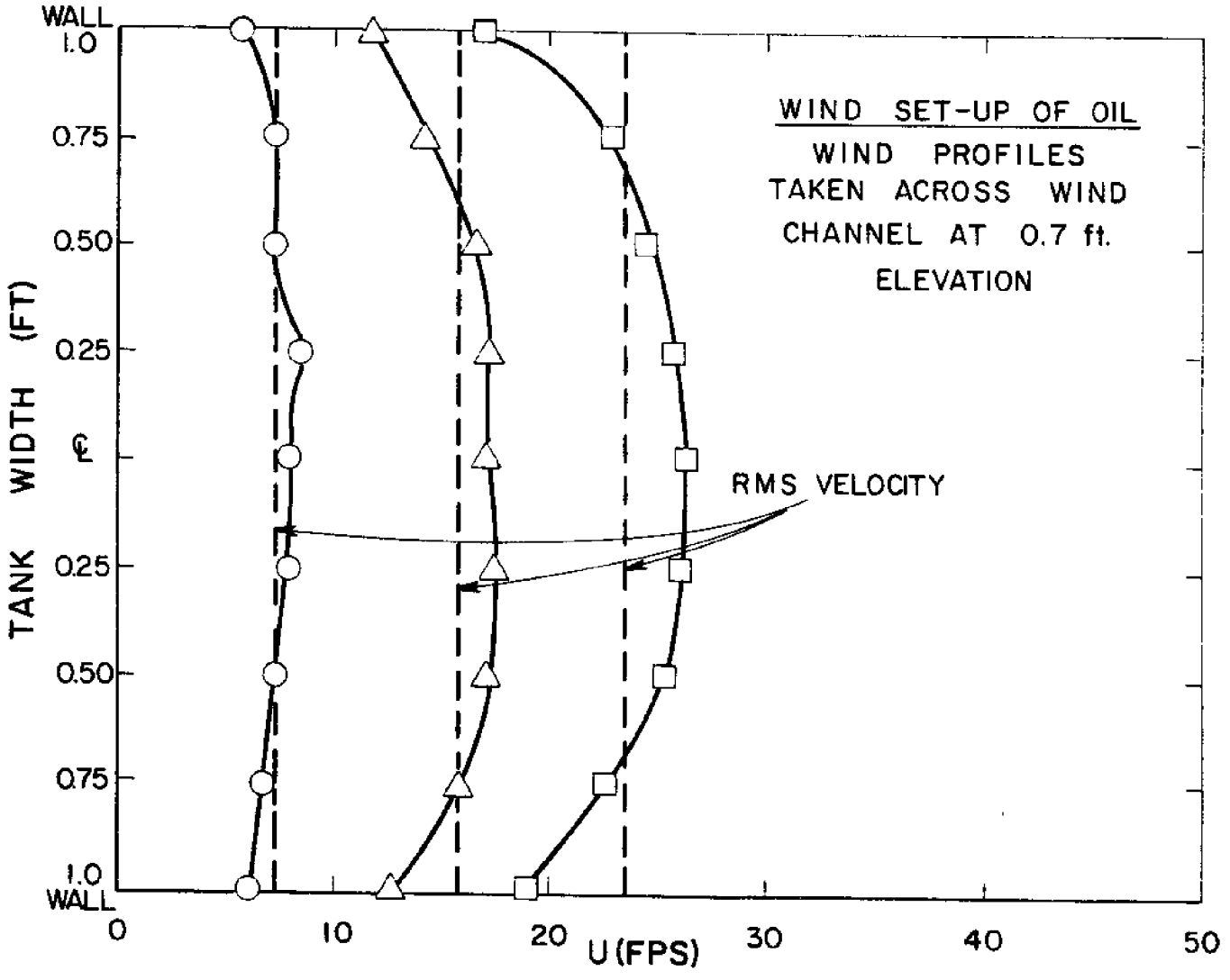

FIG. 8 - CROSS-CHANNEL WIND VELOCITY PROFILES.

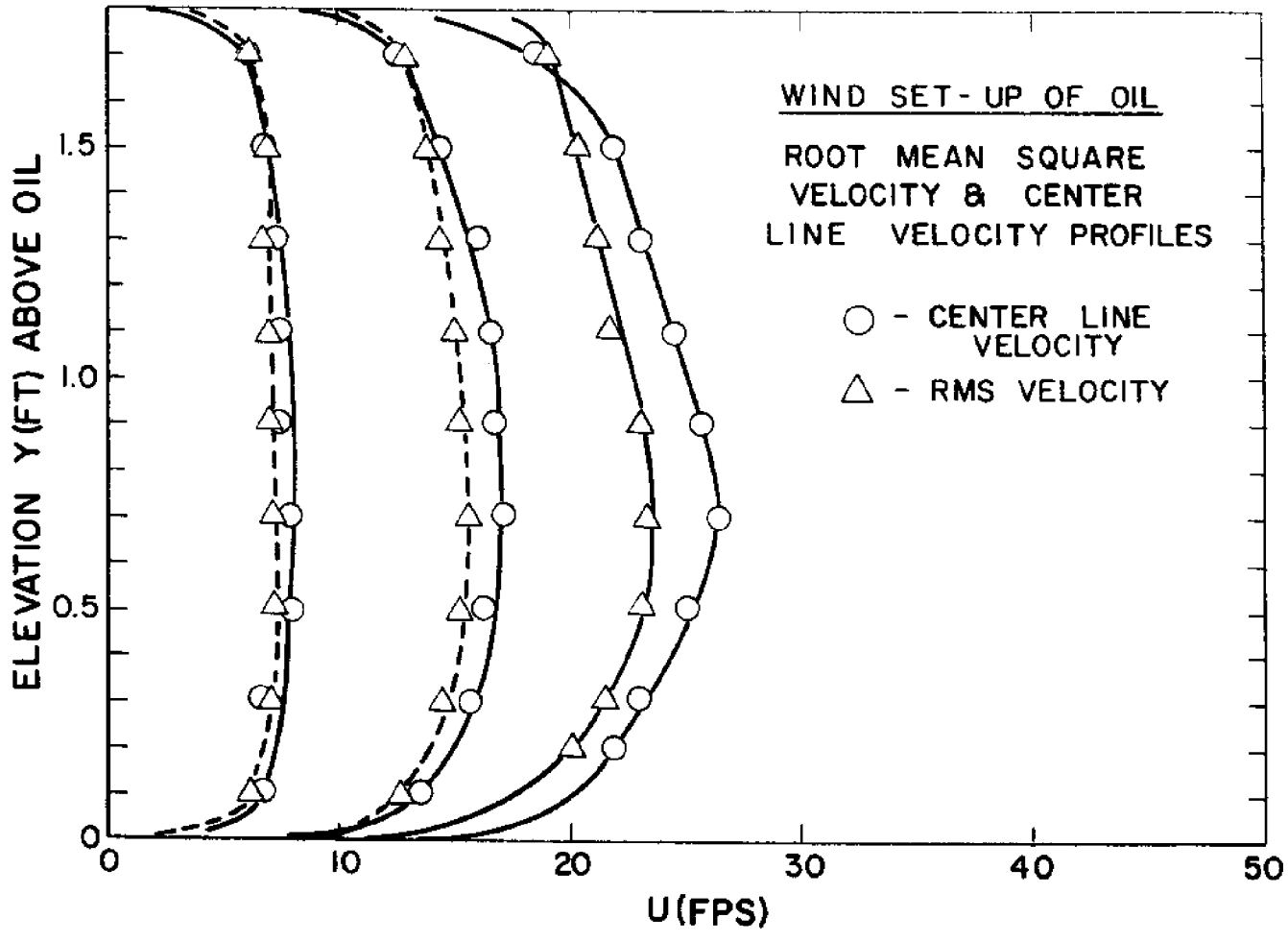

FIG. 9 – COMPARISON OF RMS AND CENTERLINE WIND VELOCITY PROFILES

allowed determination of the profile of the oil wedge floating on the water. The thickness of the oil, plotted against the horizontal distance along the oil's fetch length, shows the general shape of the oil wedge. As the wind set the oil up against the barrier, the fetch length became shorter and the oil thickness, at the down wind positions, became greater. For the oil volumes used, no fewer than two thicknesses were taken for each wind speed. Several of the runs are plotted in Figs. 20, 21 and 22, and all data taken for oil depth versus oil fetch length are shown in Appendix 2.

The oil fetch length measurement was that distance from position number one to the point where the oil wedge began. It was noted that for steady state conditions the oil wedge had a tendency to surge back and forth. No explanation could be found for this action except that possibly the power supply to the blower, which created the wind velocities, was unregulated and power surges in the electrical supply in the building caused the fan speed to vary. Also, when the wind outside the building was gusting, it could possibly have affected the pressure differential across the fan and, thereby, varied the air discharge rate.

To minimize the effects the surging of the oil might have on the data, the oil fetch length was always measured when it was believed it had reached a maximum set-up, or minimum fetch length. To insure that thickness measurements would coincide with the fetch length measurements, the thickness was measured when it appeared

to surge to the largest value. The general procedure used during the conduct of the experiment was: to establish the desired wind velocity in the wind-wave tank; take velocity profiles, while giving the oil time to establish an equilibrium set-up condition; and then take oil depth and fetch length readings.

Temperature Measurement

To insure that the effects of temperature could be accounted for in determining the oil density and viscosity, a centigrade thermometer was taped on the inside wall of the wind-wave tank. To minimize the temperature gradient effects across the glass and oil boundary, the thermometer was taped with a wedge between it and the wall. The thermometer was therefore, 1/2 to 3/4 in. from the wall with its bulb completely submerged in the oil.

With the above arrangement it was possible to read the temperature for each run through the glass tank wall. The density of the oil was corrected for temperature before being used to calculate the dimensionless Froude number. As can be seen in the Data Calculation Sheets, Appendix 3, the effects of temperature variation caused little change in the significant figures of the data calculations.

CHAPTER V

DATA REDUCTION

All data were taken manually using the equipment and apparatus described in Chapter IV. The general procedure used in obtaining the data is as follows:

1. The water level was established in the wind-wave tank.
2. The first volume of oil was placed in the tank. (Note: all runs were numbered consecutively in the order taken, e.g. 3-2-1, meaning; the third oil tested, and second volume, wind speed/run number one.)
3. All physical parameters (i.e., oil depth, barrier separation, pitot tube position, point gauge positions, height of pitot tube above still oil level, etc.) were measured and recorded.
4. A wind speed was selected that would cause the oil fetch length to begin (when set-up) at a point 10-15 feet downwind of the air intake.
5. Wind velocity profiles were taken on the tank center-line using the pitot tube and air-water inclined manometer.
6. Oil depths were taken at all positions (1 through 5) within the oil fetch length.
7. Oil temperature and oil fetch length were recorded.

8. The wind speed was increased to reduce observed fetch length and to increase oil set-up.
9. Steps 5-8 were repeated until the wind speed resulted in loss of oil over the downwind barrier due to waves and spray.
10. The second and third barrel (volume) of oil was added to the tank and steps 3-9 repeated.
11. After each volume, or at the end of a day of testing, oil samples were taken to allow determination of oil density and viscosity.
12. After all testing was completed on a given oil, the oil was removed using a vacuum pump and the tank was cleaned and prepared for the next oil. Selection of the second and third oil took place during and after testing of the previous oil. This aided in minimizing problem areas encountered in the previous tests and allowed planning the necessary techniques for handling the next test series.

The reduction of the data taken for a given oil was accomplished before testing began on the next oil. The data reduction followed a general procedure. This procedure is described as follows:

1. All wind velocity profiles were converted from manometer deflection readings to wind speed, in feet per second. Tabulation of these data can be seen

in Appendix 1.

2. All velocity profiles were plotted on graph paper. Examples of the wind profiles can be seen in Figs. 3, 4 and 5.

3. Oil depth readings were taken and recorded for each position. As the oil fetch length varied for each run, the distance from the beginning of the oil wedge to the position of oil depth measurement also varied. Each length therefore was calculated based on the distance between the positions and the total length. The results of these calculations and the oil depths are shown in Appendix 2. Additionally, all of these data were plotted on graph paper to show the profile of the oil wedge. Examples of this can be seen in Figs. 20, 21 and 22.

Using Eq. 63, where

$$d_o = \left[\frac{2KC\ \rho_w\ U^2 L}{\rho_o\ g\ (1 - \frac{\rho_o}{\rho_w})}\right]^{1/2}$$

in which $2KC = 2.3 \times 10^{-3}$, U (generally taken at 0.7 ft elevation) and ρ_o were those values associated with a particular run and oil, and with L selected in 5 ft increments, d_o was calculated. This theoretical value of d_o was plotted with the actual d_o to compare the actual set-up with a predicted value for

a given set of conditions. See Figs. 20, 21 and 22.

4. The wind velocity profiles were examined to determine the wind speed which represented that wind speed above which, if the tank cover had not existed, the profile would straighten (normally the maximum speed). The selected wind speed was corrected by applying a factor determined from the difference in the center-line velocity and the RMS velocity plotted as a function of wind velocity (at which the difference occurred). The corrected wind velocities are tabulated in Appendix 3. Other data, associated with a particular run, and used for further calculation of the dimensionless terms d_o/L and $U/\sqrt{g'L}$, are also tabulated in Appendix 3.

5. The values of d_o/L and $U/\sqrt{g'L}$ were plotted for each run. These can be seen in Figs. 10, 11, 12 and 13. These four figures show that a straight line relationship exists for each oil below certain values of $U/\sqrt{g'L}$. Above that value, the data departs from the original linear function. The data above that certain value of $U/\sqrt{g'L}$, also form a linear relationship and represent d_{o_w}/L, or that set-up caused by waves in the oil.

The original linear relationship allowed determination of the functional relationships expressed in Eq. 64 as the slope of this line is,

$$\text{Slope} = \left[\frac{2KC\ \rho_w}{\rho_o}\right]^{1/2}$$

6. Having plotted the values of d_o/L versus $U/\sqrt{g'L}$ and observed (both in the wind-wave tank and on the graphs plotted in No. 5, above) where the set-up became a function of wind and waves, the values of d_{ow}/L could be taken from the graphs and recorded. Using the fetch length L, d_{ow} could be calculated from d_{ow}/L. Using the run wind speed U, $d_{ow}/\sqrt{L}$ was plotted versus U. These data are tabulated in Appendix 4 and are plotted for each oil in Figs. 14, 15, 16 and 17. From the slope of these curves, and using Eq. 84, where,

$$\text{Slope} = \frac{d(d_{ow}/\sqrt{L})}{dU} = \left[\frac{2B\ \rho_w}{g'\ \rho_o}\right]^{1/2}$$

it was possible to evaluate the wind-wave constant, B.

7. Using the values of B determined for each oil tested and the value of the critical wind velocity U_c, (taken from the graphs plotted in No. 6 above), a plot was made comparing B and U_c versus ν, the kinematic viscosity of the oil.

8. Using Eq. 63 and substituting

$$\tau_{s_d} = KC\ \rho_a\ U^2 \quad \ldots\ldots\ldots\ (96)$$

results in,

$$d_o = \left[\frac{2\ \tau_{s_d}\ L}{\rho_o\ g\left(1 - \frac{\rho_o}{\rho_w}\right)}\right]^{1/2} \quad \ldots\ldots\ (97)$$

Rearranging,

$$\tau_{s_d} = \frac{d_o^{\,2}\ g\ \rho_o\ \left(1 - \frac{\rho_o}{\rho_w}\right)}{2L} \quad \ldots\ldots\ (98)$$

where τ_{s_d} is the shear stress calculated from oil set-up data. From,

$$I = \frac{g\ \rho_o\left(1 - \frac{\rho_o}{\rho_w}\right)}{2} \quad \ldots\ldots\ (99)$$

the constant I, for each oil, was calculated. These values were

$$I_1 = 1.59$$

$$I_2 = 1.96$$

$$I_3 = 1.31$$

where I_1, I_2 and I_3 were for oils No. 1, 2 and 3 respectively. Using these values of I and,

$$\tau_{s_d} = \frac{I\ d_o^{\,2}}{L} \quad \ldots\ldots\ (100)$$

values of τ_{s_d} were calculated for each run based on the oil depth at position number one and the associated oil fetch length. Using Eq. 96, where

$$\tau_{s_d} = KC \rho_a U^2$$

in which $K = 1$, $\rho_a = 2.37 \times 10^{-3}$ and by rearranging,

$$C_d = \frac{\tau_{s_d}}{2.37 \times 10^{-3} U^2} \quad \ldots\ldots\ldots (101)$$

values of the wind stress coefficient were calculated for each run. The results of these calculations can be seen in Appendix 5.

9. The data for the wind velocity profiles were plotted on semi-log paper, with the height Y (above the oil) on the ordinate in log scale, and the wind speed U on the abscissa in arithmetic scale. Plotting these parameters in this manner resulted in a straight line for values within the boundary layer. By extending the line to where U = 0 (through 4-6 cycles), it was possible to obtain a value, Y', which is representative of the surface roughness. Using the Karman-Prandtl relationship,

$$\frac{U}{U_*} = \frac{2.3}{\kappa_o} \log \frac{Y}{Y'}$$

where:

Y = 0.1 ft (an elevation in the boundary layer),

U = wind speed at Y,

Y' = surface roughness elevation, and

k_o = 0.4

it was possible to obtain U_*;

$$U_* = \frac{U}{5.75 \log_{10} \frac{Y}{Y'}} \quad \ldots\ldots\ldots (102)$$

or

$$U_* = \frac{U}{2.5 \ln \frac{Y}{Y'}} \quad \ldots\ldots\ldots (103)$$

as,

$$U_* = \left[\frac{\tau_{s_w}}{\rho_a}\right]^{1/2}$$

where τ_{s_w} is the shear stress based on wind profile data. Rearranging results in,

$$\tau_{s_w} = \rho_a U_*^2 \quad \ldots\ldots\ldots (104)$$

Again using Eq. 96, it can be said

$$\tau_{s_w} = K C_w \rho_a U^2 \quad \ldots\ldots\ldots (105)$$

and

$$C_w = \frac{\tau_{s_w}}{2.37 \times 10^{-3} U^2} \quad \ldots\ldots\ldots (106)$$

and calculation of the wind stress coefficient based on wind profile data was possible. This calculation

allowed a comparison to be made with the values of C, calculated using the oil set-up data, and thus helped confirm the validity of the wind profile data. The results of the above calculations can also be seen in Appendix 5.

CHAPTER VI

DISCUSSION OF RESULTS

For each run conducted, a set of dimensionless numbers, d_o/L and $U/\sqrt{g'L}$, were calculated and plotted. The data for the individual oils are plotted in Figs. 10, 11 and 12. For each oil, the data plot in a straight line as predicted by Eq. 64,

$$d_o/L = [2KC \frac{\rho_w}{\rho_o}]^{1/2} \frac{U}{g'L} \quad \ldots\ldots\ldots (64)$$

The initial slope of each of the these curves represents a constant term which relates the dimensionless numbers to the set-up due to wind only. The slopes are:

$$\text{Oil \# 1} - 2.4 \times 10^{-3}$$

$$\text{Oil \# 2} - 2.4 \times 10^{-3}$$

$$\text{Oil \# 3} - 2.53 \times 10^{-3} \quad \ldots\ldots\ldots (107)$$

Equating these values with the constant terms in Eq. 64,

$$\text{Slope} = [2KC \frac{\rho_w}{\rho_o}]^{1/2}$$

and solving for the wind stress coefficient C, when K = 1, yields the following:

$$\text{Oil \# 1} \quad C = 2.55 \times 10^{-6}$$

$$\text{Oil \# 2} \quad C = 2.47 \times 10^{-6}$$

$$\text{Oil \# 3} \quad C = 2.91 \times 10^{-6} \quad \ldots\ldots\ldots (108)$$

Fig. 13 shows the data for all three oils combined. If an envelope is drawn to enclose all the data taken, a median line can

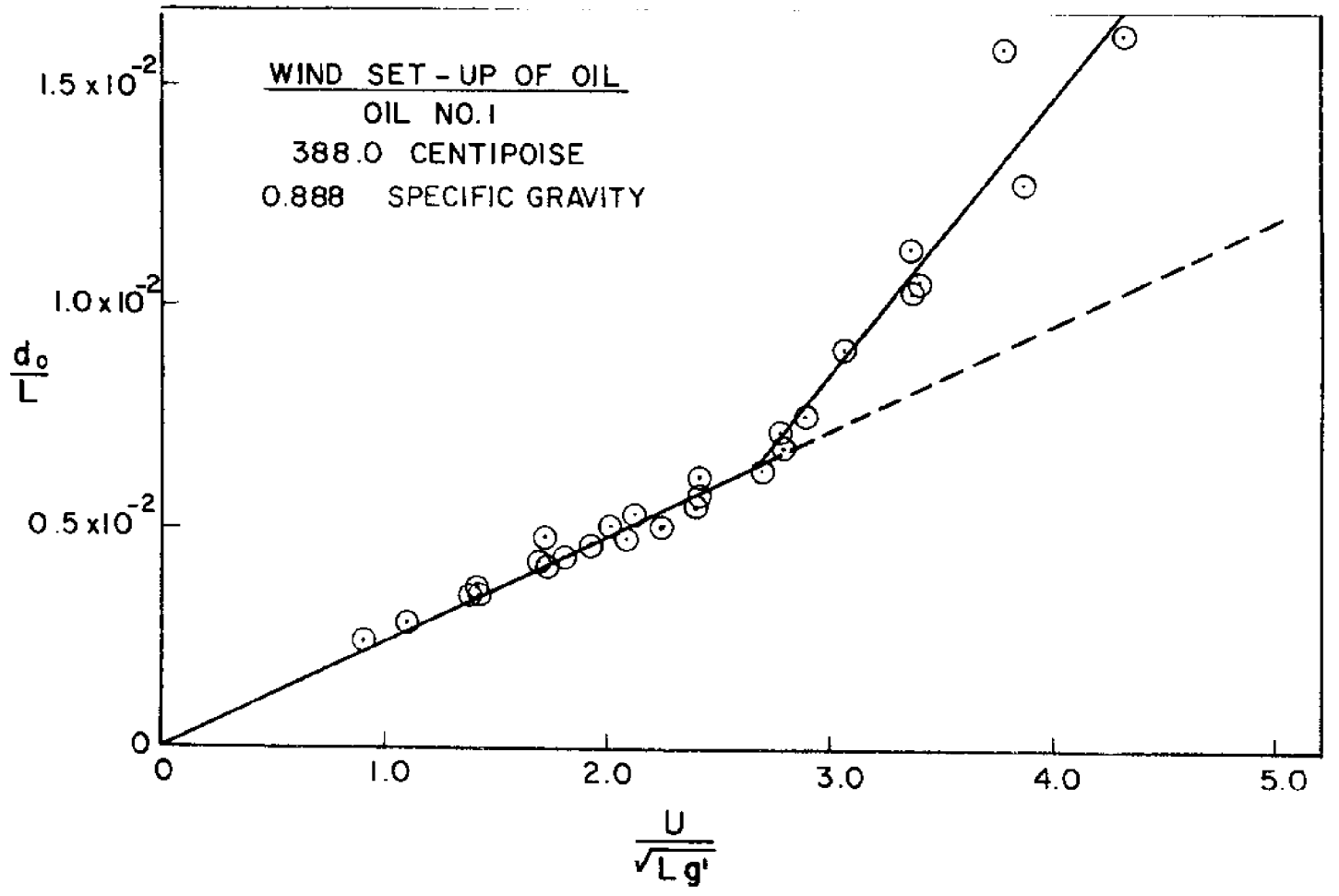

FIG. 10 – DIMENSIONLESS OIL SET - UP VERSUS FROUDE NUMBER, OIL NO. 1

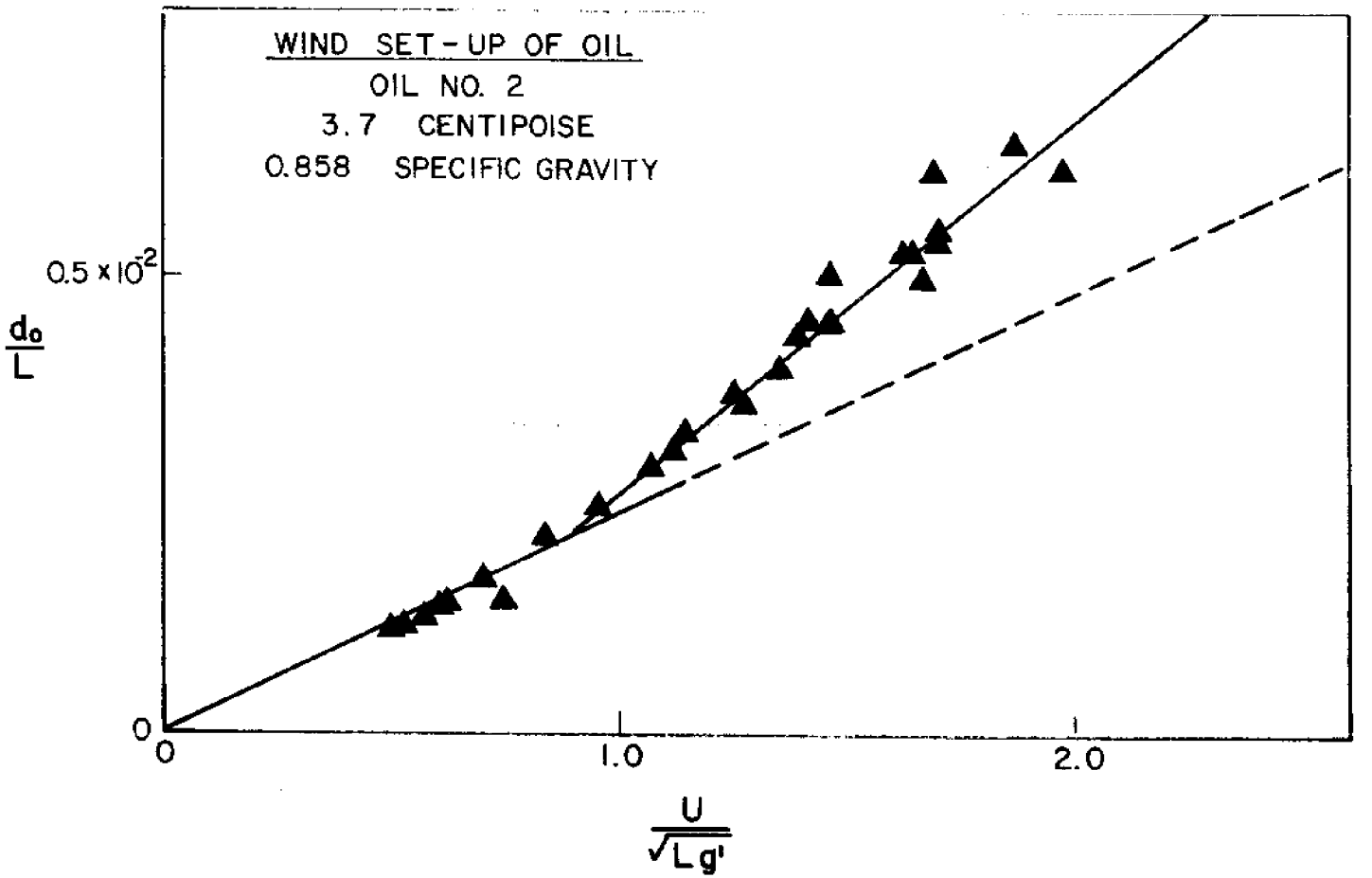

FIG. 11 – DIMENSIONLESS OIL SET – UP VERSUS FROUDE NUMBER, OIL NO. 2

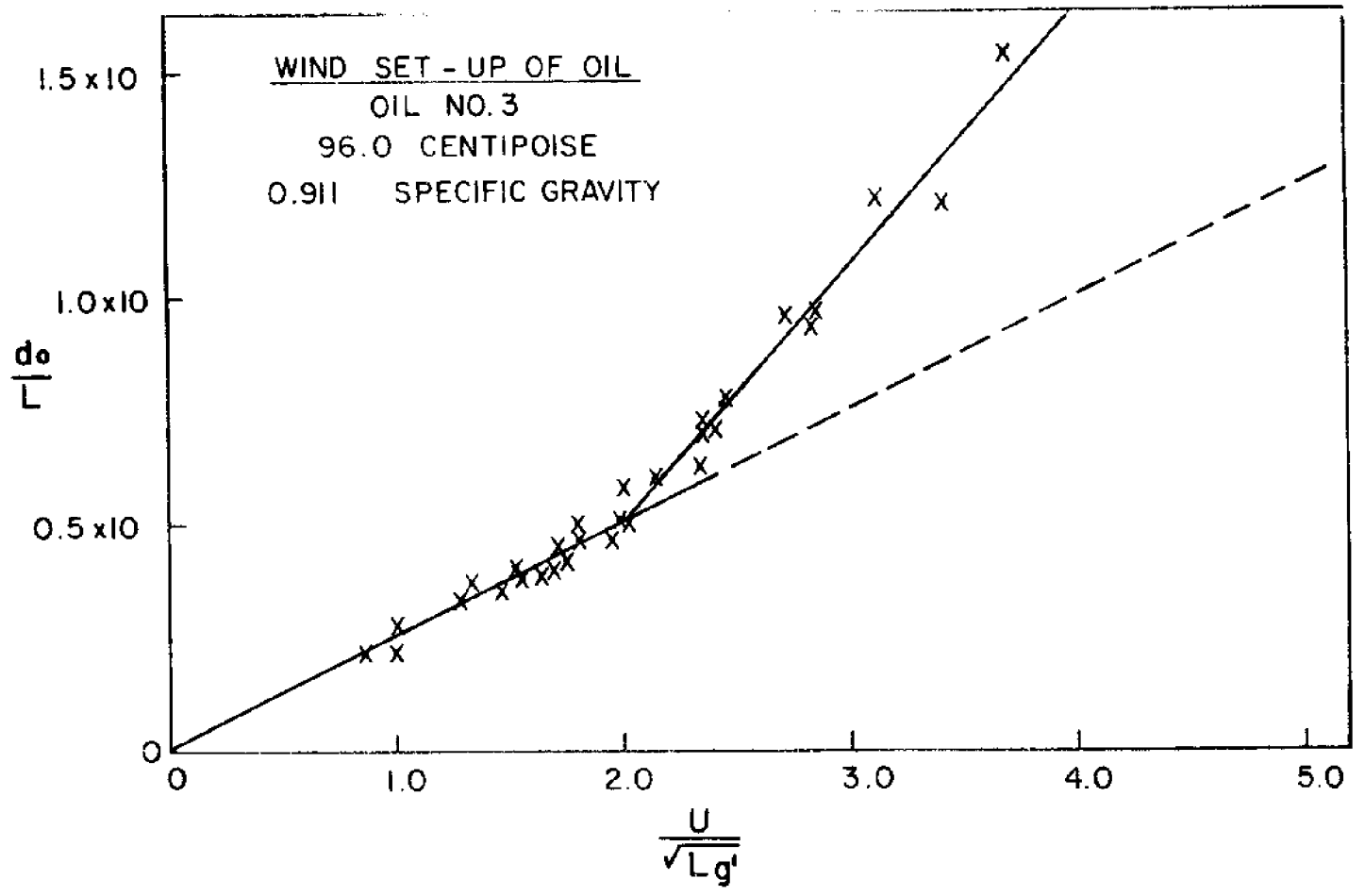

FIG. 12 – DIMENSIONLESS OIL SET - UP VERSUS FROUDE NUMBER, OIL NO. 3

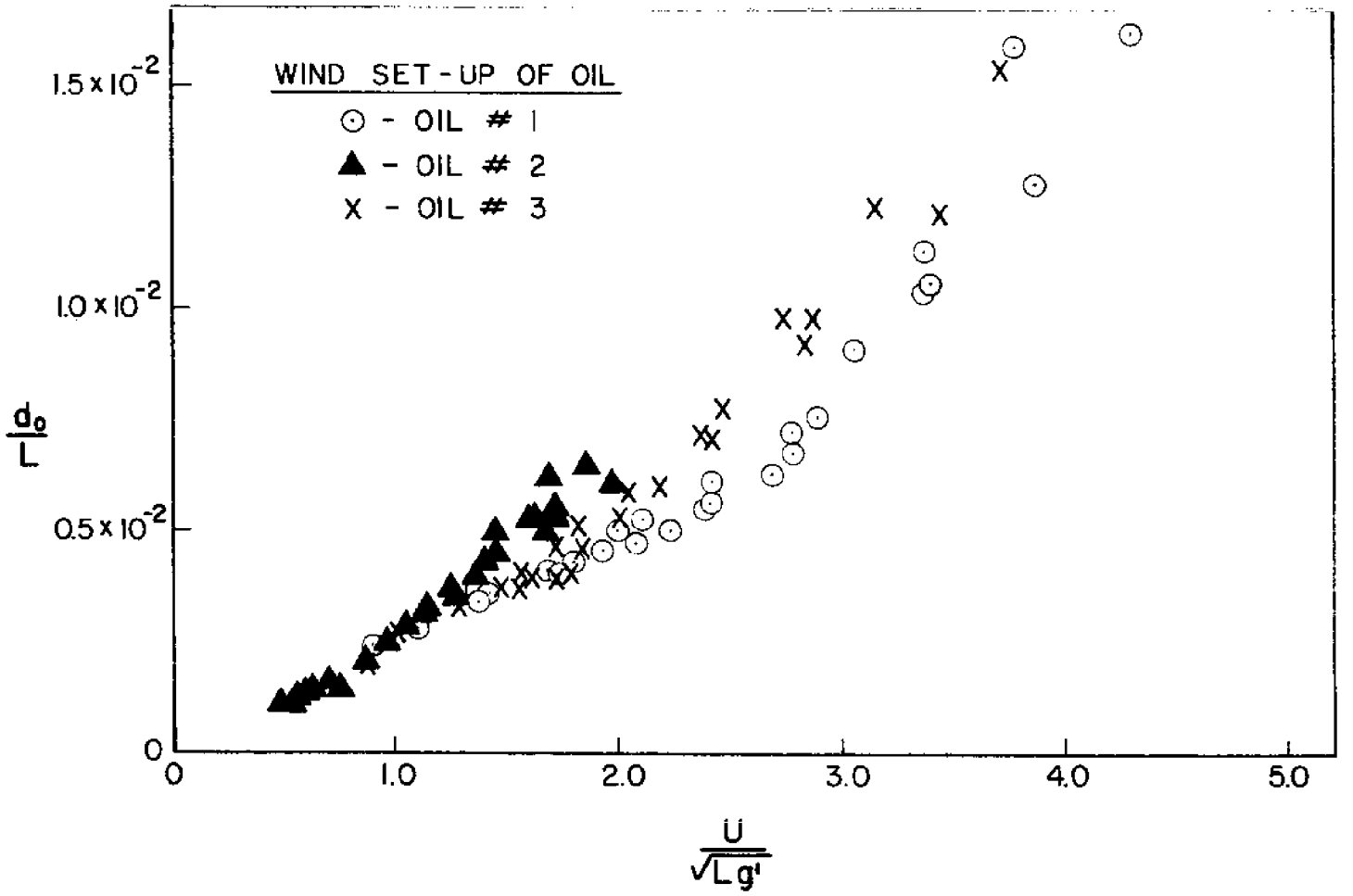

FIG. 13 - DIMENSIONLESS OIL SET-UP VERSUS FROUDE NUMBER, OIL NOS. 1, 2 AND 3

be constructed representing the entire set of data, including set-up occurring due to waves. In addition, the median slope line is representative of an oil which has a viscosity range between 4 and 440 centistokes, and an average density of 0.886. The slope of the median line is 3.0×10^{-3}. For this slope, the wind stress coefficient is, $C = 3.99 \times 10^{-6}$.

For the design of an oil containment barrier it would perhaps be more conservative to select a slope from Fig. 13 from the upper half of the enclosing envelope. This would add more weight to the data taken when waves were present in the oil, a condition more likely to occur under design conditions. However, using the median slope, it can be concluded that for engineering purposes, the set-up of oil can be expressed,

$$\frac{d_o}{L} = 3.0 \times 10^{-3} \frac{U}{\sqrt{g'L}} \quad \ldots\ldots\ldots \quad (109)$$

To predict more accurately the oil set-up due to wind and waves, it is necessary to determine separately the set-up due to wind and due to waves. To do this, values of d_{ow} were taken from Figs. 10, 11 and 12 for all data points above the initial slope line. These were plotted, using Eq. 66, in Figs. 14, 15, 16 and 17. The data for these figures are tabulated in Appendix 4. Using Eq. 68, the slope of these curves can be expressed

$$\text{Slope} = \left[\frac{2B\ \rho_w}{\rho_o\ g'}\right]^{1/2} \quad \ldots\ldots\ldots \quad (110)$$

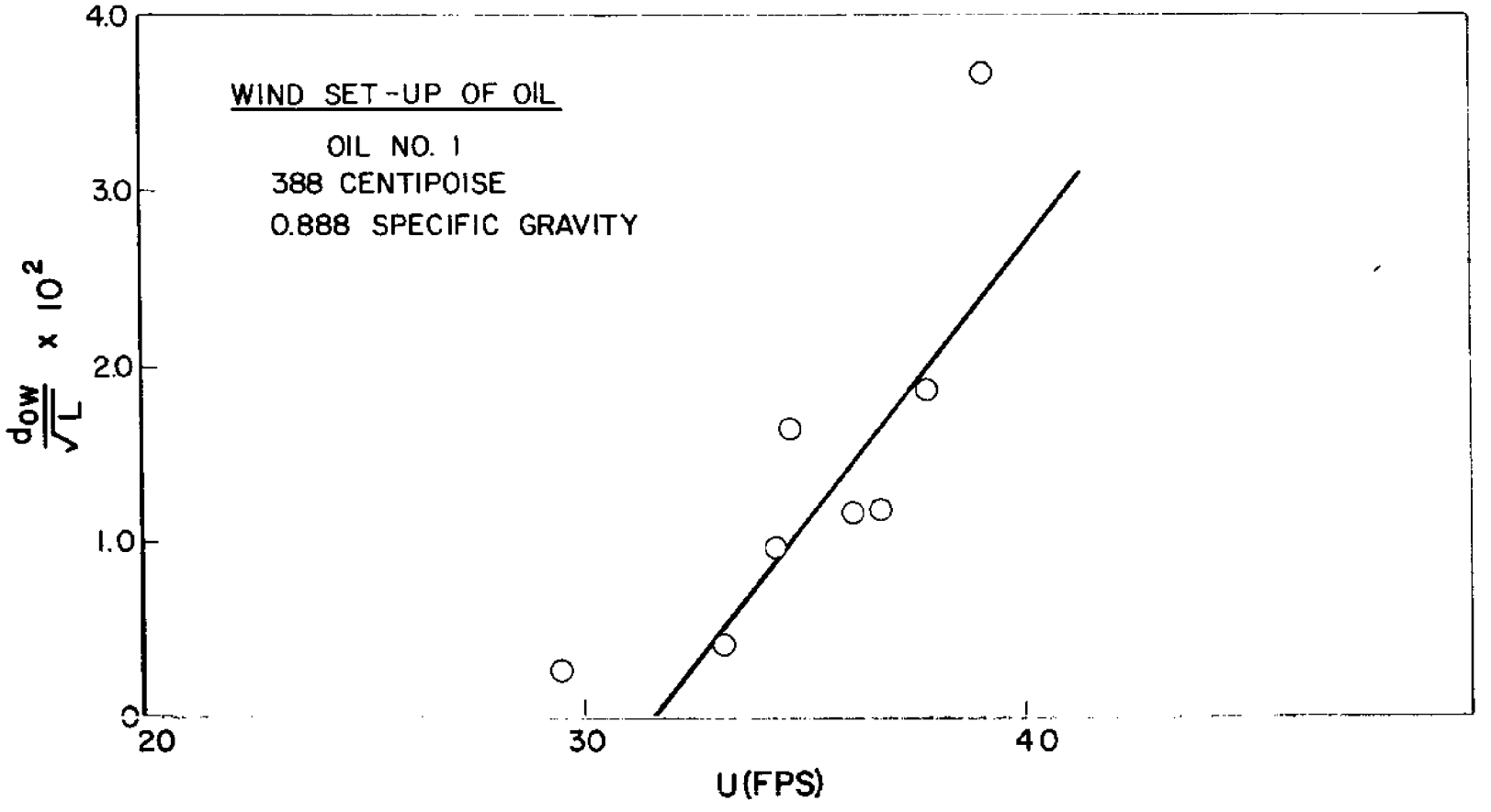

FIG. 14 - OIL SET-UP DUE TO WAVES, OIL NO. 1

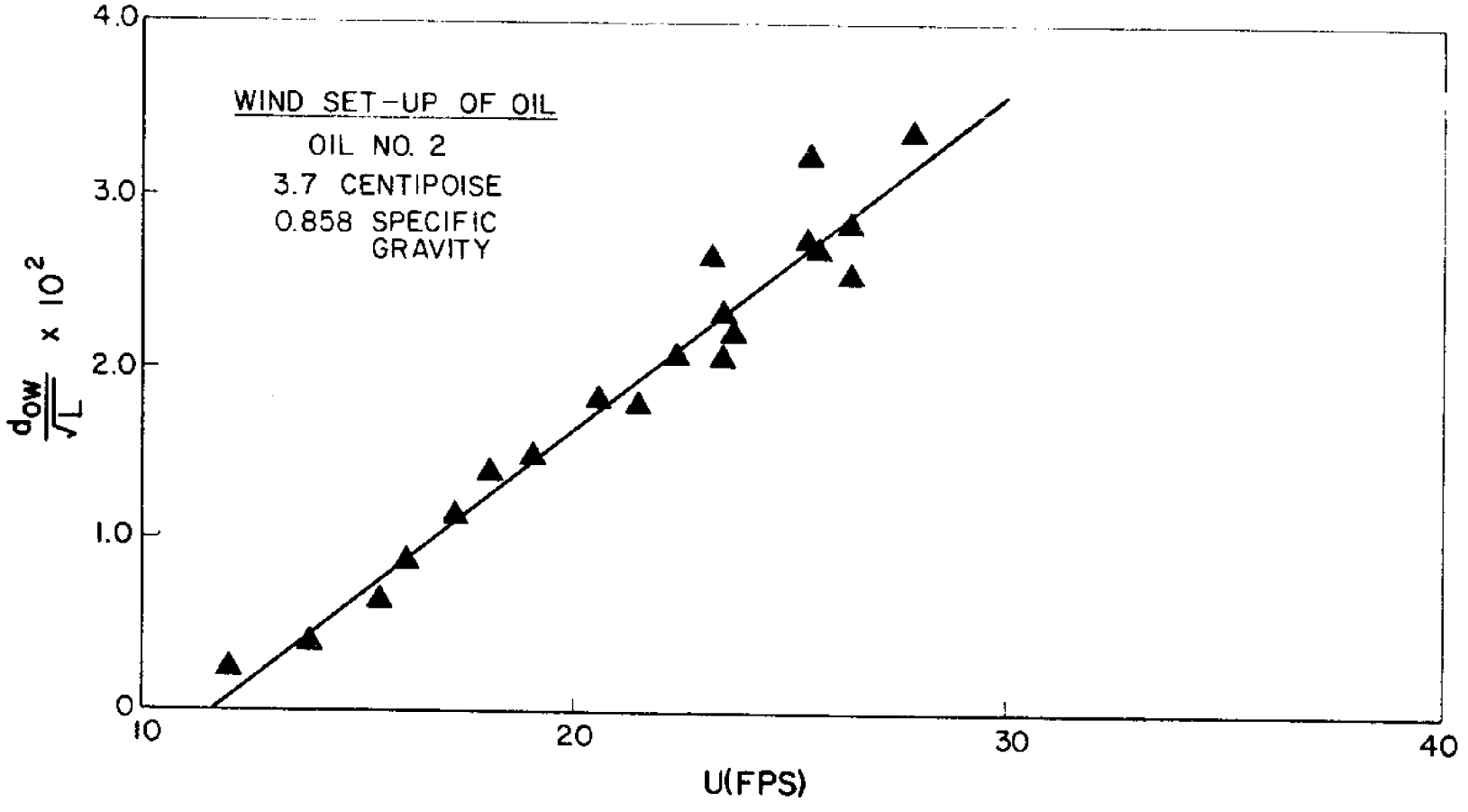

FIG. 15- OIL SET-UP DUE TO WAVES, OIL NO.2.

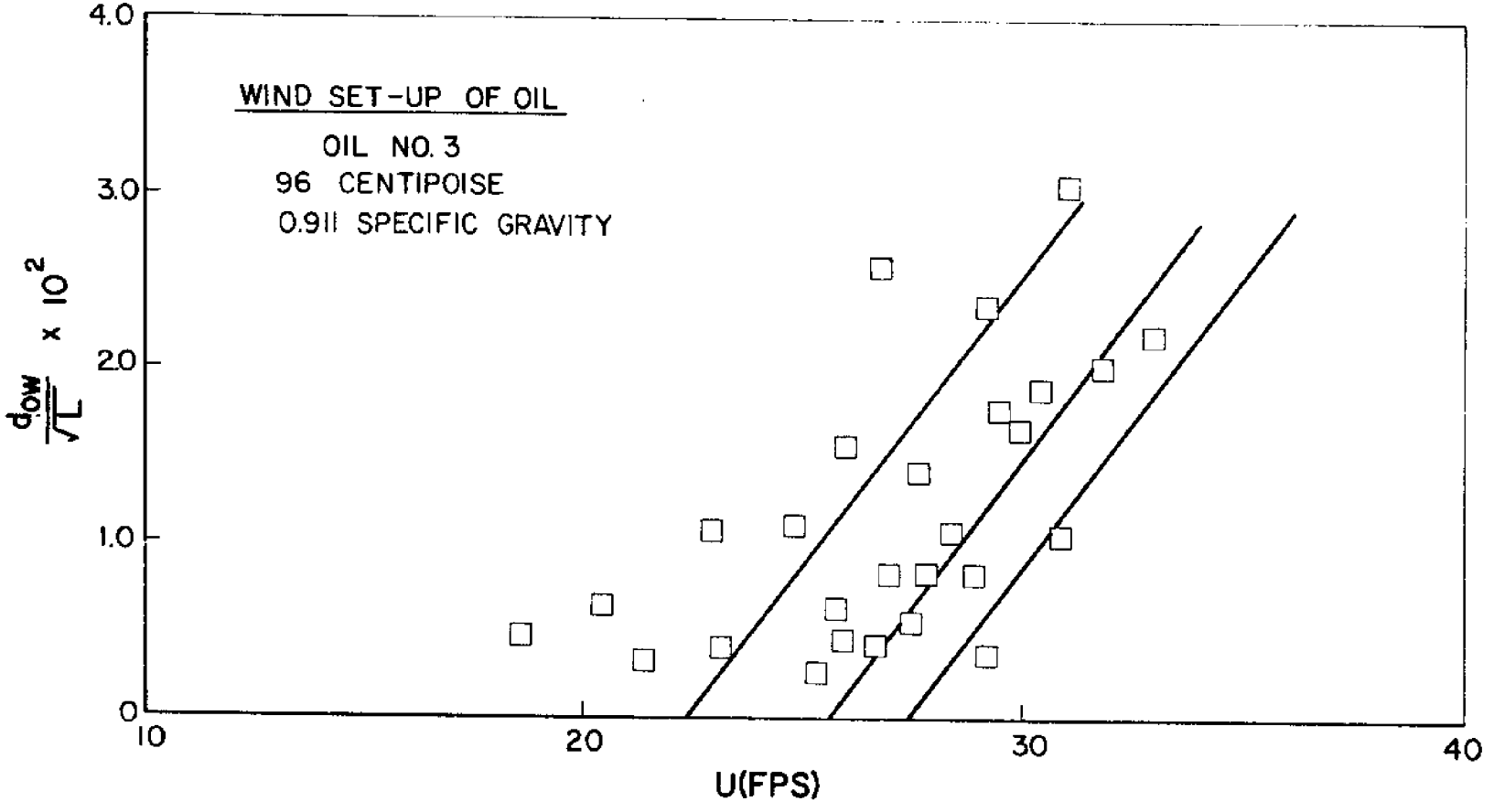

FIG. 16 - OIL SET-UP DUE TO WAVES, OIL NO. 3.

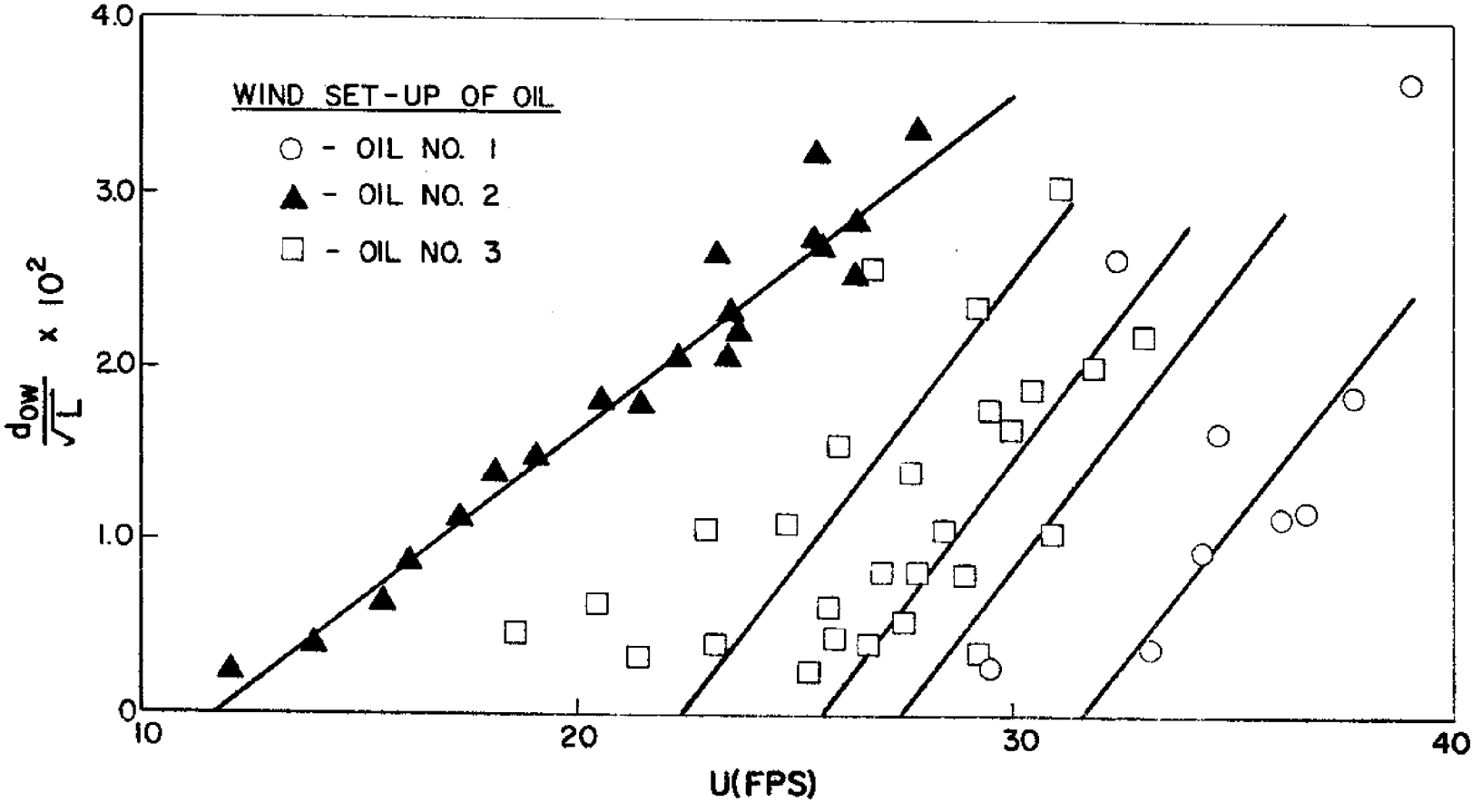

FIG. 17 - OIL SET-UP DUE TO WAVES, OIL NOS. 1, 2, AND 3.

This relationship can be used to determine the value of the wind-wave constant B. The results for each oil were as follows:

$$\text{Oil \# 1} \quad B = 16.65 \times 10^{-6}$$

$$\text{Oil \# 2} \quad B = 7.5 \times 10^{-6}$$

$$\text{Oil \# 3} \quad B = 14.4 \times 10^{-6} \quad \ldots\ldots\ldots (11)$$

In Fig. 17 it can be seen that the slope of the curves vary and change in the same direction for increasing viscosity. Corrected for the oil density, B also increases.

The values of B obtained for each oil were plotted in Fig. 18 against oil viscosity. It appears, although inconclusively, that B reaches a maximum limiting value for high viscosities. For use in engineering design, it is believed that Fig. 18 will provide the necessary wind-wave constant to allow predicting the set-up of oil.

The values of the critical wind speed, U_c, at which set-up due to wind waves begins, were determined by that point at which $d_{ow}/\sqrt{L} = 0$, as seen in Figs. 14, 15, 16 and 17. The values of U_c were as follows:

$$\text{Oil \# 1} - U_c = 31.6 \text{ fps}$$

$$\text{Oil \# 2} - U_c = 11.7 \text{ fps}$$

$$\text{Oil \# 3} - U_c = 24.0 \text{ fps} \quad \ldots\ldots\ldots (112)$$

Additionally, it was observed during testing that these wind

speeds were essentially those speeds at which waves were created in the oil and water of sufficient size to travel along the oil fetch to the point of measurement (at position No. 1). These observations support those of Van Dorn (2), who said that the waves caused a transport of liquid by their motion and thereby contributed to the set-up of the mean liquid surface level.

To develop a usable relationship, the three values of U_c were plotted in Fig. 18. As with the constant B, U_c is seen to increase with viscosity.

The values of U_c are plotted versus oil viscosity on log-log paper in Fig. 19. By extension of the resulting curve, to a viscosity equal to unity (water), the critical wind speed, taken at an elevation of 0.7 ft (21.3 cm), is 8.3 fps (2.53 m/sec). Using the Karman relationship

$$\frac{U_c}{U_c'} = \frac{1}{k_o} \ln \frac{Y}{Y'} \quad \ldots\ldots\ldots\ldots (113)$$

where U_c' is the critical wind speed at 0.7 ft, values of U_c were found (at 10, 25, 100 and 1000 cm) to be:

$$10 \text{ cm} - U_c = 1.58 \text{ m/sec}$$
$$25 \text{ cm} - U_c = 2.85 \text{ m/sec}$$
$$100 \text{ cm} - U_c = 9.80 \text{ m/sec}$$
$$1000 \text{ cm} - U_c = 24.3 \text{ m/sec} \quad \ldots\ldots\ldots (114)$$

These values of critical velocity can now be compared with

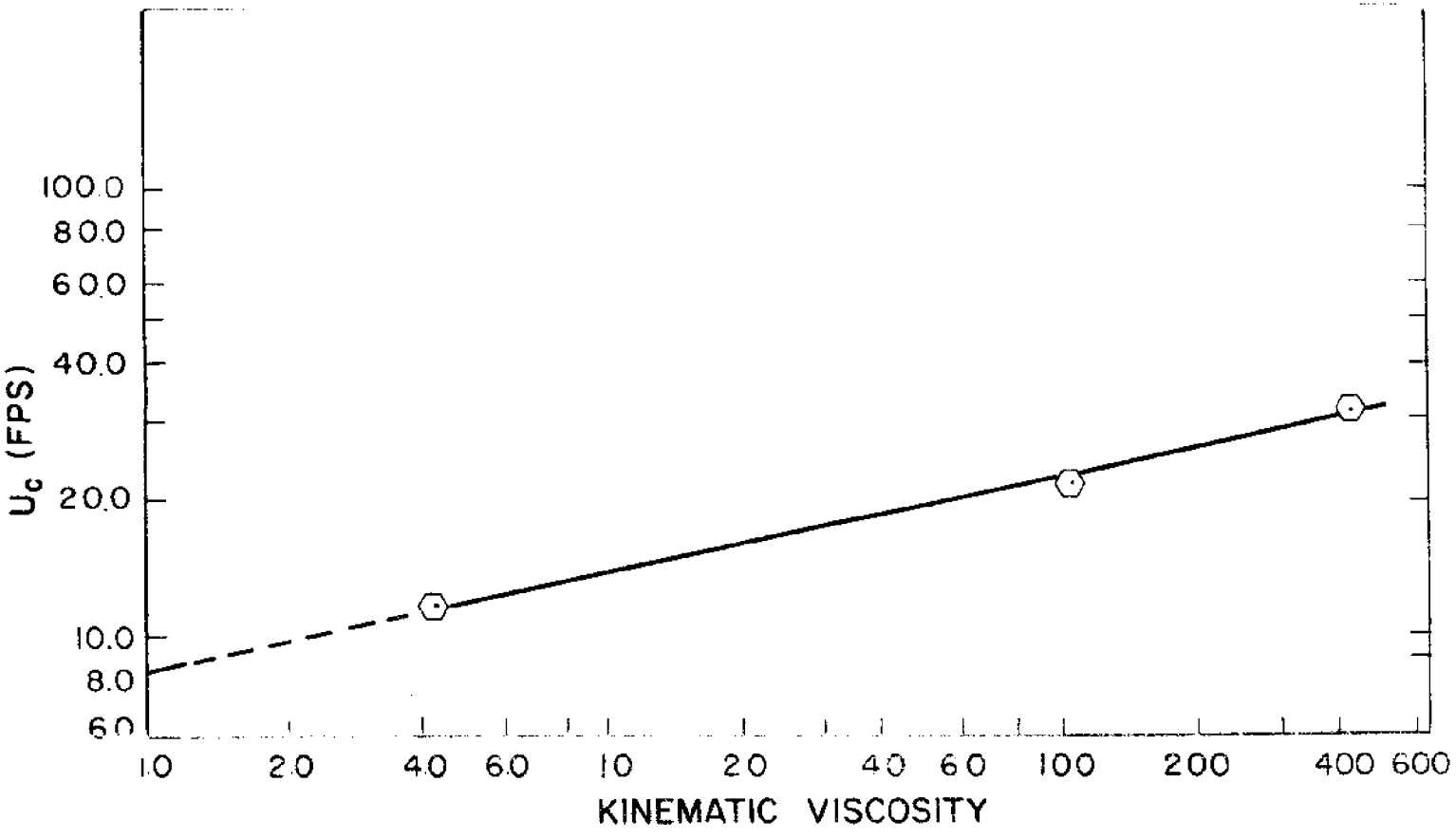

FIG. 19 -WIND SET-UP OF OIL. KINEMATIC VISCOSITY VS. CRITICAL WIND VELOCITY

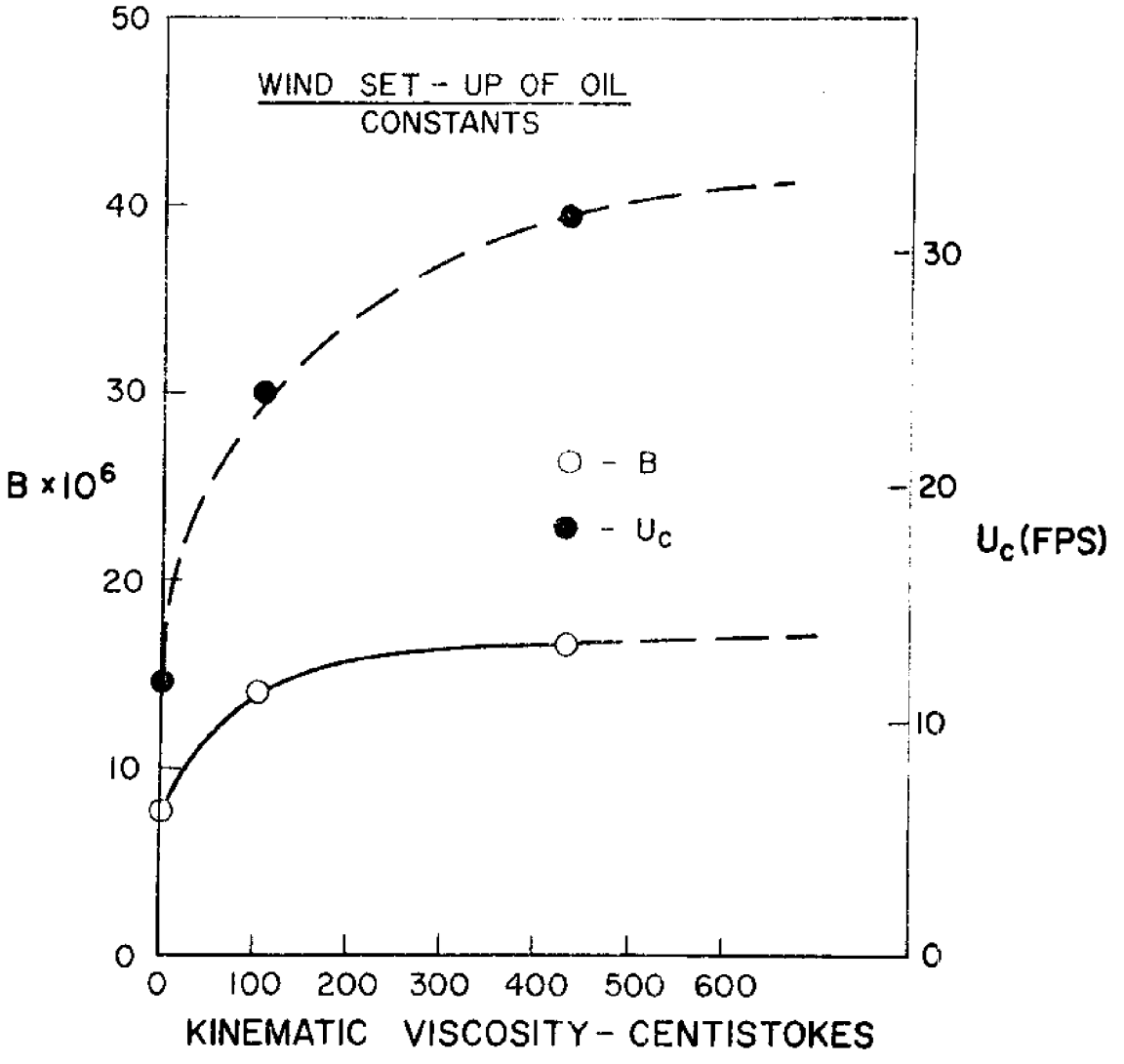

FIG. 18 - WIND-WAVE CONSTANT B, AND CRITICAL WIND VELOCITY, U_c, VERSUS OIL VISCOSITY

those obtained by Van Dorn (2) and Keulegan (1) in their determination of set-up of water by wind. The values of critical wind speed which they found were,

$$10 \text{ cm} - U_c = 3.9 \text{ m/sec (Keulegan)}$$

$$25 \text{ cm} - U_c = 3.1 \text{ m/sec}$$

$$100 \text{ cm} - U_c = 4.0 \text{ m/sec}$$

$$1000 \text{ cm} - U_c = 5.6 \text{ m/sec.}$$

The elevations of 25, 100 and 1000 cm. are elevations at which Van Dorn actually took wind velocity measurements. This indicates that a boundary layer existed, however the slope was less than predicted by the Karman equation.

The fact that the curve in Fig. 19 produces a critical velocity for water close to that obtained by Van Dorn in the field, lends support to the slope of the curve obtained for the oils tested. This slope is approximately 0.20. Keulegan (1), in Eq. 11, indicated the slope should be 0.33, using metric units.

Based on the foregoing, it is now possible to obtain the necessary significant constants to be used in Eq. 69, to predict the total set-up of oil:

$$d_{o_t} = \left[\frac{2KC\ \rho_w\ U^2 L}{\rho_o\ g'}\right]^{1/2} + \left[\frac{2BL\ \rho_w}{g'\ \rho_o}\right]^{1/2} (U - U_c) \quad . . (69)$$

Fig. 16, shows a wide range of data points associated with set-up of oil due to waves for oil No. 3. The reason for this is believed to be because of testing procedure. Each of the three

curves represents a different volume. It was observed that the amount of open water upwind of the oil wedge created a different wind speed at which wind waves would be generated of sufficient energy to penetrate the oil wedge to the point of measuring oil set-up. It was observed that for the smaller oil volumes, there was more open water in front of the oil, and a thinner oil wedge than would occur for a large oil volume. As a result, the wind waves generated in the water (a function of fetch length) became higher sooner (at lower wind speed) and were able to traverse the oil wedge more easily. This resulted in U_c being lower for the smaller volume and higher for the larger volumes.

This phenomenon was not observed in Oils No. 1 and 3. This is believed to be because Oil No. 1 was so viscous that wind waves were quickly damped and at only the very high wind speeds were waves able to penetrate the oil wedge through its full length. Additionally, too few data points were taken in the wind speed range where waves were generated to allow correlation of the "open water effect."

Oil No. 2 had a viscosity very near that of water, consequently the waves were generated regardless of the amount of open water upwind of the oil wedge. In this case the open water effect was masked by the existence of waves generated in the oil

Using the oil depths measured along the oil wedge, the oil profiles were determined. Figs. 20, 21 and 22 show the oil wedge profile for different oils and oil volumes. To allow for a means of comparison, the first term on the right hand side of Eq. 69 was

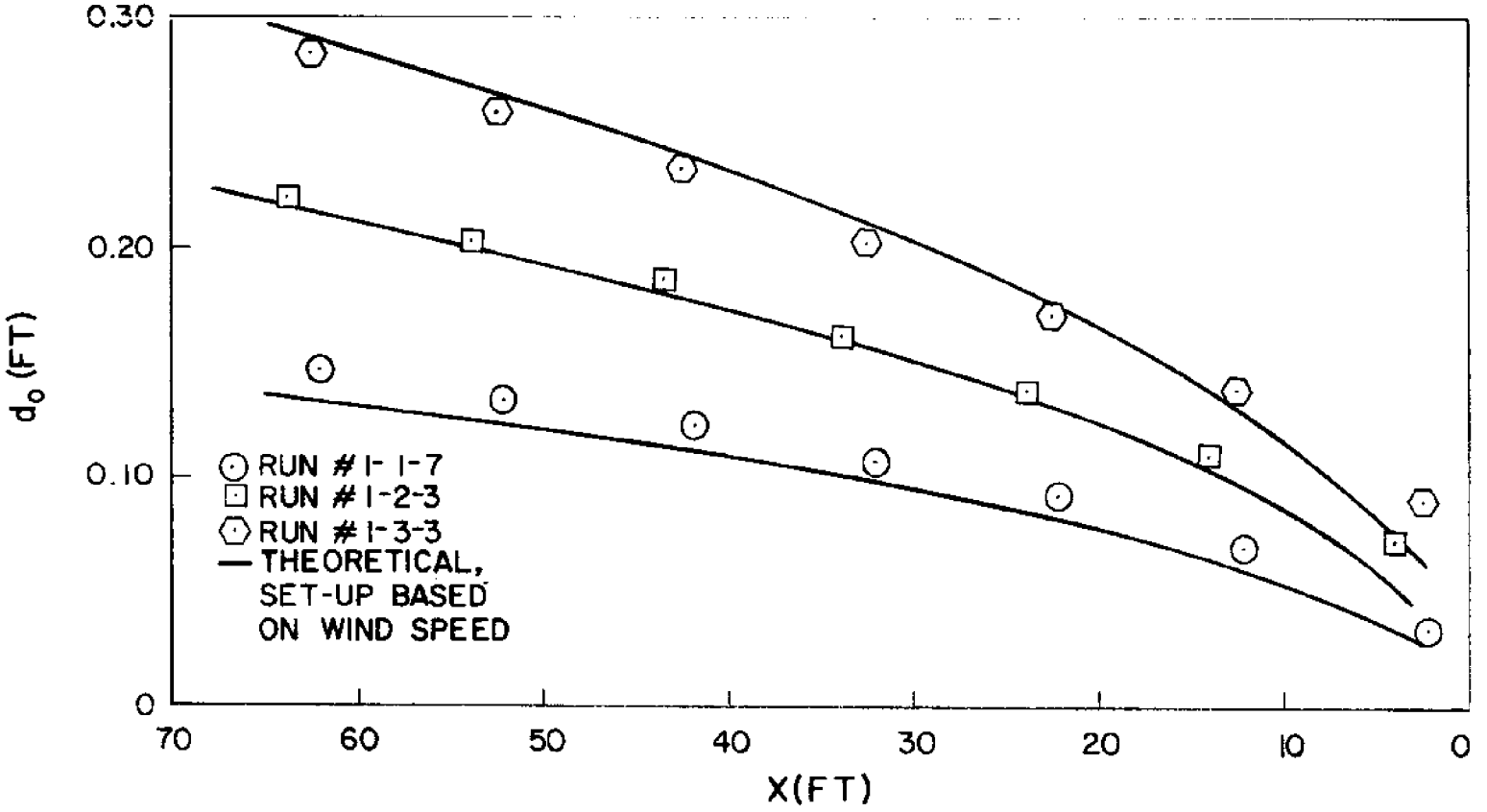

FIG. 20 - WIND SET-UP OF OIL.
OIL DEPTH VS. OIL FETCH, OIL NO. 1.

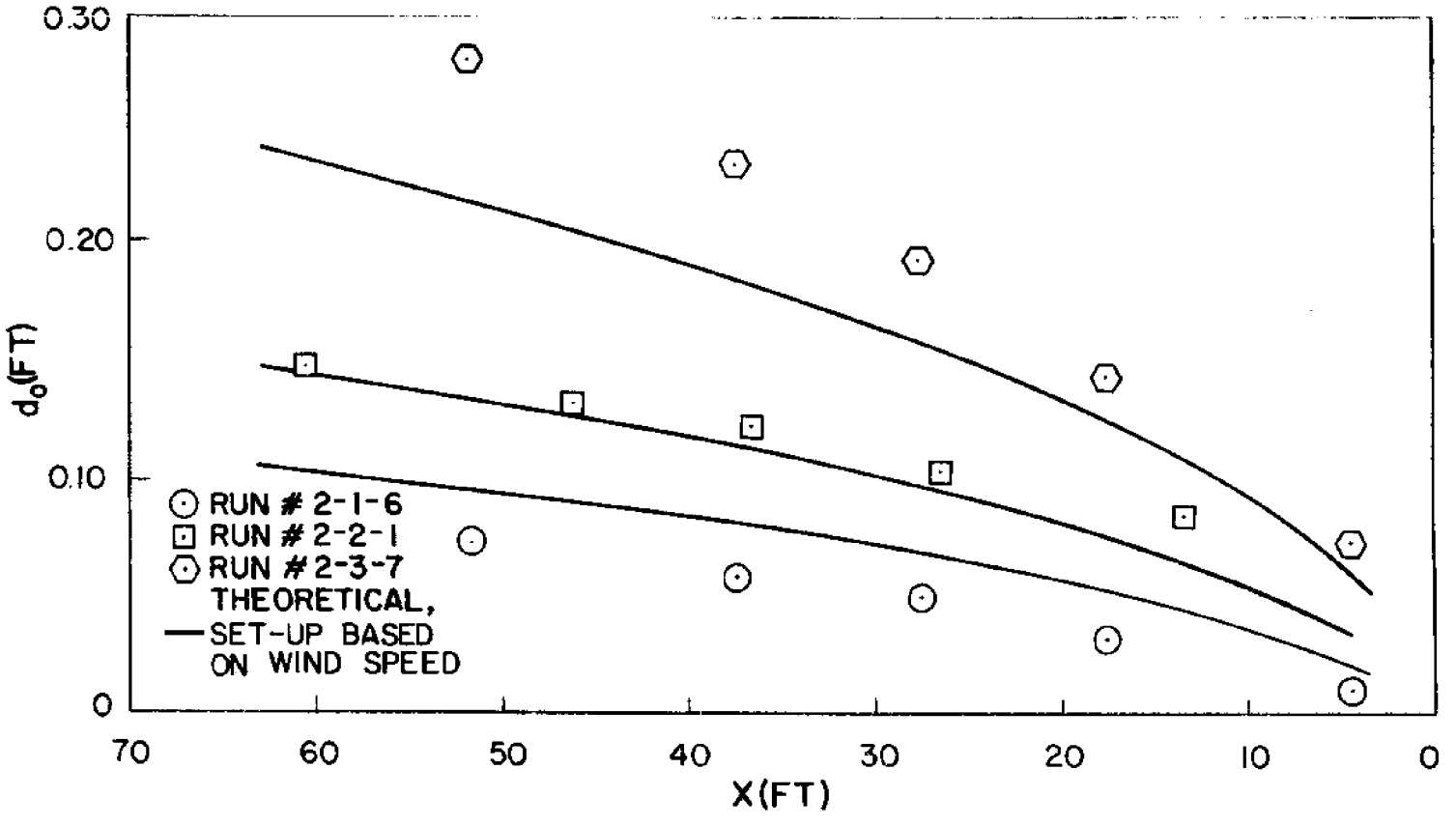

FIG. 21 - WIND SET-UP OF OIL.
OIL DEPTH VS. OIL FETCH, OIL NO. 2.

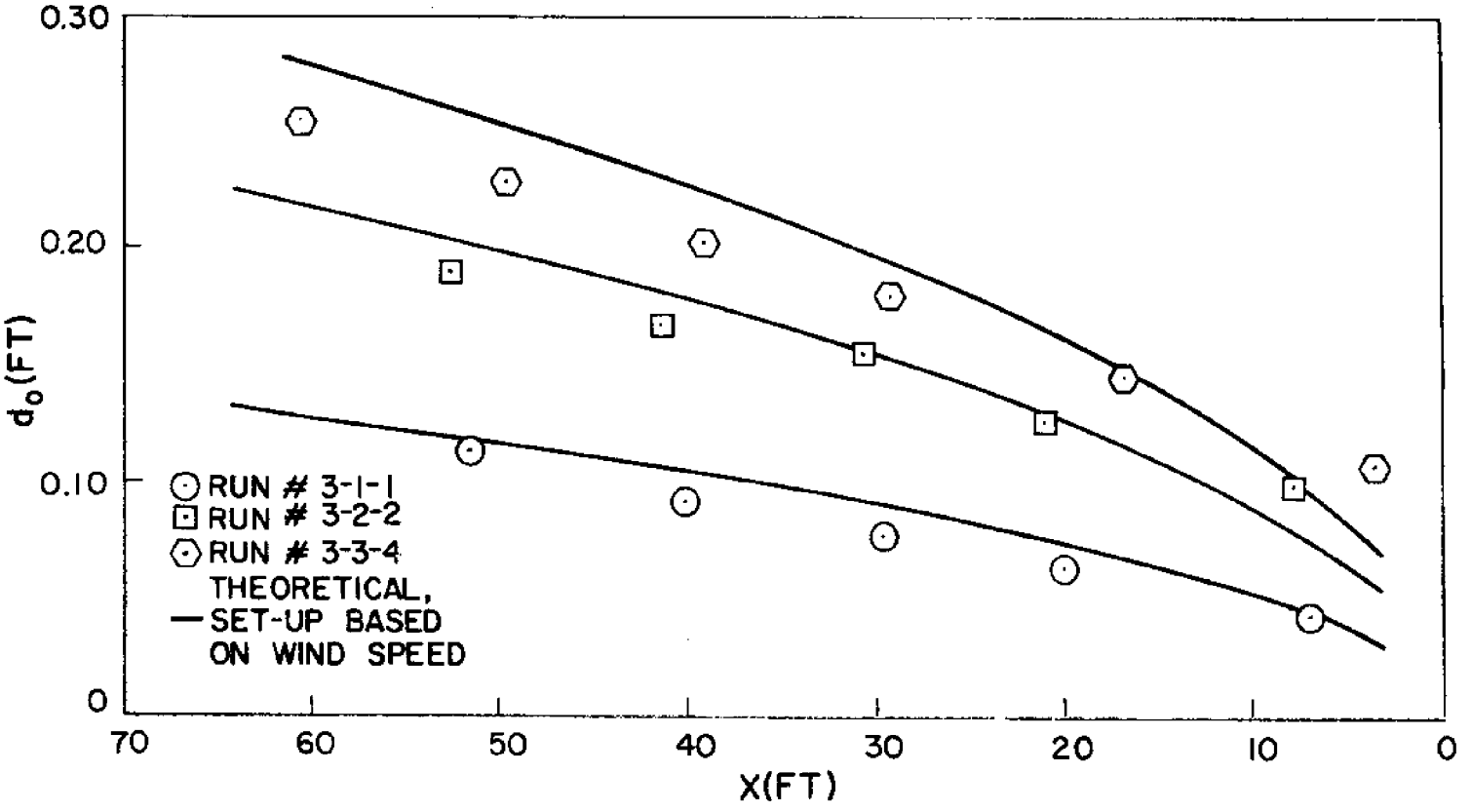

FIG. 22-WIND SET-UP OF OIL.
OIL DEPTH VS. OIL FETCH, OIL NO. 3.

used to calculate the oil depth for assumed values of L, using the run wind speed (taken at 0.7 ft elevation). The results of these calculations are the solid line in each of the figures. As can be seen, Eq. 69 closely predicts the set-up of oil, for any value of L, when no waves are generated in the oil.

Use of Eq. 69 fails however, when waves are generated in the oil. This is best seen in Fig. 21, run # 2 - 3 - 7. Using all terms in Eq. 69, which thereby predicts total set-up, and accounts for waves in the liquid, it is found that d_{o_t} = 0.422 ft at L = 50 ft. This compares favorably with the actual set-up of 0.283 ft at L = 51.67 ft. The constants B and U_c were obtained from Eqs. 111 and 112.

Run No. 3 - 3 - 10 was a run in which oil set-up was observed to be the results of wind and waves. The measured oil depth was 0.378 ft, at L = 39 ft. Using Eq. 69, for L = 39 ft the predicted set-up is 0.390 ft.

Based on the foregoing and other comparative calculations, it is believed that sufficient data were taken to substantiate the use of Eq. 69 for predicting the set-up of oil. However, additional work is believed necessary to validate the constants B and U_c, as associated with other oil viscosities.

It was stated previously that it was necessary to use a value of wind speed which represented the wind actually causing the set-up of the oil. Comparing the predicted set-up with the actual

set-up was one method of verifying the selected values of wind speed. It appears that the wind speeds selected were reasonably correct as the predicted set-up curves indicate in Figs. 20, 21 and 22.

Additional methods used to validate the wind profiles involves the comparison of shear stress as indicated by the set-up of oil and the shear stress based on the wind velocity profiles.

$$\tau_{s_d} = \frac{d_o^2 \, g \, \rho_o (1 - \frac{\rho_o}{\rho_w})}{2L}$$

was used to compute values of average shear stress based on oil depth and fetch length for each run. These values are tabulated in Appendix 5.

For comparison, the wind velocity profiles taken on the tank centerline at position No. 1, were plotted on semi-log paper, examples of which are shown in Fig. 23. As the boundary layer portion plots in a straight line, as predicted by the Karman-Prandtl relationship, Eq. 22,

$$\frac{U}{U_*} = \frac{2.3}{k_o} \log \frac{Y}{Y'}$$

it was possible to calculate the shear velocity using Eqs. 102 or 103. Then, using Eq. 104, the shear stress based on each wind velocity profile was calculated. These values are also tabulated in Appendix 5.

To present a graphic comparison between the two shear stresses,

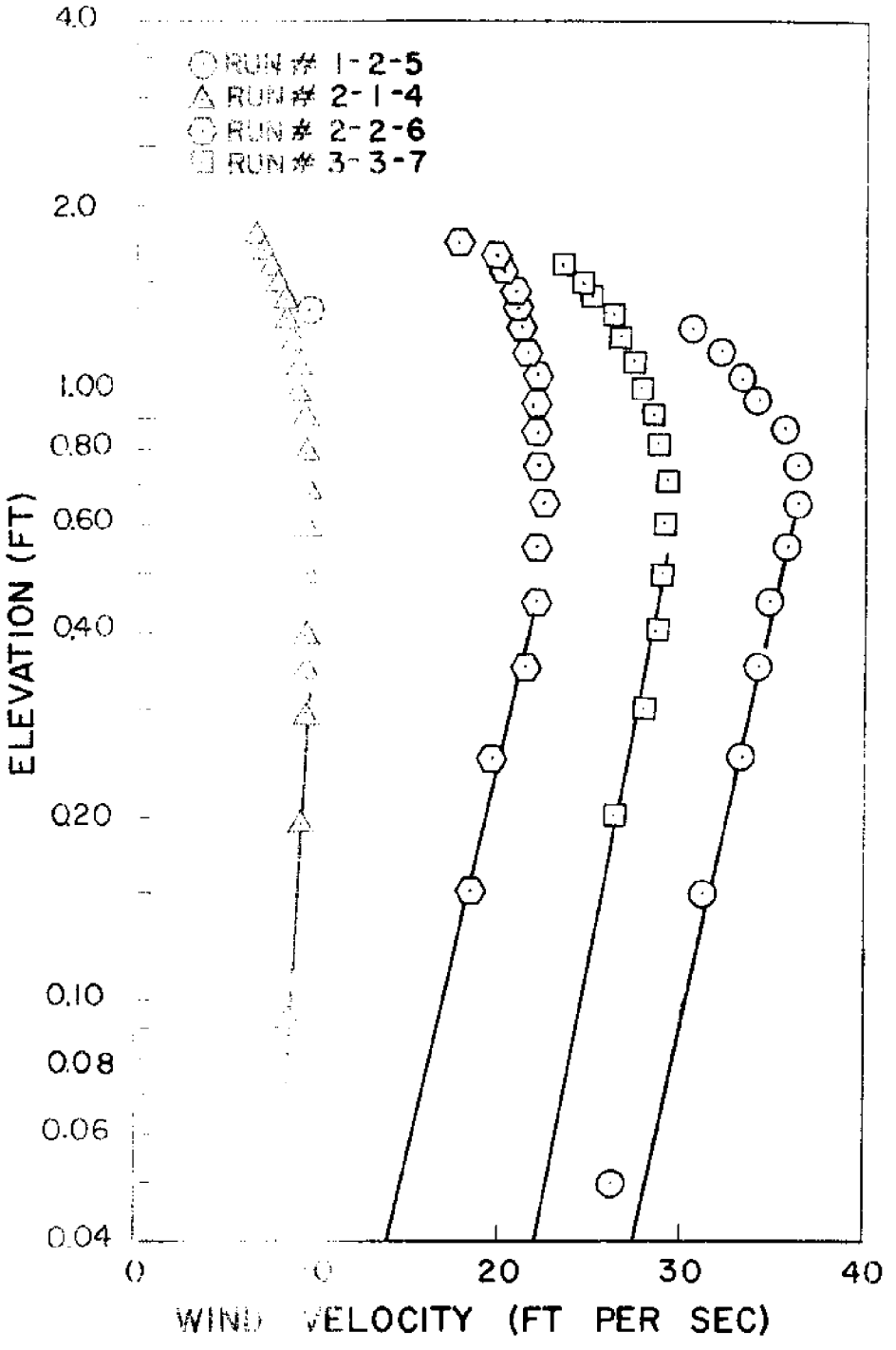

FIG. 23 - TYPICAL CENTERLINE VELOCITY PROFILES.

Fig. 24 was plotted showing τ_{s_d} versus τ_{s_w}. The results are as anticipated. Fig. 24 indicates that the shear stresses, based on the wind velocity profiles, are higher than the shear stresses based on oil set-up. As a correction factor was applied to all wind velocities used (and thereby achieving good comparison on the oil profile prediction curves), it follows that the centerline wind profiles were slightly higher in magnitude than the profile representative of the boundary layer caused by the actual shear stress.

The corrected values of wind velocity were used to calculate the dimensionless terms in Figs. 10, 11 and 12. From these plots, values of C for each oil were determined. Using these values of C, and the relationship $\tau_s = C \rho_w U^2$, taken from Eq. 63, values of shear stress were calculated. The results of these calculations were excellent and the shear stress values were similar to those obtained using Eq. 97. This procedure allowed a cross check of data calculations, a check on plotting of the data and finally a validation of the values of C as obtained from Figs. 10, 11 and 12.

As a final comparison, values of the wind stress coefficient C were calculated for τ_{s_d} and τ_{s_w}, for each run. This was done using Eq. 106,

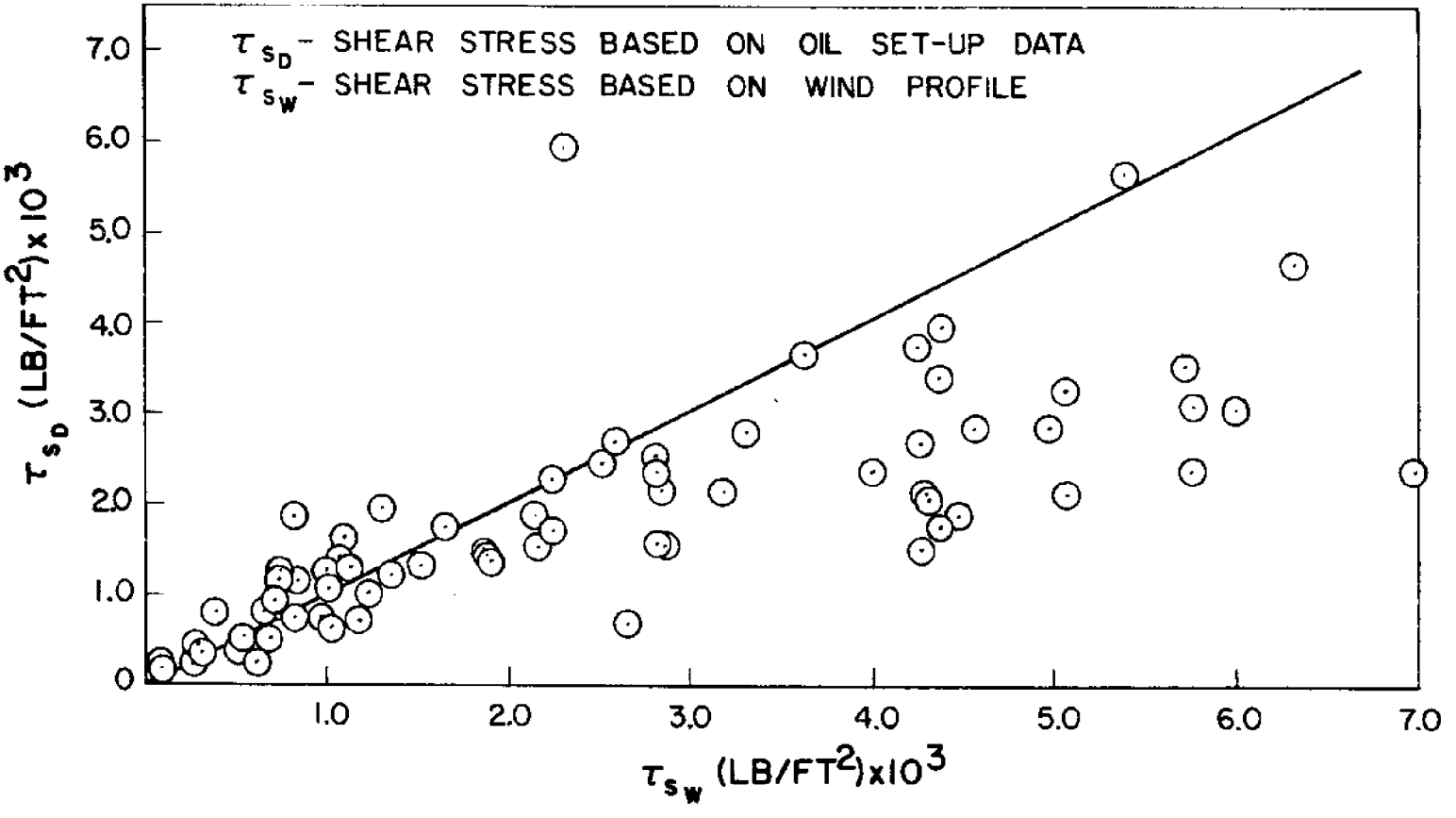

FIG. 24 - SHEAR STRESS BASED ON DATA AND WIND PROFILE

$$C = \frac{\tau}{\rho_a U^2}.$$

The values of C, for each oil, based on oil set-up data (T_{s_d}) were,

$$\text{Oil \# 1} \quad C = 1.412 \times 10^{-3}$$

$$\text{Oil \# 2} \quad C = 1.475 \times 10^{-3}$$

$$\text{Oil \# 3} \quad C = 1.537 \times 10^{-3} \quad \ldots\ldots\ldots (115)$$

The average for the three oils is $C = 1.474 \times 10^{-3}$.

The values of C, for each oil, based on the wind velocity profiles (T_{s_w}) were,

$$\text{Oil \# 1} \quad C = 2.542 \times 10^{-3}$$

$$\text{Oil \# 2} \quad C = 1.834 \times 10^{-3}$$

$$\text{Oil \# 3} \quad C = 1.689 \times 10^{-3} \quad \ldots\ldots (116)$$

The average for the three oils is $C = 2.025 \times 10^{-3}$.

Using the relationship developed by Wilson (3), for evaluating values of C, at Y = 30 ft the wind stress coefficients were found to be,

$$\text{Oil Set-Up Data} \quad C_{30} = 1.135 \times 10^{-3}$$

$$\text{Wind Profile Data} \quad C_{30} = 1.495 \times 10^{-3} \quad \ldots (117)$$

These values compare favorably with the values obtained by Wilson for light winds. His results were $C = 1.49 \times 10^{-3}$ with a standard deviation of 0.83×10^{-3}.

CHAPTER VII

CONCLUSIONS AND RECOMMENDATIONS

Conclusions

The following conclusions may be drawn from this investigation of set-up of oil on water by wind:

1. The amount of oil set-up against a barrier is a function of the wind stress on the smooth oil surface and when the wind exceeds a certain critical value (a function of oil viscosity) waves are produced and an additional set-up of oil occurs.
2. The total set-up of oil can be expressed by the equation, (Eq. 69)

$$d_{o_t} = \left[\frac{2KC\ \rho_w\ U^2 L}{\rho_o\ g'}\right]^{1/2} + \left[\frac{2B\ \rho_w\ L}{\rho_o\ g'}\right]^{1/2} (U - U_c).$$

3. The assumptions made in the development of Eq. 69 are basically correct.
4. The wind stress coefficients C, based on wind and oil set-up data, were found to compare closely with previously determined values for water set-up.
5. The wind-wave constant, B was determined to be a function of fluid viscosity and for the values of B calculated, it was found that a reasonably accurate prediction of set-up caused by wind and waves could be made.

Recommendations

It is believed that sufficient experimental work was conducted to validate the equations predicting set-up of oil without waves. However, because only three oils were tested, it is felt that insufficient data were taken to properly evaluate the wind-wave constant B and to achieve a valid relationship between oil viscosity and the critical wind velocity, U_c. Also, due to limitations in test procedure, additional testing should include more extensive evaluation of the data. Specifically, the following recommendations for any additional work in this general area are suggested toward improving the results and the technique. In addition, the following is intended as a self-criticism of the work accomplished:

1. Test at least two more oils in the 10-100 centistoke range and at least one between 100 and 400 centistokes. It is not believed necessary that consideration be given to oil density.
2. Conduct all tests using a constant water fetch length upwind of the oil wedge. This will ensure that any water waves generated will occur in the same fetch length regardless of the oil volume.
3. Use air flow straighteners both at air intake and discharge. This will prevent prerotation of the air entering the blower and create a more uniform air flow over the oil surface.

4. Conduct all tests with at least 3 ft of air space above the oil level. This should minimize the effect by the tank cover on the wind velocity profile.
5. Use the smoothest possible under surface for tank walls and top to prevent establishing large boundary layers.
6. Conduct extensive isovel determination, over the range of wind speeds used for testing, to allow proper correction factors to be applied to wind profile data.
7. Use a hot-wire anemometer for measuring wind velocity profiles (and isovels) to obtain more accurate profile information and speed up data taking and reduction.
8. Measure wave height and period spectra of waves in the water and oil fetches to determine effects of oil viscosity and density on wave damping.

REFERENCES

1 G. H. Keulegan, "Wind Tides in Small Closed Channels," Research Paper 2207, Journal of Research of the National Bureau of Standards, Vol. 46, No. 5, May 1951.

2 W. G. Van Dorn, "Wind Stress on an Artificial Pond," Journal of Marine Research, Vol. 12, No. 3, 1953.

3 B. W. Wilson, "Note on Surface Wind Stress over Water at Low and High Wind Speeds," Journal of Geophysical Research, Vol. 65, No. 10, October, 1960.

4 R. O. Reid and B. R. Bodine, "Numerical Model for Storm Surges in Galveston Bay," Journal of the Waterways and Harbors Division, Proc. ASCE, Vol. 94, No. WW1, February, 1968.

5 C. L. Bretschneider and J. I. Collins, "Prediction of Hurricane Surge, an Investigation for Corpus Christi, Texas, and Vicinity," Technical Report, Contract No. DA-41-243-CIVENG-63-69, by National Engineering Science Co., Washington, D.C.

6 T. Saville, Jr., "Wind Set-up and Waves in Shallow Water," Beach Erosion Board Technical Memorandum, No. 27, 1953.

7 Belly, Pierre- Yves, "Sand Movement by Wind," U.S. Army Coastal Engineering Research Center Technical Memorandum, No. 1, January, 1964.

8 K. Horikawa and H. W. Shen, "Sand Movement by Wind Action (on the Characteristics of Sand Traps)," Beach Erosion Board Technical Memorandum, No. 119, August, 1960.

9 R. A. Bagnold, "The Physics of Blown Sand and Desert Dunes," Methuen and Co. Ltd., London, 1954.

10 W. D. Von Gonten, Personal Communication, January, 1970.

APPENDIX 1

VELOCITY PROFILES

Run # 1-1-1

U (fps)	26.30	29.80	30.10	31.50	32.50	31.90	31.10
y (ft)	0.088	0.188	0.288	0.388	0.488	0.588	0.688
	31.95	31.48	30.37	28.84	28.35	27.21	10.00
	0.788	0.888	0.988	1.088	1.188	1.288	1.388

Run # 1-1-2

U (fps)	24.50	27.40	28.53	28.55	30.20	30.20	29.01
y (ft)	0.088	0.188	0.288	0.388	0.488	0.588	0.688
	29.15	29.18	27.90	27.02	26.10	24.60	11.60
	0.788	0.888	0.988	1.088	1.188	1.288	1.388

Run # 1-1-3

U (fps)	21.78	24.65	25.06	26.22	26.44	26.22	26.47
y (ft)	0.088	0.188	0.288	0.388	0.488	0.588	0.688
	27.20	26.03	25.30	25.29	23.80	21.15	12.20
	0.788	0.888	0.988	1.088	1.188	1.288	1.388

Run # 1-1-4

U (fps)	20.20	22.55	23.20	23.60	23.90	24.17	24.55
y (ft)	0.088	0.188	0.288	0.388	0.488	0.588	0.688
	24.55	24.00	23.60	22.41	21.82	20.92	11.23
	0.788	0.888	0.988	1.088	1.188	1.288	1.388

Run # 1-1-5

U (fps)	16.90	19.00	20.10	20.48	20.48	20.75	20.95
y (ft)	0.088	0.188	0.288	0.388	0.488	0.588	0.688
	21.00	20.75	20.37	19.40	18.00	17.50	10.37
	0.788	0.888	0.988	1.088	1.188	1.288	1.388

Run # 1-1-6

U (fps)	14.38	16.00	17.13	17.50	18.46	18.10	18.40
y (ft)	0.088	0.188	0.288	0.388	0.488	0.588	0.688
	18.30	18.40	18.40	17.58	16.75	16.75	9.51
	0.788	0.888	0.988	1.088	1.188	1.288	1.388

Run # 1-1-7

U (fps)	12.36	13.91	14.55	14.12	15.62	15.35	15.90
y (ft)	0.088	0.188	0.288	0.388	0.488	0.588	0.688
	16.05	16.05	15.62	14.40	14.30	12.22	6.47
	0.788	0.888	0.988	1.088	1.188	1.288	1.388

Run # 1-1-8

U (fps)		35.40	37.60	38.95	38.85	38.40	37.42
y (ft)		0.188	0.288	0.388	0.488	0.588	0.688
	36.40	34.75	33.60	32.60	31.20	30.80	17.52
	0.788	0.888	0.988	1.088	1.188	1.288	1.388

Run # 1-1-9

U (fps)		35.20	36.65	37.05	36.90	36.40	34.40
y (ft)		0.188	0.288	0.388	0.488	0.588	0.688
	32.80	33.20	31.80	30.80	30.20	28.50	12.58
	0.788	0.888	0.988	1.088	1.188	1.288	1.388

Run # 1-1-10

U (fps)	28.72	32.70	35.08	35.20	34.08	35.40	35.80
y (ft)	0.088	0.188	0.288	0.388	0.488	0.588	0.688
	34.06	33.10	31.95	31.10	29.60	29.25	12.95
	0.788	0.888	0.988	1.088	1.188	1.288	1.388

Run # 1-2-1

U (fps)	23.90	29.20	30.62	32.40	32.93	33.80	34.40
y (ft)	0.050	0.150	0.250	0.350	0.450	0.550	0.650
	34.40	34.05	33.50	32.40	31.21	31.19	19.30
	0.750	0.850	0.950	1.050	1.150	1.250	1.350

Run # 1-2-2

U (fps)	23.02	25.03	28.20	29.70	30.60	31.40	31.10
y (ft)	0.050	0.150	0.250	0.350	0.450	0.550	0.650
	31.10	30.80	30.15	28.96	28.[illegible]	26.50	15.30
	0.750	0.850	0.950	1.050	[illegible]	1.250	1.350

Run # 1-2-3

U (fps)	19.20	23.40	24.85	25.70	26.60	27.40	28.80
y (ft)	0.050	0.150	0.255	0.355	0.455	0.555	0.655
	28.60	27.20	26.92	26.00	25.60	23.00	15.40
	0.750	0.850	0.950	1.050	1.150	1.250	1.350

Run # 1-2-4 (a)

U (fps)	17.90	21.10	22.05	22.80	23.20	24.12	24.15
y (ft)	0.050	0.150	0.250	0.350	0.450	0.550	0.650
	24.12	24.01	23.80	23.10	22.20	19.22	12.74
	0.750	0.850	0.950	1.050	1.150	1.250	1.350

Run # 1-2-4 (b)

U (fps)	17.90	21.30	22.20	23.15	24.00	24.10	24.80
y (ft)	0.050	0.150	0.250	0.350	0.450	0.550	0.650
	24.75	24.20	23.90	23.05	22.30	21.40	16.85
	0.750	0.850	0.950	1.050	1.150	1.250	1.350

Run # 1-2-5

U (fps)	26.20	31.40	33.38	34.35	34.80	35.78	36.30
y (ft)	0.050	0.150	0.250	0.350	0.450	0.550	0.650
	36.22	35.61	34.02	33.29	32.10	30.70	9.72
	0.750	0.850	0.950	1.050	1.150	1.250	1.350

Run # 1-2-6

U (fps)	27.8[illegible]	[illegible].08	36.00	36.60	37.30	37.18	36.80
y (ft)	0.05[illegible]	[illegible].150	0.250	0.350	0.450	0.550	0.650
	35.6[illegible]	[illegible].40	33.80	32.90	31.60	30.20	11.02
	0.75[illegible]	[illegible].850	0.950	1.050	1.150	1.250	1.350

Run # 1-2-7

U (fps)		[illegible].00	37.00	38.05	39.03	39.05	38.04
y (ft)		[illegible].150	0.250	0.350	0.450	0.550	0.650
	37.[illegible]	[illegible].58	34.60	33.45	32.20	31.40	9.72
	0.75[illegible]	[illegible].850	0.950	1.050	1.150	1.250	1.350

Run # 1-3-1

U (fps)	20.71	21.70	26.61	27.70	28.40	29.10	29.58
y (ft)	0.050	0.150	0.250	0.350	0.450	0.550	0.650
	29.42	29.20	28.60	27.60	26.90	25.82	10.47
	0.750	0.850	0.950	1.050	1.150	1.250	1.350

Run # 1-3-2

U (fps)	21.50	26.60	28.40	28.65	29.70	30.12	30.70
y (ft)	0.050	0.150	0.250	0.350	0.450	0.550	0.650
	30.60	30.09	29.30	28.60	27.60	26.40	8.20
	0.750	0.850	0.950	1.050	1.150	1.250	1.350

Run # 1-3-3

U (fps)	23.70	23.80	29.70	30.80	31.60	32.00	32.10
y (ft)	0.050	0.150	0.250	0.350	0.450	0.550	0.650
	31.40	31.60	31.00	30.04	28.95	27.20	11.08
	0.750	0.850	0.950	1.050	1.150	1.250	1.350

Run # 1-3-4

U (fps)	24.25	28.10	31.30	33.10	33.28	33.65	33.80
y (ft)	0.050	0.150	0.250	0.350	0.450	0.550	0.650
	33.70	33.28	32.40	31.58	30.20	28.90	11.90
	0.750	0.850	0.950	1.050	1.150	1.250	1.350

Run # 1-3-5

U (fps)	23.90	30.40	32.00	33.60	34.20	34.75	35.40
y (ft)	0.050	0.150	0.250	0.350	0.450	0.550	0.650
	36.95	35.45	34.20	33.40	32.40	30.50	21.60
	0.750	0.850	0.950	1.050	1.150	1.250	1.350

Run # 1-3-6

U (fps)	24.95	31.82	33.40	35.20	36.00	36.90	37.10
y (ft)	0.050	0.150	0.250	0.350	0.450	0.550	0.650
	36.90	36.50	35.60	34.80	33.30	32.00	29.60
	0.750	0.850	0.950	1.050	1.150	1.250	1.350

Run

U	34.30	35.90	36.90	37.80	38.35	38.50
y	0.150	0.250	0.350	0.450	0.550	0.650
	37.90	37.10	35.50	34.60	32.90	17.22
	0.850	0.950	1.050	1.150	1.250	1.350

Run

U	34.20	35.90	36.60	39.20	39.55	39.95
y	0.150	0.250	0.350	0.450	0.550	0.650
	39.20	38.05	37.30	35.82	34.40	14.55
	0.850	0.950	1.050	1.150	1.250	1.350

Run

U	34.60	37.40	39.60	40.49	40.40	40.25
y	0.150	0.250	0.350	0.450	0.550	0.650
	38.80	37.20	36.20	35.21	34.06	10.08
	0.850	0.950	1.050	1.150	1.250	1.350

Run

U	33.70	37.20	40.60	40.95	41.15	41.08
y	0.150	0.250	0.350	0.450	0.550	0.650
	39.40	38.60	37.65	37.00	36.20	15.50
	0.850	0.950	1.050	1.150	1.250	1.350

Run # 2-1-1

U (fps)	7.04	7.66	7.94	7.94	7.94	7.94	7.94	7.66	7.66
y (ft)	0.094	0.194	0.294	0.394	0.494	0.594	0.694	0.794	0.894
	7.66	7.66	7.94	7.66	7.36	7.04	6.72	6.38	6.38
	0.994	1.094	1.194	1.294	1.394	1.494	1.594	1.694	1.794

Run # 2-1-2

U (fps)	7.36	8.21	8.21	8.21	8.50	8.50	8.21	8.21	7.94
y (ft)	0.094	0.194	0.294	0.394	0.494	0.594	0.694	0.794	0.894
	7.66	7.94	7.66	7.66	7.66	7.36	7.04	6.72	6.38
	0.994	1.094	1.194	1.294	1.394	1.494	1.594	1.694	1.794

Run # 2-1-3

U (fps)	8.50	8.76	8.76	8.76	8.76	9.02	9.02	9.02	9.02
y (ft)	0.094	0.194	0.294	0.394	0.494	0.594	0.694	0.794	0.894
	8.76	8.50	8.50	8.21	8.21	7.94	7.66	7.36	6.72
	0.994	1.094	1.194	1.294	1.394	1.494	1.594	1.694	1.794

Run # 2-1-4

U (fps)	8.76	9.26	9.51	9.51	9.51	9.51	9.51	9.51	9.51
y (ft)	0.094	0.194	0.294	0.394	0.494	0.594	0.694	0.794	0.894
	9.26	9.02	9.02	8.76	8.50	8.21	7.94	7.66	7.04
	0.994	1.094	1.194	1.294	1.394	1.494	1.594	1.694	1.794

Run # 2-1-5

U (fps)	7.36	8.21	8.76	9.72	9.72	9.72	9.72	9.51	9.51
y (ft)	0.094	0.194	0.294	0.394	0.494	0.594	0.694	0.794	0.894
	9.26	8.76	9.26	8.76	8.76	8.76	7.66	7.66	7.04
	0.994	1.094	1.194	1.294	1.394	1.494	1.594	1.694	1.794

Run # 2-1-6

U (fps)	9.51	9.51	8.50	10.40	11.62	11.23	11.23	11.62	9.51
y (ft)	0.094	0.194	0.294	0.394	0.494	0.594	0.694	0.794	0.894
	9.02	9.02	11.23	9.51	10.82	9.51	9.02	10.40	9.51
	0.994	1.094	1.194	1.294	1.394	1.494	1.594	1.694	1.794

(continued Run # 2-1-6)

	8.50
	1.894

Run # 2-1-7

U (fps)	6.70	9.02	10.82	9.96	9.51	9.96	9.02	10.82	8.50
y (ft)	0.080	0.180	0.280	0.380	0.480	0.580	0.680	0.780	0.880
	10.40	9.96	9.51	10.82	10.82	9.96	9.51	9.51	8.50
	0.980	1.080	1.180	1.280	1.380	1.480	1.580	1.680	1.780
	7.36								
	1.880								

Run # 2-1-8

U (fps)	9.96	11.23	12.02	12.02	12.40	12.40	11.62	11.62	11.62
y (ft)	0.080	0.180	0.280	0.380	0.480	0.580	0.680	0.780	0.880
	12.40	11.23	11.23	10.82	9.96	9.96	9.51	9.02	7.94
	0.980	1.080	1.180	1.280	1.380	1.480	1.580	1.680	1.780

Run # 2-1-9

U (fps)	10.82	13.45	14.08	14.40	14.40	14.08	14.40	13.45	13.45
y (ft)	0.080	0.180	0.280	0.380	0.480	0.580	0.680	0.780	0.880
	13.75	13.08	13.75	13.08	13.08	12.73	12.02	11.23	9.51
	0.980	1.080	1.180	1.280	1.380	1.480	1.580	1.680	1.780

Run # 2-1-10

U (fps)	13.45	15.60	16.19	16.47	16.47	16.19	16.19	15.89	15.89
y (ft)	0.080	0.180	0.280	0.380	0.480	0.580	0.680	0.780	0.880
	15.89	15.60	15.60	15.01	14.70	14.40	13.75	13.08	12.40
	0.980	1.080	1.180	1.280	1.380	1.480	1.580	1.680	1.780

Run # 2-2-1

U (fps)	14.70	16.19	16.73	17.00	16.73	16.73	16.73	16.47	16.47
y (ft)	0.10	0.20	0.30	0.40	0.50	0.60	0.70	0.80	0.90

16.73	15.89	15.60	15.30	15.01	14.08	13.45	11.62
1.00	1.10	1.20	1.30	1.40	1.50	1.60	1.70

Run # 2-2-2

U (fps)	15.88	17.50	17.78	18.26	18.26	18.54	18.26	17.97	17.78
y (ft)	0.10	0.20	0.30	0.40	0.50	0.60	0.70	0.80	0.90

17.50	15.70	17.31	16.74	15.88	15.31	14.46	12.74
1.00	1.10	1.20	1.30	1.40	1.50	1.60	1.70

Run # 2-2-3

U (fps)	17.50	18.73	19.21	19.21	19.21	19.02	19.21	19.02	18.54
y (ft)	0.150	0.250	0.350	0.450	0.550	0.650	0.750	0.850	0.950

18.26	17.97	17.78	17.50	17.02	15.88	15.02	13.12
1.050	1.150	1.250	1.350	1.450	1.550	1.650	1.750

Run # 2-2-4

U (fps)	18.54	19.11	20.35	20.35	20.35	20.35	20.35	20.35	19.50
y (ft)	0.150	0.250	0.350	0.450	0.550	0.650	0.750	0.850	0.950

19.02	19.02	18.26	17.97	17.78	17.31	15.88	14.46
1.050	1.150	1.250	1.350	1.450	1.550	1.650	1.750

Run # 2-2-5

U (fps)	19.68	21.68	22.35	22.06	22.06	22.06	22.35	21.68	21.49
y (ft)	0.150	0.250	0.350	0.450	0.550	0.650	0.750	0.850	0.950

21.30	20.83	20.35	19.97	19.50	18.54	17.50	15.88
1.050	1.150	1.250	1.350	1.450	1.550	1.650	1.750

Run # 2-2-6

U (fps)	18.54	19.47	21.49	22.06	22.06	22.35	22.06	22.06	22.06
y (ft)	0.150	0.250	0.350	0.450	0.550	0.650	0.750	0.850	0.950

22.35	21.87	21.49	21.30	21.02	20.35	19.97	17.97
1.050	1.150	1.250	1.350	1.450	1.550	1.650	1.750

Run # 2-2-7

U (fps)	21.68			24.89	25.20	25.30	25.49	25.49	25.30
y (ft)	0.150	0.250	0.350	0.450	0.550	0.650	0.750	0.850	0.950

24.62	24.89	24.25	23.68	22.92	21.51	20.64	19.02	
1.050	1.150	1.250	1.350	1.450	1.550	1.650	1.750	

Run # 2-2-8

U (fps)	20.64	22.11	23.87	24.25	25.49	25.68	25.68	25.87	25.68
y (ft)	0.150	0.250	0.350	0.450				0.850	0.950

25.49	25.49	24.89	25.01	24.06	21.68	22.11	19.68	
1.050	1.150	1.250	1.350	1.450	1.550	1.650	1.750	

Run # 2-2-9

U (fps)			27.39	28.34	28.68	28.68	28.82	28.53
y (ft)	0	0.250	0.350	0.450	0.550	0.650	0.850	0.950

28.24	28.39	28.20	26.91	25.87	25.61	23.68	21.49	
1.050	1.150	1.250	1.350	1.450	1.550	1.650	1.750	

Run # 2-3-1

U (fps)	20.12	21.65	22.45	23.05	23.05	22.87	22.87	22.65
y (ft)	0.150	0.250	0.350	0.450	0.550	0.650	0.750	0.850
	22.22	21.90	21.02	21.02	20.80	19.45	18.50	17.00
	0.950	1.050	1.150	1.250	1.350	1.450	1.550	1.650

Run # 2-3-2

U (fps)	21.22	22.65	23.80	24.00	24.00	23.80	23.80	23.41
y (ft)	0.150	0.250	0.350	0.450	0.550	0.650	0.750	0.850
	22.47	22.22	22.08	21.43	21.02	20.38	19.45	18.50
	0.950	1.050	1.150	1.250	1.350	1.450	1.550	1.650

Run # 2-3-3

U (fps)	22.87	24.60	25.30	25.80	25.80	25.80	25.42	25.15
y (ft)	0.150	0.250	0.350	0.450	0.550	0.650	0.750	0.850
	24.60	24.20	23.61	23.41	22.87	22.22	20.60	19.45
	0.950	1.050	1.150	1.250	1.350	1.450	1.550	1.650

Run # 2-3-4

U (fps)	20.38	22.45	23.61	24.60	25.00	25.15	25.15	25.00
y (ft)	0.150	0.250	0.350	0.450	0.550	0.650	0.750	0.850
	24.80	24.80	24.80	24.20	24.00	23.61	22.45	21.22
	0.950	1.050	1.150	1.250	1.350	1.450	1.550	1.650

Run # 2-3-5

U (fps)	23.41	25.15	26.55	27.68	27.55	27.20	27.20	26.65
y (ft)	0.150	0.250	0.350	0.450	0.550	0.650	0.750	0.850
	26.00	25.61	25.00	24.60	24.00	23.41	22.45	21.02
	0.950	1.050	1.150	1.250	1.350	1.450	1.550	1.650

Run # 2-3-6

U (fps)	23.61	25.42	26.65	27.38	27.68	27.82	27.55	27.00
y (ft)	0.150	0.250	0.350	0.450	0.550	0.650	0.750	0.850
	26.65	26.20	25.42	25.15	24.40	23.22	22.45	21.22
	0.950	1.050	1.150	1.250	1.350	1.450	1.550	1.650

Run # 2-3-7

U (fps)	23.22	25.15	27.55	28.53	28.80	28.80	28.53	28.02
y (ft)	0.150	0.250	0.350	0.450	0.550	0.650	0.750	0.850
	27.55	27.00	26.55	26.00	25.15	24.40	23.61	22.08
	0.950	1.050	1.150	1.250	1.350	1.450	1.550	1.650

Run # 2-3-8

U (fps)	22.22	24.00	25.42	26.20	27.20	27.68	27.68	27.68
y (ft)	0.150	0.250	0.350	0.450	0.550	0.650	0.750	0.850
	27.38	27.38	27.20	26.55	26.60	24.42	24.80	22.87
	0.950	1.050	1.150	1.250	1.350	1.450	1.550	1.650

Run # 2-3-9

U (fps)	27.00	28.61	29.77	30.30	30.45	30.02	29.59	29.10
y (ft)	0.150	0.250	0.350	0.450	0.550	0.650	0.750	0.850
	28.61	28.61	28.02	27.82	27.20	26.20	24.80	23.61
	0.950	1.050	1.150	1.250	1.350	1.450	1.550	1.650

Run # 3-1-1

U (fps)	8.50	9.97	10.40	10.40	10.40	10.40	10.82	10.40	10.40
y (ft)	0.05	0.15	0.25	0.35	0.45	0.55	0.65	0.75	0.85

10.40	10.40	10.40	10.40	9.00	9.00	8.50	7.45
0.95	1.05	1.15	1.25	1.35	1.45	1.55	1.65

Run # 3-1-2

U (fps)	10.40	12.04	12.40	12.04	12.04	12.40	12.40	12.40	12.63
y (ft)	0.05	0.15	0.25	0.35	0.45	0.55	0.65	0.75	0.85

11.25	12.04	11.25	11.75	11.25	10.82	10.40	8.50
0.95	1.05	1.15	1.25	1.35	1.45	1.55	1.65

Run # 3-1-3

U (fps)	12.04	14.10	14.40	14.40	14.40	14.40	14.40	14.40	14.10
y (ft)	0.05	0.15	0.25	0.35	0.45	0.55	0.65	0.75	0.85

13.77	13.45	13.45	12.72	12.40	12.40	12.40	10.82
0.95	1.05	1.15	1.25	1.35	1.45	1.55	1.65

Run # 3-1-4

U (fps)	15.35	17.50	18.50	18.50	18.50	18.50	18.50	18.50	18.00
y (ft)	0.05	0.15	0.25	0.35	0.45	0.55	0.65	0.75	0.85

17.50	16.72	16.20	16.20	15.90	15.35	15.01	14.10
0.95	1.05	1.15	1.25	1.35	1.45	1.55	1.65

Run # 3-1-5

U (fps)	17.00	18.50	19.95	19.95	19.95	19.50	19.27	19.02	19.02
y (ft)	0.05	0.15	0.25	0.35	0.45	0.55	0.65	0.75	0.85

19.02	18.50	18.00	17.50	17.80	16.72	15.90	15.35
0.95	1.05	1.15	1.25	1.35	1.45	1.55	1.65

Run # 3-1-6

U (fps)		20.80	21.30	22.10	22.10	22.10	22.10	21.65	21.65
y (ft)		0.15	0.25	0.35	0.45	0.55	0.65	0.75	0.85

21.42	21.30	20.80	20.40	20.40	19.27	19.02	17.80
0.95	1.05	1.15	1.25	1.35	1.45	1.55	1.65

Run # 3-1-7

U (fps)	21.87	23.85	24.40	24.90	24.90	24.65	24.40	23.65
y (ft)	0.15	0.25	0.35	0.45	0.55	0.65	0.75	0.85

23.65	23.45	22.50	22.30	21.87	21.65	21.00	20.19
0.95	1.05	1.15	1.25	1.35	1.45	1.55	1.65

Run # 3-1-8

U (fps)	24.40	26.35	27.20	28.00	28.15	28.15	28.28	27.65
y (ft)	0.15	0.25	0.35	0.45	0.55	0.65	0.75	0.85

27.20	27.20	26.57	25.70	25.15	23.85	23.30	22.90
0.95	1.05	1.15	1.25	1.35	1.45	1.55	1.65

Run # 3-1-9

U (fps)	24.90	27.90	28.53	29.25	29.25	29.25	29.25	28.80
y (ft)	0.15	0.25	0.35	0.45	0.55	0.65	0.75	0.85

28.28	28.15	28.00	27.87	27.90	26.57	26.20	24.40
0.95	1.05	1.15	1.25	1.35	1.45	1.55	1.65

Run # 3-2-1

U (fps)	17.90	18.40	18.62	18.62	18.62	18.62	18.40	18.62
y (ft)	0.10	0.20	0.30	0.40	0.50	0.60	0.70	0.80
	18.83	18.15	17.90	16.85	16.85	16.05	15.75	14.84
	0.90	1.00	1.10	1.20	1.30	1.40	1.50	1.60

Run # 3-2-2

U (fps)	19.35	19.77	20.25	19.77	20.09	19.77	19.77	19.65
y (ft)	0.10	0.20	0.30	0.40	0.50	0.60	0.70	0.80
	19.65	19.65	18.62	18.15	18.15	16.84	16.30	15.18
	0.90	1.00	1.10	1.20	1.30	1.40	1.50	1.60

Run # 3-2-3

U (fps)	20.93	21.45	21.55	21.55	21.55	21.55	21.45	21.19
y (ft)	0.10	0.20	0.30	0.40	0.50	0.60	0.70	0.80
	20.93	20.93	20.50	19.77	19.35	18.88	17.65	17.15
	0.90	1.00	1.10	1.20	1.30	1.40	1.50	1.60

Run # 3-2-4

U (fps)	20.43	21.75	22.05	22.05	22.05	22.05	21.55	21.45
y (ft)	0.10	0.20	0.30	0.40	0.50	0.60	0.70	0.80
	20.43	20.71	20.71	20.71	20.22	19.77	18.83	18.40
	0.90	1.00	1.10	1.20	1.30	1.40	1.50	1.60

Run # 3-2-5

U (fps)	22.75	24.25	24.42	24.42	24.42	24.25	24.25	24.25
y (ft)	0.10	0.20	0.30	0.40	0.50	0.60	0.70	0.80
	24.25	23.90	23.72	23.55	22.98	22.05	21.19	20.22
	0.90	1.00	1.10	1.20	1.30	1.40	1.50	1.60

Run # 3-2-6

U (fps)	23.35	25.10	25.75	26.22	26.10	25.55	25.90	25.90
y (ft)	0.10	0.20	0.30	0.40	0.50	0.60	0.70	0.80
	25.75	24.82	24.42	24.25	23.35	22.75	22.05	20.71
	0.90	1.00	1.10	1.20	1.30	1.40	1.50	1.60

Run # 3-2-7

U (fps)	24.42	26.21	26.91	27.10	27.42	27.42	27.42	26.48
y (ft)	0.10	0.20	0.30	0.40	0.50	0.60	0.70	0.80
	26.21	26.10	25.10	25.10	24.42	23.55	22.75	21.55
	0.90	1.00	1.10	1.20	1.30	1.40	1.50	1.60

Run # 3-2-8

U (fps)	24.25	26.43	27.75	28.08	28.08	28.08	27.96	27.75
y (ft)	0.10	0.20	0.30	0.40	0.50	0.60	0.70	0.80
	27.42	27.42	27.10	26.43	25.35	24.25	23.72	22.57
	0.90	1.00	1.10	1.20	1.30	1.40	1.50	1.60

Run # 3-2-9

U (fps)		28.70	28.90	30.08	30.20	30.20	30.08	29.60
y (ft)		0.20	0.30	0.40	0.50	0.60	0.70	0.80
	29.42	29.31	28.75	28.66	28.00	26.91	25.75	29.75
	0.90	1.00	1.10	1.20	1.30	1.40	1.50	1.60

Run # 3-2-10

U (fps)		27.42	30.43	31.50	31.80	31.80	31.90	31.80
y (ft)		0.20	0.30	0.40	0.50	0.60	0.70	0.80
	31.16	30.55	30.43	30.20	30.08	28.90	29.31	27.18
	0.90	1.00	1.10	1.20	1.30	1.40	1.50	1.60

Run # 3-3-1

U (fps)	21.65	22.96	23.05	23.30	23.30	22.96	22.50	22.10
y (ft)	0.10	0.20	0.30	0.40	0.50	0.60	0.70	0.80
	21.30	21.65	21.00	21.00	20.60	20.40	19.50	18.80
	0.90	1.00	1.10	1.20	1.30	1.40	1.50	1.60

Run # 3-3-2

U (fps)	22.96	24.05	24.65	24.65	24.65	24.65	24.65	24.65
y (ft)	0.10	0.20	0.30	0.40	0.50	0.60	0.70	0.80
	24.40	23.65	23.30	23.30	22.30	22.10	21.42	20.40
	0.90	1.00	1.10	1.20	1.30	1.40	1.50	1.60

Run # 3-3-3

U (fps)	22.10	23.65	24.40	24.90	24.05	23.85	23.65	23.85
y (ft)	0.10	0.20	0.30	0.40	0.50	0.60	0.70	0.80
	23.65	23.65	23.30	23.30	22.50	21.65	20.80	19.95
	0.90	1.00	1.10	1.20	1.30	1.40	1.50	1.60

Run # 3-3-4

U (fps)	23.65	25.15	25.52	25.70	25.70	25.70	25.52	25.52
y (ft)	0.10	0.20	0.30	0.40	0.50	0.60	0.70	0.80
	25.52	24.99	24.40	23.85	23.30	22.50	21.65	21.00
	0.90	1.00	1.10	1.20	1.30	1.40	1.50	1.60

Run # 3-3-5

U (fps)	23.65	25.30	26.00	26.20	25.82	26.00	26.00	26.20
y (ft)	0.10	0.20	0.30	0.40	0.50	0.60	0.70	0.80
	25.70	25.30	24.96	24.65	24.40	23.45	22.30	21.30
	0.90	1.00	1.10	1.20	1.30	1.40	1.50	1.60

Run # 3-3-6

U (fps)	24.05	26.57	27.38	27.57	27.65	28.00	27.87	27.57
y (ft)	0.10	0.20	0.30	0.40	0.50	0.60	0.70	0.80
	27.20	26.90	26.20	26.00	24.96	24.22	23.30	22.50
	0.90	1.00	1.10	1.20	1.30	1.40	1.50	1.60

Run # 3-3-7

U (fps)	26.57	28.00	28.80	29.08	29.08	29.22	28.80
y (ft)	0.20	0.30	0.40	0.50	0.60	0.70	0.80

28.80	27.97	27.57	26.71	26.57	24.96	24.65	23.65
0.90	1.00	1.10	1.20	1.30	1.40	1.50	1.60

Run # 3-3-8

U (fps)	26.90	29.05	30.42	30.52	30.10	30.00	30.00
y (ft)	0.20	0.30	0.40	0.50	0.60	0.70	0.80

30.10	29.80	29.08	28.68	27.75	27.02	25.67	24.75
0.90	1.00	1.10	1.20	1.30	1.40	1.50	1.60

Run # 3-3-9

U (fps)	26.43	26.75	30.42	31.12	31.12	31.12	30.98
y (ft)	0.20	0.30	0.40	0.50	0.60	0.70	0.80

30.52	30.10	29.08	29.05	27.90	26.94	26.60	25.60
0.90	1.00	1.10	1.20	1.30	1.40	1.50	1.60

Run # 3-3-10

U (fps)	26.90	29.62	31.38	32.09	32.40	32.20	32.00
y (ft)	0.20	0.30	0.40	0.50	0.60	0.70	0.80

32.00	31.60	31.38	30.80	30.10	29.71	28.03	26.94
0.90	1.00	1.10	1.20	1.30	1.40	1.50	1.60

APPENDIX 2

OIL DEPTH PROFILES

Run # 1-1-1

x (ft)	29.416	19.478	9.54
d (ft)	0.223	0.195	0.173

Run # 1-1-2

x (ft)	35.167	26.229	16.291	6.353
d (ft)	0.2[illegible]	0.194	0.166	0.134

Run # 1-1-3

x (ft)	40.[illegible]	30.39	20.45	10.51
d (ft)	0.[illegible]	0.173	0.160	0.131

Run # 1-1-4

x (ft)	45.92	35.98	26.04	16.10	6.16
d (ft)	0.190	0.172	0.152	0.124	0.082

Run # 1-1-5

x (ft)	48.25	38.31	28.37	18.43	8.49
d (ft)	0.176	0.158	0.139	0.114	0.90

Run # 1-1-6

x (ft)	56.83	46.89	35.95	26.01	16.07	6.13
d (ft)	0.159	0.147	0.129	0.111	0.089	.061

Run # 1-1-7

x (ft)	61.[illegible]	51.83	41.89	31.95	22.01	12.07	2.13
d (ft)	0.1[illegible]	0.133	0.121	0.106	0.090	0.068	.033

Run # 1-1-8

x (ft)	20.5	10.56
d (ft)	0.33	0.32

Run # 1-1-9

x (ft)	22.92	12.98
d (ft)	0.293	0.266

Run # 1-1-10

x (ft)	25.75	15.81	5.87
d (ft)	0.271	0.240	0.235

Run # 1-2-1

x (ft)	47.33	37.39	27.45	17.51	7.57
d (ft)	.267	.237	.212	.176	.134

Run # 1-2-2

x (ft)	49.20	39.26	29.32	19.38	9.44
d (ft)	.256	.232	.205	.178	.143

Run # 1-2-3

x (ft)	57.60	47.66	37.72	27.78	17.84	7.90
d (ft)	.234	.213	.199	.167	.139	.104

Run # 1-2-4 (a)

x (ft)	63.69	53.75	43.81	33.87	23.93	13.99	4.05
d (ft)	.219	.201	.183	.160	.134	.107	.070

Run # 1-2-4 (b)

x (ft)	63.50	53.56	43.62	33.68	23.74	13.80	3.86
d (ft)	.220	.204	.185	.164	.139	.111	.065

Run # 1-2-5

x (ft)	40.17	30.23	20.29	10.35
d (ft)	.289	.258	.229	.195

Run # 1-2-6

x (ft)	35.25	25.31	15.37	5.43
d (ft)	.321	.287	.257	.230

Run # 1-2-7

x (ft)	33.00	23.06	13.13
d (ft)	.342	.308	.278

Run # 1-3-1

x (ft)	66.17	56.23	46.29	36.35	26.41	16.47	6.53
d (ft)	.270	.248	.226	.203	.167	.143	.098

Run # 1-3-2

x (ft)	64.58	54.64	44.70	34.76	24.82	14.88	4.94
d (ft)	.274	.255	.228	.202	.179	.142	.092

Run # 1-3-3

x (ft)	62.25	52.31	42.37	32.43	22.49	12.55	2.61
d (ft)	.283	.258	.234	.201	.170	.137	.090

Run # 1-3-4

x (ft)	60.17	50.23	40.29	30.35	20.41	10.47	0.53
d (ft)	.284	.261	.236	.208	.174	.135	.086

Run # 1-3-5

x (ft)	58.92	48.98	39.04	29.10	19.16	9.22
d (ft)	.296	.268	.241	.205	.173	.134

Run # 1-3-6

x (ft)	56.42	46.48	36.54	26.60	16.66	6.72
d (ft)	.307	.275	.246	.213	.175	.126

Run # 1-3-7

x (ft)	49.92	39.98	30.04	20.10	10.16
d (ft)	.312	.283	.253	.222	.186

Run # 1-3-8

x (ft)	49.33	39.39	29.45	19.51	9.57
d (ft)	.334	.295	.253	.219	.188

Run # 1-3-9

x (ft)	35.67	25.73	15.79
d (ft)	.405	.362	.316

Run # 1-3-10

x (ft)	30.50	20.56
d (ft)	.485	.405

Run # 2-1-1

x (ft)	60.03	45.70	35.87	25.83	12.75
d (ft)	0.068	0.059	0.051	0.048	0.037

Run # 2-1-2

x (ft)	59.54	45.21	35.38	25.34	12.26
d (ft)	0.069	0.059	0.054	0.048	0.033

Run # 2-1-3

x (ft)	56.63	42.30	32.47	22.43	9.35
d (ft)	0.072	0.064	0.057	0.048	0.034

Run # 2-1-4

x (ft)	53.96	39.63	29.80	19.76	6.68
d (ft)	0.078	0.064	0.055	0.046	0.030

Run # 2-1-5

x (ft)	57.29	42.96	33.13	23.09	10.01
d (ft)	0.080	0.068	0.054	0.042	0.032

Run # 2-1-6

x (ft)	51.67	37.34	27.51	17.47	4.39
d (ft)	0.074	0.061	0.053	0.035	0.015

Run # 2-1-7

x (ft)	47.25	32.92	23.09	13.05
d (ft)	0.080	0.067	0.059	0.039

Run # 2-1-8

x (ft)	45.17	30.84	21.01	10.97
d (ft)	0.097	0.073	0.058	0.036

Run # 2-1-9

x (ft)	33.17	18.84	9.01
d (ft)	0.103	0.072	0.058

Run # 2-1-10

x (ft)	32.08	17.75	7.92
d (ft)	0.115	0.087	0.063

Run # 2-2-1

x (ft)	60.67	46.34	36.51	26.47	13.39
d (ft)	0.149	0.132	0.125	0.104	0.086

Run # 2-2-2

x (ft)	56.25	41.92	32.09	22.05	8.97
d (ft)	0.164	0.143	0.133	0.106	0.077

Run # 2-2-3

x (ft)	54.83	40.50	30.67	20.63	7.55
d (ft)	0.181	0.155	0.136	0.104	0.072

Run # 2-2-4

x (ft)	49.58	35.25	25.42	15.38	2.30
d (ft)	0.184	0.162	0.143	0.109	0.071

Run # 2-2-5

x (ft)	47.00	32.67	22.84	12.80
d (ft)	0.204	0.163	0.146	0.098

Run # 2-2-6

x (ft)	45.83	31.50	21.67	11.63
d (ft)	0.208	0.169	0.145	0.096

Run # 2-2-7

x (ft)	43.00	28.67	18.84	8.80
d (ft)	0.215	0.176	0.099	0.087

Run # 2-2-8

x (ft)	41.50	27.17	17.34	7.30
d (ft)	0.223	0.183	0.146	0.074

Run # 2-2-9

x (ft)	38.50	24.17	14.34	4.30
d (ft)	0.238	0.188	0.148	0.050

Run # 2-3-1

x (in)	61.67	47.34	37.51	27.47	14.39
d (in)	0.220	0.207	0.191	0.152	0.124

Run # 2-3-2

x (in)	58.17	43.84	34.01	23.97	10.89
d (in)	0.237	0.213	0.188	0.158	0.126

Run # 2-3-3

x (in)	56.50	42.17	32.34	22.30	9.22
d (in)	0.256	0.220	0.191	0.155	0.108

Run # 2-3-4

x (in)	54.50	40.17	30.34	20.30	7.22
d (in)	0.275	0.233	0.190	0.155	0.103

Run # 2-3-5

x (in)	52.75	38.42	28.59	18.55	5.47
d (in)	0.277	0.232	0.192	0.150	0.105

Run # 2-3-6

x (in)	52.50	38.17	28.34	18.30	5.22
d (in)	0.275	0.226	0.205	0.156	0.101

Run # 2-3-7

x (in)	51.67	37.34	27.51	17.47	4.39
d (in)	0.283	0.238	0.198	0.148	0.077

Run # 2-3-8

x (in)	49.25	34.92	25.09	15.05	1.97
d (in)	0.306	0.238	0.202	0.156	0.073

Run # 2-3-9

x (in)	48.17	33.84	24.01	13.97	0.89
d (in)	0.313	0.250	0.198	0.148	0.068

Run # [illegible]-1

[illegible] (ft)	51.50	40.46	29.67	20.21	7.17
[illegible] (ft)	0.114	0.094	0.076	0.064	0.043

Run # [illegible]-2

[illegible] (ft)	46.10	35.06	24.27	14.81	1.77
[illegible] (ft)	0.129	0.101	0.085	0.071	0.032

Run # [illegible]-3

[illegible] (ft)	39.17	28.13	17.34	7.88
[illegible] (ft)	0.132	0.110	0.093	0.069

Run # [illegible]-4

[illegible] (ft)	30.50	19.46	8.67
[illegible] (ft)	0.155	0.126	0.105

Run # [illegible]-5

[illegible] (ft)	29.17	17.13	6.34
[illegible] (ft)	0.165	0.139	0.107

Run # [illegible]-6

[illegible] (ft)	25.17	14.13	3.34
[illegible] (ft)	0.18	0.160	0.111

Run # [illegible]-7

[illegible] (ft)	21.83	10.79
[illegible] (ft)	0.205	0.164

Run # [illegible]-8

[illegible] (ft)	19.25	8.21
[illegible] (ft)	0.233	0.188

Run # [illegible]-9

[illegible] (ft)	17.50	6.46
[illegible] (ft)	0.269	0.198

Run # 3-2-1

x (ft)	55.25	44.21	33.42	23.96	10.92
d (ft)	0.187	0.166	0.145	0.126	0.092

Run # 3-2-2

x (ft)	52.17	41.13	30.34	20.88	7.84
d (ft)	0.192	0.168	0.154	0.125	0.097

Run # 3-2-3

x (ft)	50.75	39.71	28.92	19.46	6.42
d (ft)	0.204	0.177	0.155	0.133	0.092

Run # 3-2-4

x (ft)	46.58	35.54	24.75	15.29
d (ft)	0.214	0.186	0.159	0.13[illegible]

Run # 3-2-5

x (ft)	42.67	31.63	20.84	11.38
d (ft)	0.239	0.191	0.167	0.133

Run # 3-1-6

x (ft)	49.50	38.46	27.67	18.21
d (ft)	0.228	0.201	0.175	0.138

Run # 3-2-7

x (ft)	38.50	27.46	16.67	7.21
d (ft)	0.239	0.208	0.185	0.137

Run # 3-2-8

x (ft)	37.83	26.79	16.00	6.54
d (ft)	0.266	0.223	0.194	0.139

Run # 3-2-9

x (ft)	30.75	19.71	8.92
d (ft)	0.299	0.240	0.205

Run # 3-2-10

x (ft)	28.42	17.38	6.[illegible]
d (ft)	0.347	0.266	0.2[illegible]

Run # 3-3-1

x (ft)	64.08	53.04	42.25	32.[illegible]	19.[illegible]	7.[illegible]
d (ft)	0.239	0.218	0.199	0.183	0.[illegible]	0.095

Run # 3-3-2

x (ft)	60.50	49.46	38.67	29.[illegible]	16.[illegible]	4.[illegible]
d (ft)	0.245	0.222	0.202	0.[illegible]	0.[illegible]	0.092

Run # 3-3-3

x (ft)	63.58	52.54	41.75	32.29	19.25	11.4[illegible]
d (ft)	0.246	0.221	0.203	0.180	0.145	0.104

Run # 3-3-4

x (ft)	60.33	49.29	38.50	29.[illegible]	16.00	3.16
d (ft)	0.253	0.228	0.204	0.[illegible]	0.[illegible]	0.105

Run # 3-3-5

x (ft)	57.24	46.20	35.[illegible]	25.[illegible]	1.[illegible]
d (ft)	0.264	0.233	0.21[illegible]	0.[illegible]	0.[illegible]

Run # 3-3-6

x (ft)	54.67	43.63	32.84	23.[illegible]	10.[illegible]
d (ft)	0.279	0.241	0.221	0.[illegible]	0.[illegible]

Run # 3-3-7

x (ft)	50.50	39.46	28.67	19.[illegible]	6.[illegible]
d (ft)	0.301	0.259	0.229	0.[illegible]	0.[illegible]

Run # 3-3-8

x (ft)	45.92	34.88	24.09	14.[illegible]	1.[illegible]
d (ft)	0.327	0.279	0.240	0.[illegible]	0.[illegible]

Run # 3-3-9

x (ft)	44.25	33.21	22.42	12.[illegible]
d (ft)	0.344	0.287	0.249	0.[illegible]

Run # 3-3-10

x (ft)	39.00	27.96	17.17	7.[illegible]
d (ft)	0.378	0.313	0.282	0.208

DATA CALCULATIONS APPENDIX 3

Run #	d_o(ft)	L(ft)	$d_o/L \times 10^3$	F°	Specific Gravity	Wind Speed U (fps)	$\sqrt{Lg(1-\rho_o/\rho_w)}$	$\frac{U}{\sqrt{Lg(1-\rho_o/\rho_w)}}$
1-1-1	0.223	29.42	7.55	64.6	.8906	29.44	10.17	2.89
1-1-2	0.216	35.17	6.12	66.5	.8913	26.84	11.14	2.41
1-1-3	0.201	40.33	4.98	66.9	.8915	23.81	11.92	2.00
1-1-4	0.190	45.92	4.16	68.0	.8919	21.47	12.71	1.09
1-1-5	0.176	48.25	3.65	68.0	.8919	18.16	13.06	1.39
1-1-6	0.159	56.83	2.80	67.3	.8916	15.56	14.12	1.10
1-1-7	0.149	61.77	2.41	66.4	.8913	13.20	13.20	.895
1-1-8	0.330	20.50	16.20	65.8	.8911	36.70	8.51	4.31
1-1-9	0.293	22.92	12.80	64.6	.8906	34.64	8.96	3.87
1-1-10	0.271	25.75	10.56	64.8	.8907	32.37	9.53	3.40

Run #	d_o(ft)	L(ft)	d_o/L x10^3	F°	Specific Gravity	Wind Speed U (fps)	$\sqrt{Lg(1-\sigma_o/\sigma_w)}$	$\frac{U}{\sqrt{Lg(1-\sigma_o/\sigma_w)}}$
1-2-1	0.267	47.33	5.64	63.7	.8883	31.22	12.96	2.41
1-2-2	0.256	49.20	5.21	65.9	.8892	27.86	13.22	2.11
1-2-3	0.234	57.60	4.06	66.2	.8893	24.79	14.39	1.72
1-2-4a	0.219	63.69	3.43	66.5	.8894	20.81	15.04	1.38
1-2-4b	0.220	63.50	3.47	64.4	.8886	21.24	15.01	1.42
1-2-5	0.289	40.17	7.20	65.8	.8891	33.12	11.97	2.77
1-2-6	0.321	35.25	9.11	66.5	.8894	34.31	11.21	3.06
1-2-7	0.342	33.00	10.36	66.6	.8894	36.18	10.72	3.37

Run #	d_o(ft)	L(ft)	d_o/L x10^3	F°	Specific Gravity	Wind Speed U (fps)	$\sqrt{Lg(1-\rho_o/\rho_w)}$	$\frac{U}{\sqrt{Lg(1-\rho_o/\rho_w)}}$
1-3-1	0.270	66.17	4.07	65.1	.8908	26.03	15.26	1.71
1-3-2	0.274	64.58	4.24	65.5	.8910	27.01	15.05	1.80
1-3-3	0.283	62.25	4.55	66.5	.8914	28.48	14.81	1.92
1-3-4	0.284	60.17	4.73	66.9	.8915	30.25	14.58	2.08
1-3-5	0.296	58.92	5.00	66.9	.8915	31.95	14.35	2.23
1-3-6	0.307	56.42	5.45	66.5	.8914	33.58	14.08	2.39
1-3-7	0.312	49.92	6.25	66.5	.8914	35.04	13.04	2.69
1-3-8	0.334	49.33	6.78	67.0	.8915	36.75	13.19	2.79
1-3-9	0.405	35.67	11.32	66.9	.8815	37.76	11.20	3.37
1-3-10	0.485	30.50	15.90	66.7	.8914	39.09	10.37	3.77

Run #	d_o(ft)	L(ft)	d_o/L x10^3	F°	Specific Gravity	Wind Speed U (fps)	$\sqrt{Lg(1-\rho_o/\rho_w)}$	$\frac{U}{\sqrt{Lg(1-\rho_o/\rho_w)}}$
2-1-1	0.068	60.03	1.13	64.1	.8595	8.16	16.65	0.490
2-1-2	0.069	59.54	1.15	64.1	.8595	8.86	16.59	0.534
2-1-3	0.072	56.63	1.27	64.1	.8595	9.34	16.16	0.578
2-1-4	0.078	53.96	1.44	64.1	.8595	9.88	15.78	0.626
2-1-5	0.080	57.29	1.40	63.7	.8594	9.99	16.27	0.614
2-1-6	0.074	51.67	1.43	64.4	.8597	11.62	15.45	0.752
2-1-7	0.080	47.25	1.69	64.4	.8597	10.40	14.77	0.704
2-1-8	0.097	45.17	2.14	64.7	.8598	12.08	14.45	0.836
2-1-9	0.103	39.17	2.10	65.1	.8599	13.87	12.38	1.120
2-1-10	0.115	39.99	2.88	65.5	.8601	15.57	12.17	1.279

Run #	d_o(ft)	L(ft)	d_o/L x10^3	F°	Specific Gravity	Wind Speed U (fps)	$\sqrt{Lg(1-\rho_o/\rho_w)}$	$\frac{U}{\sqrt{Lg(1-\rho_o/\rho_w)}}$
2-2-1	0.149	60.67	2.45	66.2	.8603	16.04	16.74	0.958
2-2-2	0.164	56.25	2.91	65.8	.8602	17.29	16.11	1.073
2-2-3	0.181	54.83	3.30	65.8	.8602	18.05	15.81	1.142
2-2-4	0.184	49.58	3.71	65.5	.8601	19.03	15.14	1.257
2-2-5	0.204	47.00	4.34	65.5	.8601	20.51	14.74	1.391
2-2-6	0.208	45.83	4.54	65.7	.8602	20.60	14.54	1.417
2-2-7	0.215	43.00	5.00	65.8	.8602	23.45	14.09	1.664
2-2-8	0.223	41.50	5.37	65.8	.8602	23.68	13.85	1.710
2-2-9	0.238	38.50	6.18	66.0	.8603	26.31	13.34	1.972

Run #	d_o(ft)	L(ft)	d_o/L x10^3	F°	Specific Gravity	Wind Speed U (fps)	$\sqrt{Lg(1-\rho_o/\rho_w)}$	$\frac{U}{\sqrt{Lg(1-\rho_o/\rho_w)}}$
2-3-1	0.220	61.67	3.57	65.5	.8596	21.39	16.88	1.267
2-3-2	0.237	58.17	4.00	65.5	.8596	22.23	16.41	1.355
2-3-3	0.256	56.50	4.53	64.9	.8584	23.60	16.15	1.461
2-3-4	0.275	54.50	5.04	64.9	.8584	23.22	15.86	1.464
2-3-5	0.277	52.75	5.25	64.7	.8583	25.35	15.60	1.625
2-3-6	0.275	52.50	5.24	64.7	.8583	25.55	15.59	1.639
2-3-7	0.283	51.67	5.48	64.7	.8583	26.40	15.45	1.709
2-3-8	0.306	49.25	6.21	64.7	.9593	25.48	15.08	1.690
2-3-9	0.313	48.17	6.50	64.7	.8583	27.78	14.92	1.862

Run #	d_o(ft)	L(ft)	d_o/L x10^3	F°	Specific Gravity	Wind Speed U (fps)	$\sqrt{Lg(1-\rho_o/\rho_w)}$	$\frac{U}{\sqrt{Lg(1-\rho_o/\rho_w)}}$
3-1-1	0.114	51.50	2.21	70.9	.9090	10.82	12.38	.874
3-1-2	0.129	46.10	2.80	74.5	.9075	12.07	11.72	1.030
3-1-3	0.132	39.17	3.37	74.8	.9075	13.82	10.80	1.280
3-1-4	0.155	30.50	5.08	74.8	.9075	17.30	9.58	1.806
3-1-5	0.165	28.17	5.86	75.2	.9075	18.55	9.16	2.025
3-1-6	0.182	25.17	7.23	74.8	.9075	20.44	8.66	2.360
3-1-7	0.205	21.83	9.39	74.8	.9075	22.91	8.06	2.842
3-1-8	0.333	19.25	12.10	74.5	.9075	26.02	7.57	3.437
3-1-9	0.269	17.50	15.37	74.5	.9075	26.76	7.22	3.706

Run #	d_o(ft)	L(ft)	d_o/L x10^3	F°	Specific Gravity	Wind Speed U (fps)	$\sqrt{Lg(1-\rho_o/\rho_w)}$	$\frac{U}{\sqrt{Lg(1-\rho_o/\rho_w)}}$
3-2-1	0.187	55.25	3.38	75.6	.9065	17.50	12.90	1.356
3-2-2	0.192	52.17	3.68	75.6	.9065	18.49	12.54	1.474
3-2-3	0.204	50.75	4.02	75.6	.9065	19.11	12.36	1.546
3-2-4	0.214	46.58	4.59	75.6	.9065	20.40	11.85	1.721
3-2-5	0.219	42.67	5.13	76.3	.9060	22.54	11.34	1.988
3-2-6	0.228	49.50	4.61	75.9	.9060	23.92	12.20	1.961
3-2-7	0.239	38.50	6.21	75.9	.9060	25.23	10.76	2.345
3-2-8	0.266	37.83	7.03	75.4	.9065	25.78	10.66	2.418
3-2-9	0.299	30.75	9.72	75.6	.9065	27.63	9.62	2.872
3-2-10	0.347	28.42	12.21	75.6	.9065	29.10	9.25	3.146

Run #	d_o(ft)	L(ft)	d_o/L x10^3	F°	Specific Gravity	Wind Speed U (fps)	$\sqrt{Lg(1-\rho_o/\rho_w)}$	$\frac{U}{\sqrt{Lg(1-\rho_o/\rho_w)}}$
3-3-1	0.239	64.08	3.73	75.2	.9065	21.58	13.86	1.557
3-3-2	0.245	60.50	4.05	76.5	.9065	22.85	13.47	1.696
3-3-3	0.246	63.58	3.87	74.8	.9070	22.66	13.81	1.641
3-3-4	0.253	60.33	4.19	76.6	.9065	23.72	13.45	1.764
3-3-5	0.264	57.24	4.61	76.6	.9065	23.95	13.10	1.828
3-3-6	0.279	54.67	5.10	74.8	.9070	25.64	12.81	2.002
3-3-7	0.301	50.50	5.96	76.3	.9067	26.67	12.31	2.166
3-3-8	0.327	45.92	7.12	76.4	.9065	27.82	11.74	2.370
3-3-9	0.344	44.25	7.77	76.4	.9065	28.44	11.52	2.469
3-3-10	0.378	39.00	9.69	76.6	.9065	29.49	10.81	2.728

APPENDIX 4

d_{o_w}, SET-UP DUE TO WAVES

RUN #	d_{o_w}	L	$\sqrt{L}$	$d_{o_w}\sqrt{L}x10^2$	U(fps)
1-1-1	0.014	29.42	5.42	0.258	29.44
1-1-8	0.119	20.50	4.53	2.626	32.37
1-1-9	0.078	22.92	4.79	1.628	34.64
1-1-10	0.059	25.75	5.08	1.161	36.70
1-2-5	0.010	40.17	6.34	0.394	33.12
1-2-6	0.056	35.25	5.94	0.942	34.31
1-2-7	0.066	33.00	5.74	1.149	36.10
1-3-9	0.113	37.76	6.14	1.840	37.76
1-3-10	0.201	30.50	5.52	3.641	39.09
2-1-8	0.017	45.17	6.72	0.253	12.08
2-1-9	0.023	33.17	5.76	0.399	13.87
2-1-10	0.035	32.08	5.66	0.618	15.57
2-2-1	0.069	60.67	7.79	0.886	16.04
2-2-2	0.084	56.25	7.50	1.120	17.29
2-2-3	0.101	54.83	7.41	1.363	18.05
2-2-4	0.104	49.58	7.04	1.477	19.03
2-2-5	0.124	47.00	6.86	1.808	20.51
2-2-6	0.122	45.83	6.77	1.802	20.60
2-2-7	0.135	43.00	6.56	2.057	23.45
2-2-8	0.143	41.50	6.44	2.220	23.68
2-2-9	0.158	38.50	6.21	2.544	26.31

RUN #	d_{ow}	L	$\sqrt{L}$	$d_{ow}\sqrt{L}x10^2$	U(fps)
2-3-1	0.140	61.67	7.86	1.781	21.39
2-3-2	0.157	58.17	7.63	2.058	22.23
2-3-3	0.176	56.50	7.52	2.340	23.60
2-3-4	0.195	54.50	7.38	2.642	23.22
2-3-5	0.197	52.25	7.23	2.725	25.35
2-3-6	0.195	52.50	7.25	2.690	25.55
2-3-7	0.203	51.67	7.19	2.823	26.40
2-3-8	0.226	49.25	7.02	3.219	25.48
2-3-9	0.233	48.17	6.94	3.357	27.78
3-1-5	.024	28.17	5.31	0.452	18.55
3-1-6	.032	25.37	5.02	0.637	20.44
3-1-7	.050	21.83	4.67	1.070	22.91
3-1-8	.066	19.25	4.39	1.503	26.02
3-1-9	.106	17.50	4.18	2.535	26.76
3-2-7	.015	38.50	6.21	0.241	25.23
3-2-8	.038	37.83	6.15	0.618	25.78
3-2-9	.077	30.75	5.54	1.389	27.63
3-2-10	.126	28.42	5.33	2.364	29.10
3-3-7	.028	50.50	7.11	0.393	26.67
3-3-8	.055	45.92	6.78	0.811	27.82
3-3-9	.071	44.25	6.65	1.067	28.44
3-3-10	.109	39.00	6.24	1.746	29.49
3A-1-4	0.017	24.75	4.98	0.347	21.30
3A-1-5	0.019	23.83	4.88	0.391	23.10
3A-1-6	0.052	22.50	4.74	1.095	24.80
3A-1-7	0.038	21.00	4.58	0.825	26.90

RUN #	d_{o_w}	L	$\sqrt{L}$	$d_{o_w}/\sqrt{L} \times 10^2$	U(fps)
3A-1-8	0.071	18.67	4.32	1.640	29.95
3A-1-9	0.124	16.33	4.08	3.040	31.10
3A-2-4	0.025	36.17	6.01	0.422	25.90
3A-2-5	0.031	34.75	5.89	0.532	27.40
3A-2-6	0.045	32.33	5.68	0.797	28.90
3A-2-7	0.102	29.00	5.38	1.887	30.40
3A-2-8	0.115	28.00	5.29	2.170	33.00
3A-3-6	0.023	46.50	6.82	0.340	29.25
3A-3-7	0.067	41.67	6.46	1.030	30.80
3A-3-8	0.123	37.67	6.16	2.000	31.80

APPENDIX 5

WIND STRESS COEFFICIENTS

Run #	T_{s_d} (lb/ft^2)$\times 10^3$ Shear Stress Based on Oil Set-Up Data	$C_d \times 10^3$ Wind Stress Coefficient Based on T_{s_d}	T_{s_w} (lb/ft^2)$\times 10^3$ Shear Stress Based on Wind Profile Data	$C_w \times 10^3$ Wind Stress Coefficient Based on T_{s_w}
1-1-1	2.69	1.309	4.25	2.069
1-1-2	2.11	1.236	3.19	1.868
1-1-3	1.59	1.183	2.18	1.622
1-1-4	1.25	1.144	1.36	1.245
1-1-5	1.02	1.305	1.21	1.548
1-1-6	0.71	1.237	0.84	1.464
1-1-7	0.57	1.380	0.72	1.743
1-1-8	8.45	2.647	18.71	5.860
1-1-9	5.96	2.096	2.66	0.936
1-1-10	4.53	1.824	10.85	4.369
1-2-1	2.39	1.035	5.77	2.498
1-2-2	2.12	1.152	4.32	2.348
1-2-3	1.51	1.036	4.30	2.952
1-2-4(9)	1.20	1.169	2.67	2.602

Run #	τ_{s_d} (lb/ft^2)x10^3	C_dx10^3	τ_{s_w} (lb/ft^2)x10^3	C_wx10^3
1-1-4(6)	1.21	1.132	2.67	2.497
1-2-5	3.27	1.257	5.05	1.942
1-2-6	4.65	1.666	6.31	2.262
1-2-7	5.64	1.826	5.40	1.748
1-3-1	1.75	1.089	4.39	2.734
1-3-2	1.85	1.069	4.47	2.585
1-3-3	2.05	1.066	5.33	2.252
1-3-4	2.13	0.982	5.09	2.347
1-3-5	2.36	0.975	6.99	2.888
1-3-6	2.66	0.995	8.97	3.357
1-3-7	3.10	1.065	5.76	1.979
1-3-8	3.59	1.122	7.54	2.356
1-3-9	7.31	2.163	23.50	6.955
1-3-10	12.26	3.385	13.72	3.789
	Average	1.412		2.542
2-1-1	0.15	0.950	0.11	0.722
2-1-2	0.16	0.862	0.12	0.666
2-1-3	0.18	0.875	0.14	0.671
2-1-4	0.22	0.969	0.11	0.502

Run #	τ_{s_d} (lb/ft^2)x10^3	C_dx10^3	τ_{s_w} (lb/ft^2)x10^3	C_wx10^3
2-1-5	0.22	0.930	0.17	0.715
2-1-6	0.21	0.657	0.27	0.847
2-1-7	0.27	1.052	0.61	2.380
2-1-8	0.41	1.185	0.54	1.552
2-1-9	0.63	1.380	1.01	2.210
2-1-10	0.81	1.408	0.67	1.158
2-2-1	0.70	1.150	1.18	1.935
2-2-2	0.76	1.073	0.99	1.392
2-2-3	1.17	1.515	0.75	0.960
2-2-4	1.34	1.560	1.10	1.281
2-2-5	1.74	1.748	1.65	1.655
2-2-6	1.85	1.840	2.18	2.170
2-2-7	2.10	1.610	2.86	2.193
2-2-8	2.35	1.771	4.01	3.020
2-2-9	2.88	1.755	4.98	3.040
2-3-1	1.53	1.414	2.87	2.645
2-3-2	1.76	1.505	2.26	1.935
2-3-3	2.27	1.720	2.24	1.695
2-3-4	2.72	2.130	2.61	2.042
2-3-5	2.85	1.875	4.58	3.020

Run #	τ_{s_d} (lb/ft^2)x10^3	C_dx10^3	τ_{s_w} (lb/ft^2)x10^3	C_wx10^3
2-3-6	2.82	1.825	3.30	2.135
2-3-7	3.04	1.839	6.00	3.360
2-3-8	3.73	2.420	4.26	2.770
2-3-9	3.97	2.172	4.38	2.398
	Average	1.475		1.834
3-1-1	0.33	1.186	0.38	1.362
3-1-2	0.45	1.300	0.30	0.865
3-1-3	0.58	1.280	0.55	1.205
3-1-4	1.03	1.455	1.01	1.425
3-1-5	1.27	1.559	1.02	1.253
3-1-6	1.64	1.655	1.11	1.20
3-1-7	2.52	2.025	2.84	2.285
3-1-8	3.69	2.300	3.64	2.270
3-1-9	3.42	3.200	4.38	2.585
3-2-1	0.83	1.145	0.38	0.518
3-2-2	0.93	1.149	0.73	0.905
3-2-3	1.07	1.238	———	———
3-2-4	1.29	1.308	1.14	1.115
3-2-5	1.47	1.219	1.88	1.560
3-2-6	1.37	1.010	1.92	1.415

Run #	T_{s_d} (lb/ft^2)x10^3	C_dx10^3	T_{s_w} (lb/ft^2)x10^3	C_wx10^3
3-2-7	1.94	1.285	1.31	0.869
3-2-8	2.44	1.549	2.53	1.607
3-2-9	3.81	2.105	———	———
3-2-10	5.55	2.770	8.29	4.130
3-3-1	1.17	1.061	0.86	0.782
3-3-2	1.30	1.050	1.54	1.242
3-3-3	1.25	1.028	0.73	0.603
3-3-4	1.39	1.042	1.88	1.408
3-3-5	1.59	1.169	2.82	2.070
3-3-6	1.86	1.192	0.83	0.529
3-3-7	2.35	1.397	2.83	1.682
3-3-8	3.05	1.663	7.49	4.075
3-3-9	3.50	1.823	5.74	2.990
3-3-10	4.80	2.330	7.59	3.680
	Average	1.534		1.689

Average of 3 Oils

$$C_d = 1.475 \times 10^{-3}$$

$$C_w = 2.205 \times 10^{-3}$$

APPENDIX G - LIST OF SYMBOLS

In the dimensions used below

F is the force dimension

L is the length dimension

T is the time dimension

M is the mass dimension

Symbol	Description	Units	Dimensions
A	Dimensionless wind stress coefficient as defined by Keulegan (1)		
a_x	Total fluid acceleration in the x-direction	$\frac{ft}{sec^2}$	$\frac{L}{T^2}$
a_z	Total fluid acceleration in the z-direction	$\frac{ft}{sec^2}$	$\frac{L}{T^2}$
B, B'	Dimensionless wind-wave coefficient		
C, C'	Dimensionless wind stress coefficient		
C_d	Dimensionless wind stress coefficient based on oil set-up data		
C_w	Dimensionless wind stress coefficient based on wind profile data		

LIST OF SYMBOLS (Continued)

Symbol	Description	Units	Dimensions
C_{30}	Dimensionless wind stress coefficient at 30 ft elevation		
d_o	Oil set-up due to wind	ft	L
d_{o_t}	Total oil set-up	ft	L
d_{ow}	Oil set-up due to waves	ft	L
d_{ox}	Depth of oil at any point x along oil fetch length	ft	L
d_w	Water depth	ft	L
F_o	Force on control volume from right	lbs	$\frac{ML}{T^2}$
F_w	Force on control volume from left	lbs	$\frac{ML}{T^2}$
F_x	Forces in the x-direction	lbs	$\frac{ML}{T^2}$
f	Function designation in Eq. 3, 7, 9, 56, 75 and 77		
f'	Function designation in Eq. 76 and 78		
G	A dimensionless constant expressing a relationship between the density of oil and the density of air		

LIST OF SYMBOLS (Continued)

Symbol	Description	Units	Dimensions
g	Acceleration of gravity	$\frac{ft}{sec^2}$	$\frac{L}{T^2}$
g_x	Acceleration of gravity in the z-direction	$\frac{ft}{sec^2}$	$\frac{M}{LT^2}$
g'	Densimetric acceleration of gravity	$\frac{ft}{sec^2}$	$\frac{M}{LT^2}$
H	Vertical rise in the water level in the air-water inclined manometer	ft	L
h	Water depth	ft	L
I	Constant used to describe the oil parameters in Eq. 99 and Eq. 100		
K	Numerical constant showing the ratio of surface and bottom shear stress		
k	Numerical constant defined by Wilson (3) in Eq. 18.		
k_o	Karman's constant equal to 0.40		
L	Water or oil fetch length	ft	L
m	Constant equal to the number of variables used in dimensionless analysis		

LIST OF SYMBOLS (Continued)

Symbol	Description	Units	Dimensions
n	Dimensionless flow form constant		
n'	Constant equal to the number of dimensions used in dimensional analysis		
P	Fluid pressure	$\frac{lb}{ft^2}$	$\frac{M}{LT^2}$
P_o	Free air stream pressure	$\frac{lb}{ft^2}$	$\frac{M}{LT^2}$
P_s	Stagnation pressure	$\frac{lb}{ft^2}$	$\frac{M}{LT^2}$
R	Horizontal air-water inclined manometer deflection of water	ft	L
S	Water set-up due to wind	ft	L
dS	Differential water set-up due to wind	ft	L
S_1	Set-up of water due to wind	ft	L
S_2	Set-up of water due to waves	ft	L
t	Time	sec	T
U	Wind speed	$\frac{ft}{sec}$	$\frac{L}{T}$

LIST OF SYMBOLS (Continued)

Symbol	Description	Units	Dimensions
U_o	Formula characteristic wind velocity as defined by Keulegan (1) in Eq. 10	$\frac{ft}{sec}$	$\frac{L}{T}$
$\bar{U}_o$	Used in Eq. 90 to define dimensionless wind speed	$\frac{ft}{sec}$	$\frac{L}{T}$
U'	Wind velocity at z'	$\frac{ft}{sec}$	$\frac{L}{T}$
U_*	Wind shear velocity	$\frac{ft}{sec}$	$\frac{L}{T}$
U_c	Critical wind velocity at which waves are generated in the fluid	$\frac{ft}{sec}$	$\frac{L}{T}$
U'_c	Critical wind velocity at 0.7 ft elevation	$\frac{ft}{sec}$	$\frac{L}{T}$
u	Wind velocity in the x-direction	$\frac{ft}{sec}$	$\frac{L}{T}$
u_s	Water surface velocity	$\frac{ft}{sec}$	$\frac{L}{T}$
V	Oil volume	ft^3	L^3
w	Wind velocity in the z-direction	$\frac{ft}{sec}$	$\frac{L}{T}$
x	Any distance along water or oil fetch length	ft	L
dx	Differential fetch length	ft	L

LIST OF SYMBOLS (Continued)

Symbol	Description	Units	Dimensions
Y	Elevation above still oil level	ft	L
z	Any elevation above a surface which is creating a boundary layer in the wind profile	ft	L
z_o	Equivalent roughness height of a surface creating a boundary layer	ft	L
z_1, z_2 etc.	Any elevation above a surface creating a boundary layer at points 1, 2, etc.	ft	L
z'	Elevation of focal point describing an equivalent roughness associated with sand grain diameter	ft	L
α	Dimensionless wind stress parameter for water surface without waves		
β	Dimensionless wind stress parameter for water surface with waves		
γ	Defined by Van Dorn (2) as $(\rho_w/\rho_a)\alpha^2$		
γ_a	Specific weight of water	$\frac{lbs}{ft^3}$	$\frac{M}{L^2T^2}$
γ_w	Specific weight of water	$\frac{lbs}{ft^3}$	$\frac{M}{L^2T^2}$

LIST OF SYMBOLS (Continued)

Symbol	Description	Units	Dimensions
θ	The angle the air-water manometer makes with the horizontal plane		
τ	Fluid shear stress	$\frac{lbs}{ft^2}$	$\frac{M}{L^2}$
τ_b	Bottom shear stress	$\frac{lbs}{ft^2}$	$\frac{M}{L^2}$
τ_s	Surface shear stress		
τ_{s_d}	Surface shear stress based on oil set-up data	$\frac{lbs}{ft^2}$	$\frac{M}{L^2}$
τ_{s_w}	Surface shear stress based on wind profile data	$\frac{lbs}{ft^2}$	$\frac{M}{L^2}$
ρ_a	Mass density of air	$\frac{lb\ sec^2}{ft^4}$	$\frac{M}{L^3}$
ρ_o	Mass density of oil	$\frac{lb\ sec^2}{ft^4}$	$\frac{M}{L^3}$
ρ_w	Mass density of water	$\frac{lb\ sec^2}{ft^4}$	$\frac{M}{L^3}$
μ	Fluid viscosity	$\frac{lb\ sec}{ft^2}$	$\frac{M}{LT}$
μ_o	Oil viscosity	$\frac{lb\ sec}{ft^2}$	$\frac{M}{LT}$
ν	Kinematic viscosity	$\frac{ft^2}{sec}$	$\frac{L^2}{T}$